Processing of Hemp Fibre Using Enzyme/Fungal Treatment for Composites

A thesis submitted in fulfilment of the requirements for the degree of PhD of Science at The University of Waikato

2009

Yan Li

Abstract

Hemp fibres compete very well with glass fibres in terms of their specific strength and stiffness and so can replace glass fibres as reinforcement in composites. Combining them with thermoplastics results in potentially cheap recyclable composite materials. The adhesion between the hemp fibre and thermoplastics such as polypropylene is a major factor in the mechanical properties of the composite. Interfacial bonding can be improved by modifications to the fibres, the matrix or both the fibres and the matrix. The aim of this thesis was to investigate low cost and efficient fibre treatment methods with low environmental impact such as bag retting and white rot fungi, and chelator/enzyme treatments which could be applied to hemp fibre in order to create better bonding fibre for potentially recyclable composite materials.

Bag retting was carried out by keeping fresh green hemp fibres in a sealed plastic bag for 1 to 2 weeks to allow natural retting to occur under sealed conditions. For white rot fungi treatments, the dried non-retted hemp fibres were gamma irradiated, and then inoculated with white rot fungi for 2 weeks. Chelator/enzyme treatment was achieved by immersing the fresh green non-retted hemp fibres in solutions consisting of either EDTMP.Na5 (ethylene diamine tetra (methylene phosphonic acid pentasodium salt) or pectinase (P2401) and laccase (53739) for 6 hours.

Several characterization techniques, namely wet chemical analysis, Fourier-transform infrared (FT-IR), scanning electron microscopy (SEM), fibre density testing, X-ray diffraction (XRD), differential thermal analysis (DTA) and thermogravimetric analysis (TGA), zeta potential and single fibre tensile testing were used to assess the effect of treatment on hemp fibres. Wet chemical analysis and FT-IR, were used to measure the chemical compounds present in untreated and treated hemp fibres and showed all treatments removed non-cellulosic

compounds from hemp fibre. The separation of untreated and treated fibres was investigated by visual inspection. An examination of surface morphology of hemp fibres carried out using SEM revealed that all treated fibres had cleaner hemp surfaces than untreated ones. The fibre density testing showed that the treated fibre had higher density than untreated fibre. XRD was carried out to assess modification of the crystallinity of fibres and the results showed hemp fibre crystallinity index increased in all treated fibres. Differential thermal analysis (DTA) and thermogravimetric analysis (TGA) were used to obtain the activation energies and relative thermal stability of fibres, and indicated that all treatments improved fibre thermal stability. Zeta potential indicated that all treated fibres were more hydrophilic than untreated fibre. Single fibre tensile testing was used to obtain the tensile strength of untreated and treated fibres and it was found that the tensile strength of all treated fibres was reduced.

Short fibre composites were produced by extrusion and injection moulding. Fibres, polypropylene (PP) and a maleated polypropylene (MAPP) coupling agent were compounded using a twin-screw extruder, and then injection moulded into composite tensile test specimens. It was found that all fibre treatments increased the tensile strength of composites. White rot fungi *Schizophyllum commune* (S.com) treated fibre gave the highest tensile strength of 45 MPa, an increase of 28% compared to composites using untreated fibre. Both the single fibre pull-out test and the Bowyer and Bader model were used to determine the interfacial shear strength (IFSS) of untreated fibre and S.com treated fibre composites. The results obtained from both methods showed that IFSS of the treated fibre composites was higher than that for untreated fibre composites. This supports that the hemp fibre interfacial bonding with PP was improved by white rot fungi treatment. The Bowyer and Bader model was also used to calculate the tensile strength of untreated and S.com treated short fibre composites and results closely match the experimentally values.

Long hemp fibre composite sheets were fabricated by film stacking and hot-press forming. Layers of PP film, PP/MAPP powder and hemp fibre were stacked alternately and the stack then was compressed in a hot press. The long fibre composites containing white rot fungi *Schizophyllum commune* (S.com) treated fibre had the highest tensile strength of 73 MPa, an increase of 44% compared to composites using untreated fibre. The simple "rule of mixtures" was modified by taking account of voids, and then was used to calculate the tensile strength of the composites. The modified modeling gave the same trend for strength as observed experimentally, which showed that tensile strength of the treated fibre composites, was higher than that for untreated fibre composites. This supports that the hemp fibre interfacial bonding with PP is improved by treatment.

Preface

This thesis is submitted as a fulfillment of the requirements for the Ph.D. of science degree. The study was carried out during 2006 to 2009 at the Department of Engineering, the University of Waikato, New Zealand. The project was financially supported by a Technology in Industry Fellowship (TIF) provided by Technology New Zealand and Nic Foreman of Hemptech

The study has been supervised by:

Dr. Kim Pickering Chief Supervisor

Dr. Johan Verbeek 2nd Supervisor

Dr. Mark Lay 3rd Supervisor

Published papers

1. Li Y, Pickering KL. The effect of chelator and white rot fungi treatments on long hemp fibre-reinforced composites. Comp Sci Tech (2009) 69: p.1265-1270
2. Li Y, Pickering KL, Farrell RL. Determination of interfacial shear strength of white rot fungi treated hemp fibre reinforced polypropylene. Comp Sci Tech (2009) 69: p.1165-1171
3. Li Y, Pickering KL, Farrell RL. Analysis of green hemp fibre reinforced composites using bag retting and white rot fungal treatments. Industrial Crops & Products (2009) 29: p. 420-426
4. Li Y, Pickering KL. Hemp fibre reinforced composites using chelator and enzyme treatments. Comp Sci Tech (2008) 68: p.3293-3298
5. Pickering KL, Li Y, Farrell RL. Fungal and alkali modification of hemp fibre reinforced composite. Key Eng Mat (2007) 334-335: p. 493-496
6. Pickering KL, Li Y, Farrell RL. Lay M. Interfacial modification of hemp fibre reinforced composites using fungal and alkali treatment. Journal of Biobased Materials and Bioenergy (2007) 1: p.109-117

Oral presentations

Fungal and alkali interfacial modification of hemp fibre reinforced composites. 5th Asian-Australasian Conference on Composite materials (ACCM-5) 27-30 November, 2006. Hong Kong

Acknowledgements

There have been many people who have helped with the development of this thesis and if I have forgotten to thank anyone, my sincerest apologies.

Firstly, I would like to thank my wonderful daughter for her being here with me through all these years in Hamilton. I would like to give special thanks to my husband, who has always supported me in what I've done.

I would like to think my supervisor Kim Pickering for her kindly encouragement, resolute assistance and guidance. I would also like to give thanks to my two co-supervisors, Dr. Johan Verbeek and Dr. Mark Lay. I would also like to thank Roberta Farrell and her research team for their fungal treatment supporting. I also appreciate all the support I have had from composite group, Gareth Beckerman, Dalour Beg, Saiful Islam Moyeenuddin Sawpan and Poom Pingkarawat. Without the help of all of these people this thesis would never have been completed.

I would next like to thank the technicians in laboratory whose advice, expertise and help has been a tremendous importance in the completion of this thesis. These people include Yuanji Zhang, Paul Ewart and Helen Turner.

I would like to thank the Technology in Industry Fellowship (TIF) for their financial assistance. I would also like to offer thanks to my industrial supervisor, Nic Foreman.

Table of Contents

ABSTRACT ..... **I**

PREFACE ..... **IV**

ACKNOWLEDGEMENTS ..... **VI**

TABLE OF CONTENTS ..... **VII**

LIST OF TABLES ..... **XIII**

LIST OF FIGURES ..... **XV**

CHAPTER 1: INTRODUCTION **1**

1.1 Background to the Study 1

1.2 Objectives 3

1.3 Outline 4

CHAPTER 2: LITERATURE REVIEW **6**

2.1 Natural Fibres 6

2.1.1 Natural Fibre Classifications ***6***

2.1.2 Comparison of Natural Fibres ***7***

2.1.3. Industrial Hemp ***8***

2.1.4. Hemp Plant Anatomy ***10***

2.1.5 Cell Wall Organization ***13***

2.1.6 Chemical Composition of Hemp Fibres ***15***

Cellulose ***15***
Hemicellulose ***17***
Lignin ***17***
Pectin ***18***
Wax ***18***
Minerals ***18***

2.2 Matrix 18

2.2.1 Polypropylene ***20***

2.3 Interfacial Bonding 22

2.3.1 Wettability ***22***

2.3.2 Surface Energy ***22***

2.3.3 Interfacial Bonding Mechanisms ***24***

Mechanical Interlocking **24**
Electrostatic Bonding **25**
Chemical Bonding **26**
Reaction or Interdiffusion Bonding **26**

2.4 TREATMENTS OF NATURAL FIBRE AND MATRIX 27

2.4.1 Hemp Fibre Treatment ***27***

2.4.1.1 Bew and Tank Treatment **28**
2.4.1.2 Bag Retting **28**
2.4.1.3 White Rot Fungi Treatment **28**
2.4.1.4 Alkali Treatment **30**
2.4.1.5 Chelator/Enzyme Treatment **31**
2.4.1.5.1 EDTA and EDTMP ***31***
2.4.1.5.2 Pectinase Treatment ***32***
2.4.1.5.3 Laccase Treatment ***32***

2.4.2 Matrix Treatment ***32***

2.4.2.1 Maleic Anhydride Grafted Polypropylene (MAPP) **33**
2.4.2.2 Silane Treatment **35**

2.5 ANALYTICAL TECHNIQUES FOR NATURAL FIBRES 35

2.5.1 Wet Chemical Analysis of Hemp Fibre ***36***

2.5.2 Fourier -Transform Infrared (FTIR) Analysis of Hemp Fibre ***36***

2.5.3 Scanning Electron Microscopy (SEM) ***36***

2.5.4 X-ray Diffraction ***37***

2.5.4.1 Crystalline Cellulose **39**
2.5.4.2 Crystallinity Index of Fibre **40**
2.5.4.3 The Effect of Crystallinity on Fibre Properties **40**

2.5.5 Measurement of Fibre Density ***41***

2.5.6 Thermal Analysis ***41***

2.5.6.1 DTA and TGA **41**
2.5.6.2 Activation Energy **43**
2.5.6.3 Thermal Stability of Hemp Fibre **44**

2.5.7 Zeta Potential ***44***

2.5.7.1 The Electric Double Layer **44**
2.5.7.2 Shear Plane, Zeta Potential and Isoelectric Point (IEP) **46**
2.5.7.3 The Cellulose Fibre Surface **46**
2.5.7.4 Fungi Treated Cellulose Fibre **48**

2.6 PROCESSING OF FIBRE THERMOPLASTIC COMPOSITES 48

2.6.1 Short Natural Fibre Reinforced Composites ***50***

Fibre Length **50**
Fibre Orientation **50**
Fibre Volume Fracture **51**
2.6.1.1 Processing of Short Fibre Reinforced Thermoplastic Composites **52**
Extrusion Compounding ***52***
Injection Moulding ***53***

2.6.2 long Natural Fibre Aligned Composites ***55***

2.6.2.1 Film Stacking and Hot-press Forming **55**

2.7 COMPOSITE INTERFACIAL SHEAR STRENGTH 56

2.7.1 The Single Fibre Pull-Out Test ***56***

2.7.2 The Single Fibre Fragmentation Test ***59***

2.8 COMPOSITES STRENGTH PREDICTION 62

2.8.1 Rule of Mixtures Model (Parallel and Series Model) ***62***

2.8.2 Hirsch Model ***63***

2.8.3 Modified Rule of Mixtures (Kelly-Tyson Model) ***64***

2.8.4 Bowyer-Bader Model ***65***

2.8.4.1 Determination of Interfacial Strength (IFSS) Using Bowyer-Bader Model **66**
2.8.4.2 Assumptions of Bowyer-Bader Model **67**

2.8.5 Modified of Rule of Mixtures by Taking Account of Void Content ***67***

CHAPTER 3:MATERIALS METHODS **70**

3.1 INTRODUCTION 70

3.2 MATERIALS 71

3.3 EXPERIMENTAL METHODS 72

3.3.1 Bag Retting and Fungal Treatments ***72***

3.3.2 Chelator/Enzyme Treaments ***73***

3.3.3 AnalyticalTechniques for Hemp Fibre ***74***

Wet Chemical Analysis of Fibre **74**
Scanning Electron Microscopy (SEM) **77**
FTIR Spectra **77**
X-Ray Diffraction **77**
Fibre Density Test **78**
Thermal Analysis **79**

Zeta potential....79
Single Fibre Tensile Testing....80
The Single Fibre Pull-Out Test....81
3.3.4 Composite Fabrication....82
3.3.4.1 Extrusion and Injection Moulding....82
3.3.4.2 Film Stacking and Hot-Pressing of long Fibre Composite Sheet....84
3.3.5 Assessment of Composite....85
3.3.5.1 Composite Tensile Testing....85
3.3.5.2 Fibre Lengrh distribution and Fibre Diameter....85
3.3.5.3 Composite Density....85
3.3.5.4 Fibre Weight Content....86
CHAPTER 4: RESULTS AND DISCUSSION....87
4.1 BAG RETTING AND WHITE-ROT FUNGI TREATMENTS....87
4.1.1 Separation of Bag Retted and White Rot Fungi Treated Fibre....87
4.1.2 Wet Chemical Analysis of Bag Retted and White Rot Fungi Treated Fibre....88
4.1.3 FTIR Spectra of Bag Retted and White Rot Fungi Treated Fibre....89
4.1.4 Morphology of Bag Retted and White Rot Fungi Treated Fibre....90
4.1.5 X-Ray Diffraction of Bag Retted and White Fungi Treated Fibre....94
4.1.6 Density of Bag Retted and White Rot Fungi Treated Fibre....95
4.1.7 Thermal Analysis of Bag Retted and White Rot Fungi Treated Fibre....96
4.1.8 Zeta Potential of Bag Retted and White Rot Fungi Treated Fibre....98
4.1.9 Tensile Strength and Young's Modulus of Untreated, Bag Retted and White Rot Fungi treated Fibre....99
4.2 CHELATOR/ENZYME TREATMENTS....102
4.2.1 Separation of Chelator/enzyme Treated Fibre....102
4.2.2 Wet Chemical Analysis of Chelator/enzyme Treated Fibre....103
4.2.3 FTIR Spectra of Chelator/enzyme Treated Fibre....104
4.2.4 Morphology of Chelator/enzyme Treated Fibre....105
4.2.5 X-Ray Diffraction of Chelator/enzyme Treated Fibre....108
4.2.6 Density of Chelator/enzyme Treated Fibre....109
4.2.7 Thermal Analysis of Chelator/enzyme Treated Fibre....109
4.2.8 Zeta Potential of Chelator/enzyme Treated Fibre....111

4.2.9 Tensile Strength and Young's Modulus of Chelator/enzyme Treated Fibre ***112***

4.3 COMPOSITES RESULTS 114

4.3.1 Tensile Strength and Young's Modulus of Untreated, Bag Retted and White Rot Fungi Treated Short Fibre Composite ***114***

4.3.2 Tensile Strength and Young's Modulus of Chelator/enzyme treated Short Fibre Composite ***118***

4.3.3 Environmental and Economic Consideration of Chelator/enzyme Treatment ***120***

4.3.4 Assessment of Chelator and White Rot Fungi Treatment Effect on the Tensile Strength of Long Aligned Fibre Composite ***121***

4.4 COMPOSITES TENSILE STRENGTH MODELLING 124

4.4.1 Modelling for the Tensile Strength of Short Fibre Composite ***124***

4.4.1.1 Fibre Contrubution to Composite Strengths ***124***

4.4.1.1.1 Determination of IFSS Using the Single Fibre Pull-Out Tast ***124***

4.4.1.1.2 Determination of IFSS and Orientation Factor (K_1) Using the Bowyer and Bader Mode ***126***

Fibre Volume Fraction ***126***

Fibre Length Distribution and Fibre Diameter ***126***

Critical Fibre Length at ε_1 *and* ε_2 ($L_{\varepsilon 1}$ and $L_{\varepsilon 2}$) ***128***

Sub-critical and Super-critical Fibre length ***129***

Interfacial Shear Strength (IFSS) and Orientation Factor (K_1) ***130***

4.4.1.1.3 Determination of Critical Fibre Length for Short Fibre Composites ***131***

4.4.1.1.4 Fibre orientation of Injection Moulded Compositest ***132***

4.4.1.2 Matrix Contribution to Composite Strength **132**

4.4.1.3 Total Predicted Composite Strength **134**

4.4.2 Modelling for the Tensile Strength of Long Aligned Fibre Composite ***134***

4.4.2.1 Composite Density (ρ_c) **134**

4.4.2.2 Fibre Weight Content, Void Volume Content (V_p), Fibre Volume Content (V_f) and Matrix Volume Content (V_m) of Composite **135**

4.4.2.3 Comparison of Composite Strength with Models **136**

CHAPTER 5: CONCLUSIONS **139**

5.1 BAG RETTING AND WHITE ROT FUNGAL TREATMENTS 139

5.2 CHELATOR/ENZYME TREATMENTS 139

5.3 COMPOSITE RERSULTS 139

5.4 COMPOSITE TENSILE STRENGTH MODELLING 140

CHAPTER 6: RECOMMENDATIONS 142

REFERENCES.....143

List of Tables

Table 2.1 Chemical classification of natural fibres 7

Table 2.2 Chemical Composition and Properties of plant fibres 8

Table 2.3 Primary and secondary bast fibres 12

Table 2.4 Summary of advantages and disadvantages of thermosets and thermoplastic polymer 20

Table 2.5 Price and physical properties of various polymers.....21

Table 2.6 Summary of factors affecting white rot fungi growth on non-wood fibre.....30

Table 3.1 Description of bag retting and white-rot fungi treatments.....73

Table 3.2 Description of chelator/enzyme treatments.....74

Table 4.1.1 Result of wet chemical analysis for untreated, bag retted and white-rot fungi treated fibre.....89

Table 4.1.2 Crystallinity index of untreated, bag retted and white-rot fungi treated fibre 95

Table 4.1.3 Density of untreated, bag retted and white-rot fungi treated fibre ...96

Table 4.1.4 Summary of thermal analysis for untreated, bag retted and white-rot fungi treated fibre 98

Table 4.1.5 Tensile strength and Young's modulus of untreated, bag retted and white-rot fungi treated fibre 100

Table 4.2.1 Wet chemical analysis of untreated and chelator/enzyme treated fibres 104

Table 4.2.2 Crystallinity index of untreated and chelator/enzyme treated fibres.....109

Table 4.2.3 Density of untreated and chelator/enzyme treated fibre.....109

Table 4.2.4 Summary of thermal analysis of chelator/enzyme treated fibre 111

Table 4.2.5 Tensile strength and Young's modulus of chelator/enzyme treated and untreated fibres.....114

Table 4.3.1 Tensile strength and Young's modulus of untreated, bag retted

and white-rot fungi treated short fibre composites.....115

Table 4.3.2 Tensile strength and Young's modulus of chelator/enzyme treated short fibre composites.....118

Table 4.3.3 Relative environmental, economic and composite strength summary for each chelator/enzyme treatment.....121

Table 4.3.4 Tensile strength of short and long aligned fibre composites.....122

Table 4.4.1 IFSS from single fibre pull-out test for untreated and treated fibre specimens.....125

Table 4.4.2 Average length and diameter of fibre in composites.....127

Table 4.4.3 IFSS and K_I of untreated and treated fibre composites obtained according the Bowyer and Bader model.....130

Table 4.4.4 Tensile strength of untreated and white rot fungi (S.com) treated short fibre composites obtained according to the Bowyer and Bader modal.... 133

Table 4.4.5 Density of fibre and composite.....135

Table 4.4.6 The weight content of fibre and matrix, the volume content of void, fibre and matrix.....136

Table 4.4.7 The matrix stress at the failure strain of the composite.....138

Table 4.4.8 Experimental composite tensile strength compared to calculated values using mathematical model.....138

List of Figures

Figure 2.1 Three distinct varieties of cannabis 10

Figure 2.2 Male and female plants of industrial hemp fibre 11

Figure 2.3 Cross section of a hemp stem 11

Figure 2.4 Cell wall of plant 14

Figure 2.5 Model of the structural organisation of the three major constituents in the cell wall of wood fibres 14

Figure 2.6 The molecular structure and arrangement of cellulose 15

Figure 2.7 Crystalline segments alternating with regions of amorphous in cellulose 16

Figure 2.8 The structure of hemicellulose 16

Figure 2.9 The structure of lignin 17

Figure 2.10 Schematic details of a droplet contact angle and its surface free energy components 23

Figure 2.11 Schematic of mechanical interlocking 25

Figure 2.12 Schematic of electrostatic bonding 25

Figure 2.13 Schematic of chemical bonding 26

Figure 2.14 Schematic of reaction bonding involving polymers 27

Figure 2.15 SEM of the tips of a number of hyphae 29

Figure 2.16 Maleic anhydride grafted PP 33

Figure 2.17 Reaction mechanisms of MAPP with the cellulose fibre surface 34

Figure 2.18 Fracture surfaces showing the influence of MAPP in composites 34

Figure 2.19 HR-Cryo-FE-SEM and TEM micrograph shows fungal hyphae make fine holes on the fibre surface 37

Figure 2.20 Typical X-ray system 38

Figure 2.21 X-ray diffractograms of untreated and alkali treated fibre 40

Figure 2.22 Schematic representation of a DTA/TGA instrument 42

Figure 2.23 A schematic of the structure of the electric double layer 45

Figure 2.24 A typical plot of zeta potential versus pH for cellulose fibre 47

Figure 2.25 Types of flow in thermoplastic composites processing 49

Figure 2.26 Changes in fibre orientation during processing 51

Figure 2.27 Schematic representation of twin screw extruder 53

Figure 2.28 Schematic diagram of screw injection moulding machine 54

Figure 2.29 Schematic of the single fibre pullout test 57

Figure 2.30 Typical force-displacement curve for the single fibre pull-out test ...58

Figure 2.31 Schematic of the single fibre fragmentation test 60

Figure 3.1 Density apparatus 78

Figure 3.2 SDT 2960 Simultaneous DTA-TGA analyser 79

Figure 3.3 Single fibre mounting 80

Figure 3.4 Instron-4204 tensile testing machine 81

Figure 3.5 The single fibre pull-out specimen 82

Figure 3.6 ThermoPrism TSE-16-TC twin-screw extruder 83

Figure 3.7 BOY15-S injection-moulding machine 83

Figure 3.8 Layers of thermoplastic sheet, PP/MAPP powder and hemp fibre.....84

Figure 4.1.1 Digital pictures for untreated, bag retted and white-rot fungi treated fibre 88

Figure 4.1.2 FTIR spectra of untreated, bag retted and white-rot fungi treated fibre 90

Figure 4.1.3 SEM of untreated hemp fibre 91

Figure 4.1.4 SEM of 1 week bag retted hemp fibre.....91

Figure 4.1.5 SEM of 2 weeks bag retted hemp fibre 92

Figure 4.1.6 SEM of D2B treated hemp fibre 92

Figure 4.1.7 SEM of Pyc treated hemp fibre 93

Figure 4.1.8 SEM of S.com treated hemp fibre 93

Figure 4.1.9 X-ray diffraction traces for untreated, bag retted and white-rot fungi treated fibre 94

Figure 4.1.10 DTA curve of untreated, bag retted and white-rot fungi treated fibre showing exothermic peaks.....97

Figure 4.1.11 TGA curve of untreated, bag retted and white-rot fungi treated fibre showing three major weight loss regions 97

Figure 4.1.12 Zeta potential of untreated, bag retted and white-rot fungi treated fibre 99

Figure 4.1.13 Single fibre tensile strength of untreated, bag retted and white-rot fungi treated fibre 101

Figure 4.1.14 Young's modulus of untreated, bag retted and white-rot fungi treated fibre 101

Figure 4.2.1 Digital pictures for untreated and chelator/enzyme treated fibres 103

Figure 4.2.2 FTIR spectra of untreated fibre and chelator/enzyme treated fibres 105

Figure 4.2.3 SEM of E treated hemp fibre 106

Figure 4.2.4 SEM of E2 treated hemp fibre 106

Figure 4.2.5 SEM of E+P treated hemp fibre 107

Figure 4.2.6 SEM of E+L treated hemp fibre 107

Figure 4.2.7 X-ray diffraction traces for untreated and chelator/enzyme treated fibres 108

Figure 4.2.8 DTA curve of chelator/enzyme treated fibre 110

Figure 4.2.9 TGA curve of chelator/enzyme treated fibre 110

Figure 4.2.10 Zeta potential of chelator/enzyme treated fibre 112

Figure 4.2.11 Single fibre tensile strength of untreated and chelator/enzyme treated fibres 113

Figure 4.2.12 Young's modulus of untreated and chelator/enzyme treated fibres 113

Figure 4.3.1 Tensile strength of untreated, bag retted and white-rot fungi treated short fibre composites 116

Figure 4.3.2 Young's modulus of untreated, bag retted and white-rot fungi treated short fibre composites 116

Figure 4.3.3 SEM of untreated short fibre composite fracture surface 117

Figure 4.3.4 SEM of S.com treated short fibre composite fracture surface 117

Figure 4.3.5 Tensile strength of chelator /enzyme treated short fibre composites 119

Figure 4.3.6 Young's modulus of chelator /enzyme treated short fibre composites 119

Figure 4.3.7 SEM of E2 treated fibre short composite fracture surface 120

Figure 4.3.8 SEM of untreated fibre long aligned composite fracture surface .. 123

Figure 4.3.9 SEM of S.com treated long aligned fibre composite fracture surface 123

Figure 4.4.1 Single fibre pull-out test force –displacement curve for untreated and treated fibre specimens..... 125

Figure 4.4.2 Fibre length distribution in untreated short fibre composite 127

Figure 4.4.3 Fibre length distribution in white rot fungi (S.com) treated short fibre composite 128

Figure 4.4.4 A typical tensile stress-strain curves of S.com treated hemp short fibre composites..... 129

Figure 4.4.5 Stress-strain curve for polyproplyene used to obtain the matrix stress at the failure strain of each long aligned fibre composites 137

Chapter 1: Introduction

1.1 Background to the Study

The use of natural fibre composites is increasing world-wide. Natural fibre composite materials have been utilized in sports products such as surf boards and snowboards as well as in the furniture industry as structural material because of their good strength and stiffness in combination with low density. In addition, natural fibre composites have been adopted by the automotive industry where lower weight can increase transport capacity and decrease fuel consumption. In fact, all of the European automotive manufacturers are aiming to largely replace glass fibre composites with recyclable or biodegradable natural fibre composites. The total application of natural fibres in the European automotive sector is expected to rise to 100,000 ton by 2010 [1] [2].

Industrial hemp fibre is one of the strongest, stiffest, and lightweight natural fibres and therefore has the potential to replace glass fibre in composites to give similar specific properties. Moreover, hemp fibre has other advantages compared to synthetic materials in being biologically degradable and CO_2-neutral [3] [4][14]. Thus, hemp fibre could be considered as one of the most suitable fibres for reinforcement in composites.

Thermoplastic matrices are increasingly being used in preference to thermosets for industrially fabricated natural fibre composites mainly because their composites are easier to recycle and faster to process than thermosets composites. Hemp fibre reinforced thermoplastic composites can be produced by combining hemp fibre with a thermoplastic matrix such as polypropylene and polyethylene.

Strength and stiffness are mainly obtained from the hemp fibre; the thermoplastic matrix is meant to thoroughly surround and bind the fibres to enable load transfer into the fibres and protect them against environmental influence. The interfacial bonding between hemp fibre and the thermoplastic matrix is very important for the properties of the composite. Inherently, common thermoplastic matrices including polypropylene, do not bond well with hemp fibre. Modifications can be made to the matrix in order to improve interfacial bonding. The most successful approach for improving interfacial bonding has been to add a small quantity of maleated polypropylene to polypropylene to increase its hydrophillicity, and thus make it more compatible with natural fibre and enable covalent and hydroxyl bonding [5][6].

In addition to improving interfacial bonding, treatments can be used to separate hemp fibres from their bundles, remove non-cellulosic compounds and modify the fibre surface. Traditionally, dew retting, tank retting and chemical methods have been used successfully to separate hemp fibre bundles and remove non-cellulosic material to increase the access to cellulose hydroxyl groups which can take part in bonding [4][7]. However, dew retting is labour intensive, takes several weeks and the retted fibres are usually inconsistent in quality. Tank retting causes high environmental pollution due to unacceptable wastewaters from the organic fermentation. Chemical methods such as alkali treatment are, now losing popularity mainly based on environmental grounds. Thus, there is the potential for more sustainable potentially economically viable fibre treatments including bag retting, white rot fungi treatment and chelator/enzyme treatment to be developed to enable hemp fibres to be used as reinforcement in composites.

It is reported that bag retting could be used as pre-treatment of separating green hemp fibre bundles [8]. An advantage of bag retting is that the fibres are protected from other environmental factors that may lead to unwanted degradation of the

fibre. A further benefit of bag retting is that it causes significantly less water pollution compared to tank retting. Therefore, bag retting could be used to improve fibre/matrix interfacial bonding by separating fibre bundles.

White rot fungi can selectively degrade non-cellulosic compounds, particularly lignin at a faster rate than they degrade wood cellulose. It has also been reported that fungi produce an extensive system of hyphae, which can make fine holes on the fibre surface and may roughen the surface of the hemp fibres [9]. Some researchers have used High-resolution Cryo-Field Emission Scanning Electron Microscopy (HR-Cryo-FE-SEM) to reveal fungal hyphae attacking fibre walls producing fine holes on the fibre surfaces. Therefore, white rot fungi could potentially be used to remove non-cellulosic components and modify hemp fibre surfaces in order to improve fibre/matrix interfacial bonding.

Some published reports have described the effect of enzymatic degradation of non-cellulosic compounds on hemp fibres [10][11]. Pectinases degrade pectin and laccases modify lignin. However, waxes and other non-cellulosic compounds can be a barrier to these enzymes. In order to achieve good results, these enzyme treatments have been preceded by pre-treatments such as chelator treatments with EDTA (Ethylene Diamine Tetra-acetic Acid) [12].

1.2 Objectives

The first objective of this study was to investigate bag retting and white rot fungi treatments, which could be applied to hemp fibre for removing non-cellulosic compounds, separating hemp fibre from its bundles, as well as increasing the roughness of hemp fibre surfaces, thus improving interfacial bonding with polypropylene.

The second objective of this study was to use EDTMP.Na5 and combined EDTMP.Na5 and enzyme treatments, which are also environmentally friendly methods to separate hemp fibre from its bundles, remove non-cellulosic compounds as much as possible, and therefore, increase the access to cellulose hydroxyl groups which can take part in bonding.

The third objective was to assess the effect of treatment on interfacial shear strength (IFSS) for injection moulded short fibre composites using the single fibre pull-out test and mathematical modeling using the Bowyer and Bader model and predict the tensile strength of short fibre composite using the Bowyer and Bader model.

The fourth objective was to use film-stacking and hot pressing to fabricate long aligned fibre reinforced thermoplastic composites and assess the effect of treatments on tensile strength and compare the results with those calculated using a modified model based on the simple "rule of the mixtures" which takes into account void content.

1.3 Outline

The thesis consists of 6 chapters. Chapter 1 (introduction) gives a general background and the objectives of this study and the outline of the thesis.

Chapter 2 (literature review) addresses the relevant background of the performed work. It is intended to provide the necessary detailed insight into issues directly related to the experimental work. The purpose of this chapter is also to provide a broad understanding of hemp fibres, matrix, fibre and matrix treatments, and analytical techniques for hemp fibre, composite fabrication, and composites interfacial shear strength, and composite tensile strength predictions.

Chapter 3 (material and methods) presents materials, and experimental work carried out in the course of the project.

Chapter 4 (results and discussion) gives the obtained experimental results and discusses in relation to background knowledge presented in Chapter 2. This chapter forms the central part of the thesis and consists of 4 sections:

- The effects of bag retting and white rot fungi treatment on hemp fibre are presented in Section 4.1. The methods used to measure the effects of bag retting and white rot fungi treatments on hemp fibre include wet chemical analysis, FTIR, visual inspection, fibre density test, X-ray diffraction (XRD), SEM, zeta potential, fibre density, thermal analysis, single fibre tensile testing.
- The effects of EDTMP.Na5 and combined EDTMP.Na5 and enzyme treatments on hemp fibre are presented in Section 4.2.
- The assessment of treatment effect on the tensile strength of short fibre composites and long aligned fibre composites is given in Section 4.3
- The prediction of the tensile strength of short fibre composite and long aligned fibre composites is shown in Section 4.4

Chapter 5 presents the main conclusions of the investigations.

Chapter 6 proposes future work based on the results and considerations of this study.

Chapter 2: Literature Review

This literature review is in eight sections, which give extensive discussion relating to the background of natural fibre composites. These sections are:

- Natural fibres
- Matrices
- Interfacial bonding
- Treatments for natural fibres and matrices
- Analytical techniques for natural fibres
- Processing of fibre thermoplastic composites
- Composite interfacial shear strength
- Composite strength prediction

2.1 Natural Fibres

This section addresses the relevant background of natural fibres. It includes natural fibre classifications, comparison of natural fibres, plant anatomy of industrial hemp, as well as cell wall organization and chemical composition of hemp fibre

2.1.1 Natural Fibre Classifications

Natural organic fibres can be derived from either plant or animal sources. The main chemical structures are based on cellulose for plant fibres and proteins for animal fibres (Table 2.1). Cellulose-based fibres from plants are of most interest for composite materials because they tend to be stronger and stiffer then their animal counterparts. Cellulose fibres can be classified into five categories depending on the origin of the fibre, namely:

1. Bast fibres. These fibres come from the inner bark (phloem or bast) of the stems of dicotyledonous plants. Strong bast fibres include jute, flax, hemp, and kenaf.
2. Grasses and reeds. These fibres come from the stems of monocotyledonous plants such as bamboo and sugar cane.
3. Leaf fibres. Leaf fibres are fibres that run lengthwise through the leaves of most monocotyledonous plants such as sisal, henequen, abaca and esparto.
4. Seed and fruit hairs. These are fibres that come from seed-hairs and flosses, including cotton and coconut.
5. Wood fibres. These fibres come from the xylem of angiosperm (hardwood) and gymnosperm (softwood) trees. Examples include pine, maple, yellow poplar and spruce.

Table 2.1: Chemical classification of natural fibres [15]

Chemical type	Categories	Examples
Cellulose based	Bast fibres	Jute, flax, hemp and kenaf
	Grasses and reeds	Bamboo and sugar cane
	Leaf fibres	Sisal, henequen, abaca and esparto
	Seed and fruit hairs	Cotton and coconut
	Wood fibres	Pine, maple, yellow poplar and spruce
Protein based	Silk, wool and hair	

2.1.2 Comparison of Natural Fibres

Properties of natural fibres such as fibre variability, crystallinity, mechanical properties, and bonding to the matrix should be considered when selecting suitable cellulose fibres for use in composites. Mechanical properties are most

important when selecting a cellulose fibre to give the best reinforcement in a composite material. Table 2.2 shows the chemical composition and properties of plant fibres. It can be seen that the strongest cellulose fibre are hemp, sisal and flax, with hemp and flax having the highest Young's modulus values. Therefore, the most suitable cellulose fibres for use in composite materials are hemp and flax. Flax is more widely accessible and slightly cheaper than hemp. Hemp, however, has the advantages of being extremely disease and pest resistant, and can be planted at higher densities to prevent weeds from growing between the plants. Pesticides and herbicides are therefore not required for growing hemp.

Table 2.2: Chemical composition and properties of plant fibres [15] [13]

Fibre	Cellulose (wt%)	Lignin (wt%)	Hemicellulose (wt%)	Pectin (wt%)	Tensile strength (MPa)	Young's modulus (GPa)
Flax	65-85	1-4	18-20	5-12	500-900	50-70
Hemp	60-77	3-10	18-22	5-15	350-800	30-60
Jute	45-63	12-25	13-20	4-10	200-450	20-55
Kenaf	45-57	8-13	21	3-5	-	-
Sisal	50-64	-	10-14	-	100-850	9-22
Abaca	60	12-13		1	-	-
Coir	30	40-45	0.15-0.25	-	-	-
Cotton	80-90	-	5.7	0-1	-	-
Soft wood	40-45	26-34	-	0-1	98-170	10-50
Hard wood	40-50	20-30	-	0-1	-	-

2.1.3 Industrial Hemp

Hemp is an herbaceous plant of the species *cannabis sativa*. Hemp grows successfully at a density of at least 150 plants per square metre, and reaches a height of two to five metres in a three month growing season. Due to its relationship with marijuana, industrial hemp has been banned in many countries. In New Zealand, it was illegal to grow hemp between the 1930's and 2001. In October 2001, nine growers were issued licenses to trial a crop of hemp for industrial purposes.

The essential difference between industrial hemp and marijuana is the amount of THC (Tetrahydrocannabinols) component within the plant. THC is a psychoactive chemical thought to have a range of detrimental effects on human beings, including low blood pressure, euphoria and long term degeneration of brain activity. There is ongoing debate as to whether the narcotic hemp plant is actually a different variety of plant, or actually the industrial variety bred to produce high levels of THC. Some say there is only one variety, whilst others say that there are three distinct varieties of cannabis, namely: *Cannabis ruderalis*, a small spindly plant; *Cannabis Indica*, a large bushy many branched variety supposedly the high THC cultivar; and *Cannabis sativa L*, the tall industrial hemp variety (see Figure 2.1). Industrial hemp in its natural state is a low THC plant. Scientific analysis of "wild" hemp in the USA, Vietnam and Australia shows an average THC content of 0.6wt%. It is only through intensive selection that high THC cultivars are maintained and the genetic expression of THC can be fixed at a low THC level. It is generally accepted that a content of 2wt% is required to have noticeable effect on the human body [16].

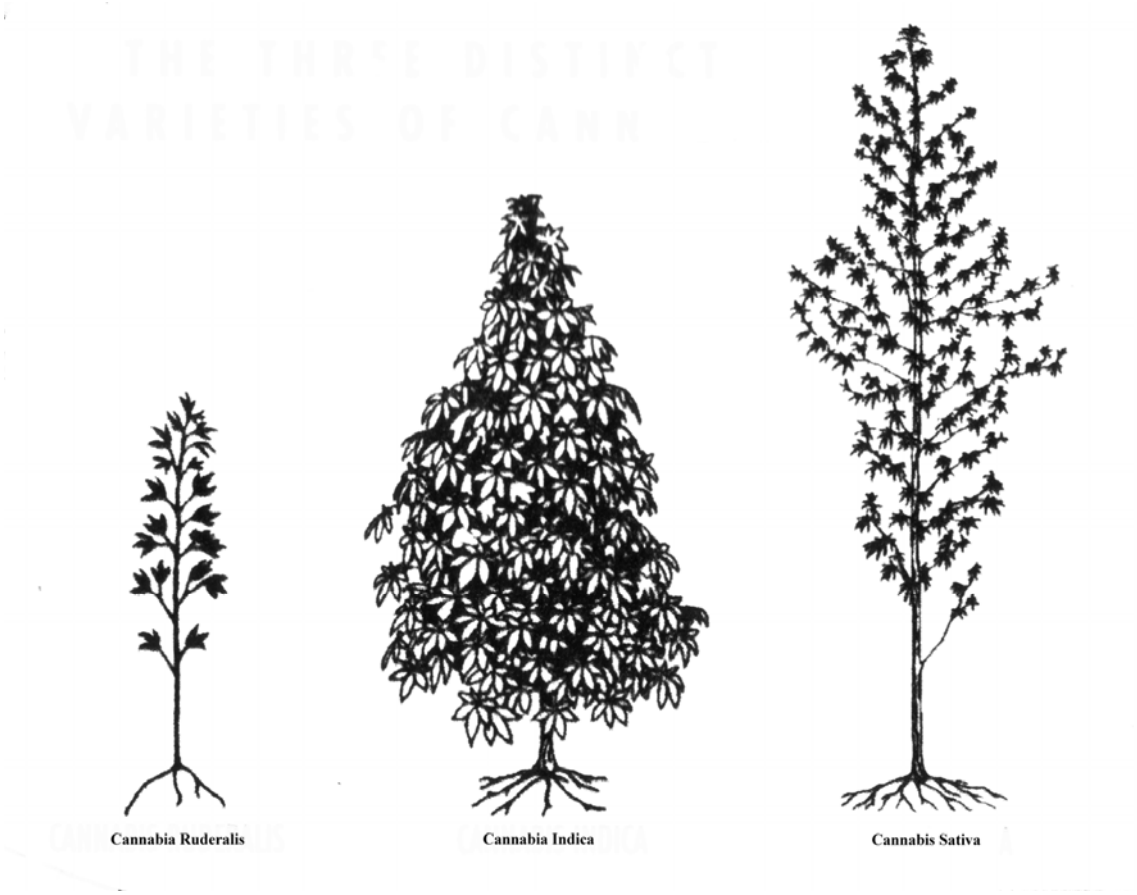

Figure 2.1: Three distinct varieties of cannabis

2.1.4 Hemp Plant Anatomy

Industrial hemp has separate male and female plants with different growth characteristics (see Figure 2.2). The male plants tend to be taller and more slender with only a few leaves surrounding the flowers, while female plants are shorter and stocky with many leaves. The male plant bears the pollen and the female produces the seeds. Throughout history, it has been known that male plants have superior, finer and stronger fibres than the female plants. Fibre quality reduces significantly once the reproductive process starts. Unfortunately the male plant usually starts the process before the female and once the male's flowering is complete the plant dies [16].

a. Male hemp b. Female hemp

Figure 2.2: Male and female plants of industrial hemp fibre

A cross section of the hemp stem can be seen in Figure 2.3, which shows different layers [17]. The hemp stem consists of a wood layer, surrounded by an outer layer of bark consisting of cambium, bast fibre, and epidermis.

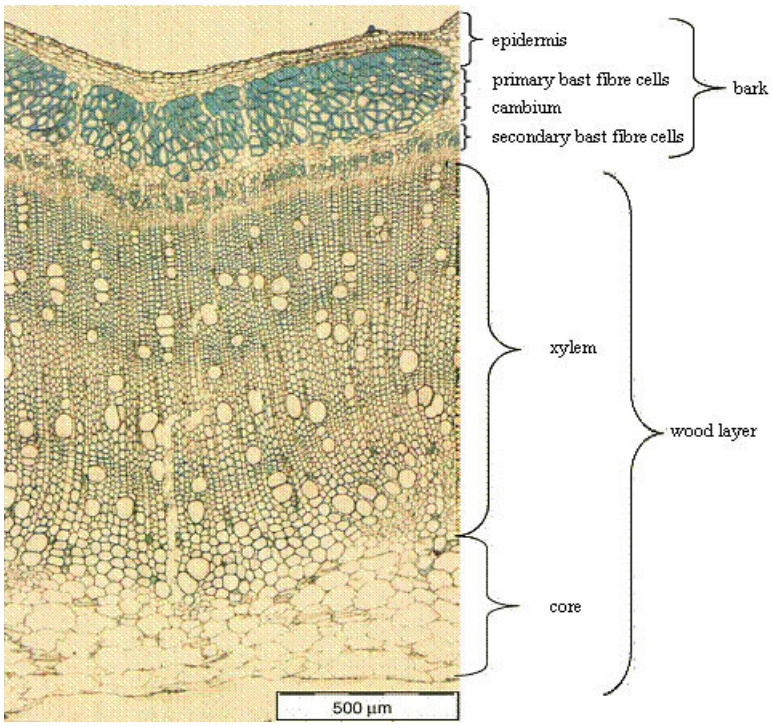

Figure 2.3: Cross section of a hemp stem showing (from exterior to interior) layers of epidermis, bast fibre, cambium, xylem and core [17]

- **Epidermis**: The epidermis (outer layer) mainly contains pectin. The outside of the epidermis, consists of waxy substances and its function is to protect the plant from drying [17].
- **Primary and secondary fibre cells**: Bast fibres are present in bundles and can be categorised as being either primary or secondary bast fibres; the primary bast fibres are long and are mostly found nearer the outer surface, whilst the secondary fibres are of medium length and dominate the inner regions of the bark. Primary bast fibres are the most valuable part of the stalk; they are generally considered to be amongst the strongest known natural fibres [16]. A comparison between primary and secondary bast fibres can be seen in Table 2.3.

Table 2.3: Primary and secondary bast fibres [18]

	Primary bast fibres	Secondary bast fibres
Diameter (μm)	28-38	18-22
Length (mm)	25-40	18-25
Tensile strength (MPa)	<1000	<300
Cellulose (%w/w)	55-85	32-50
Density (g/cm^3)	1.5	1.5

- **Cambium:** Cambium separates the wooden and bast fibre layers from the epidermis and cortex wood.
- **Xylem:** This consists of short, thick and strong-walled cells, which provide mechanical strength for the plant. The chips produced mechanically from the xylem layer are referred to as shive. Shive fibres are short, high in lignin and not very strong. In the present study the term "fibre" is used only for bast fibres.
- **Core:** The core layer is the innermost part of the wooden layer, consisting of loosely packed core cells [17].

2.1.5 Cell Wall Organization

At the cellular level, one of the main features distinguishing plants from the animal kingdom is the presence of a rigid *cell wall* surrounding the cells. The complex structure of the cell wall consists of a number of layers (see Figure 2.4), which include the middle lamella, primary wall and secondary wall [19]**.**

- **Middle lamella:** This is the pectin–rich intercellular material cementing together the primary walls of adjacent plant cells.
- **Primary wall**: This is formed after the middle lamella and consists of a rigid skeleton of cellulose microfibrils embedded in a gel-like matrix composed of pectic compounds and hemicellulose.
- **Secondary wall**: This is formed after cell enlargement is completed. The secondary wall is extremely rigid and provides compression strength. It is made of cellulose, hemicellulose and lignin. The secondary wall is often layered.
- **Structural organization of the chemical constituents:** it is generally accepted that pectin is present in the middle lamella between cells of all types and the primary wall. Lignin is distributed throughout the primary and secondary cell walls, with the highest concentration being found in the middle lamella. Cellulose dominates the secondary cell walls. The hemicellulose is thought to be bound to the cellulose microfibrils by hydrogen bonds forming a layer around the fibrils, and these cellulose/hemicellulose units are then encapsulated by lignin (see figure 2.4 and 2.5)[20].

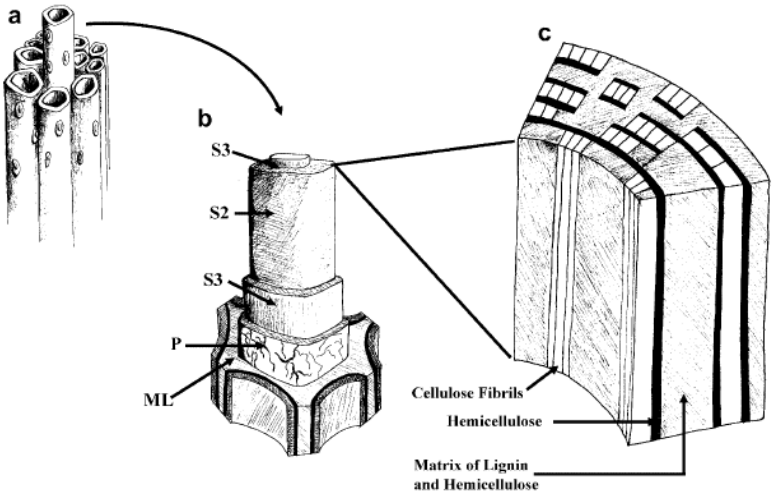

Figure 2.4: Cell wall of plant. a: adjacent cells, b: cell wall layers. S1, S2, S3 secondary cell wall layers, P primary wall, ML middle lamella. c: distribution of lignin, hemicellulose and cellulose in the secondary wall [19]

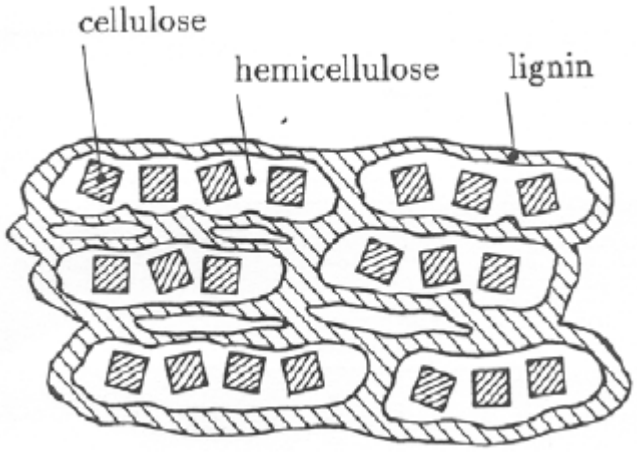

Figure 2.5 Model of the structural organisation of the three major constituents in the cell wall of wood fibres [20].

2.1.6 Chemical Composition of Hemp Fibre

The cell wall of hemp fibre is a complex structure consisting mainly of cellulose, hemicellulose, lignin, pectin and minor contents of wax, and minerals.

Cellulose

Cellulose consists of glucan units (see Figure 2.6) which are joined to form a uniform molecular chain [15]. Cellulose acts as the reinforcing material in the cell wall. The cellulose molecules are laid down in microfibrils in which there is extensive hydrogen bonding between cellulose chains producing a strong crystalline structure. Cellulose is usually composed of crystalline segments alternating with regions of amorphous cellulose (see Figure 2.7). Most plant derived cellulose is highly crystalline and may contain as much as 80% crystalline cellulose [21][22]. Crystalline cellulose is highly packed, and only the very strongest acids and alkalis can modify the crystalline lattice of cellulose.

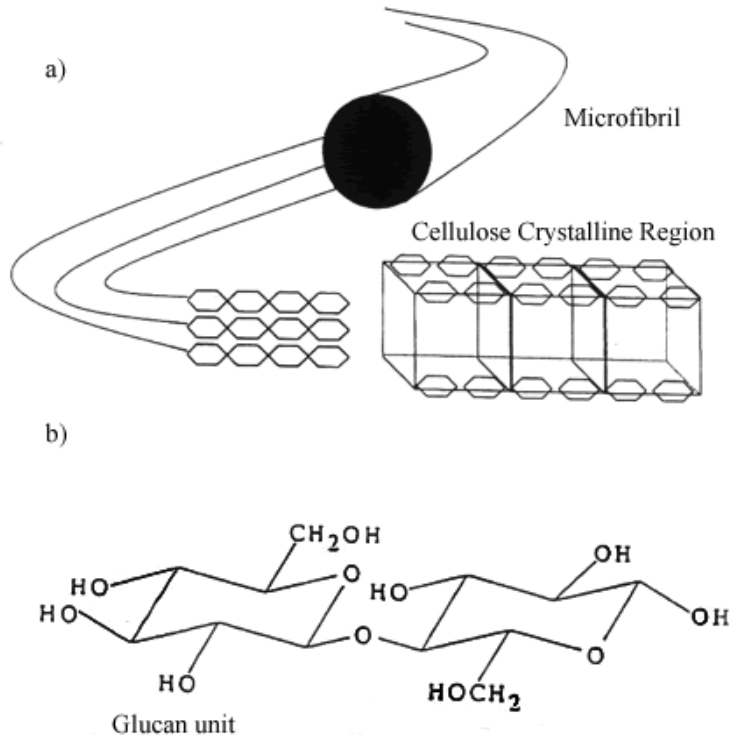

Figure 2.6: The molecular structure and arrangement of cellulose [15]

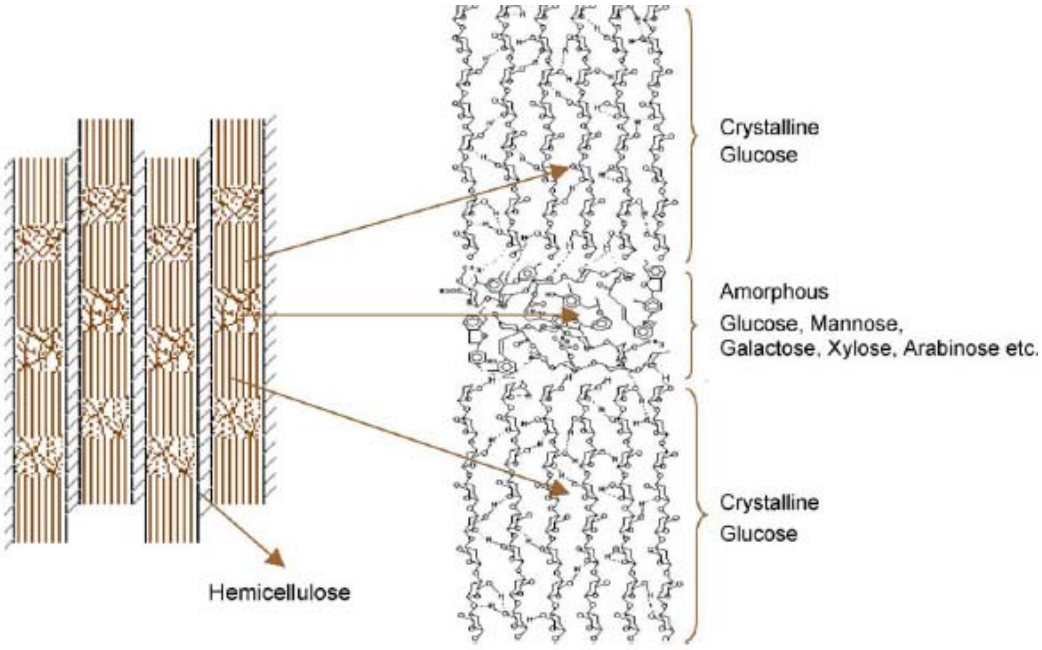

Figure 2.7: Crystalline segments alternating with regions of amorphous in cellulose [22]

Hemicellulose

Hemicellulose has a heterogeneous and branched structure consisting of a collection of polysaccharide polymers containing mainly the sugars D-xylopyranose, D-glocopyranose, Dgalactopyranose, L-arabinofuranose, D-mannopyranose, and Dglucopyranosyluronic acid with small quantities of other sugars (Figure 2.8), which can be extracted in 17-18% alkaline solutions. The role of hemicellulose is to provide linkage between cellulose and lignin. Due to its amorphous structure, its hydroxyl groups are much more accessible to water than those of cellulose [15].

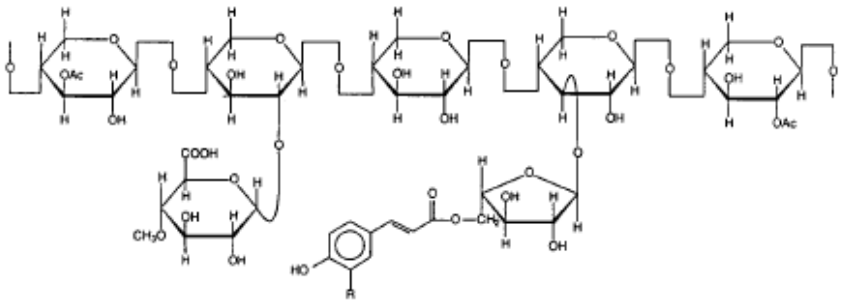

Figure 2.8: The structure of hemicellulose

Lignin

Lignin is considered to consist of three dimensional phenyl propane networks held together by ether and carbon-carbon bonds (Figure 2.9). Lignin is insoluble in most solvents, due to its high molecular weight and complex structure. The double bonds in lignin give the plant fibres a dark color. If lignin is oxidized and the double bonds are broken, the fibre that it is part of will become lighter [15][21]. Lignin is a much less hydrophilic material than hemicellulose and cellulose.

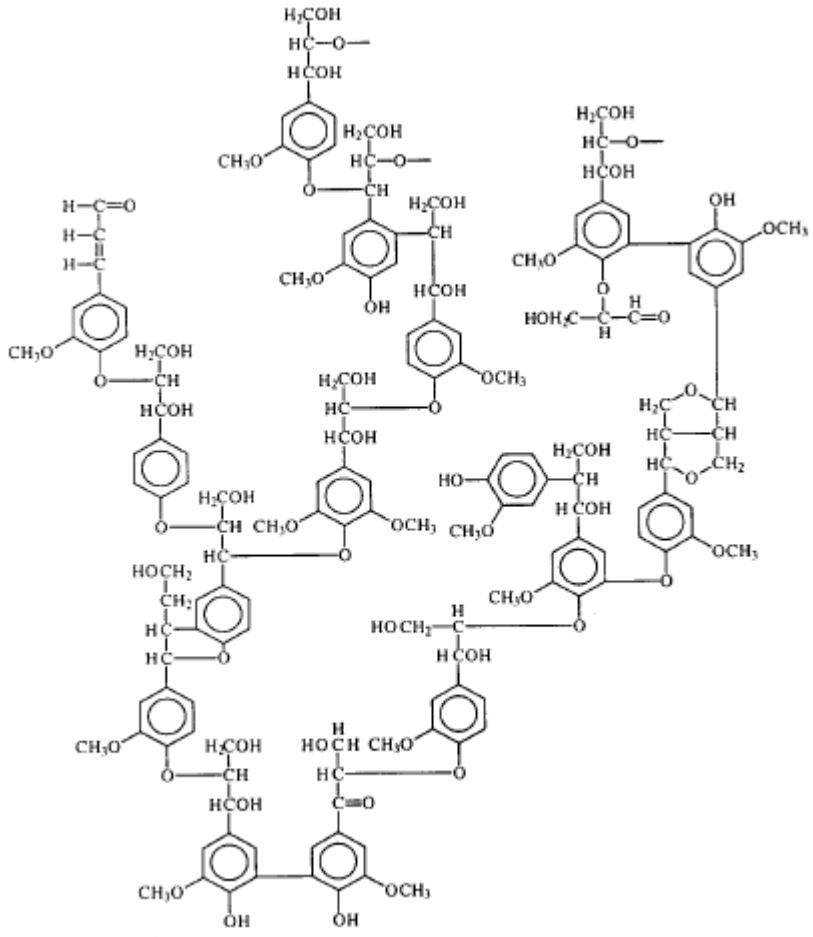

Figure 2.9: Typical structure of lignin [15]

Pectin

Pectins are irregular and heteropolysaccharides which accumulate in the primary wall and middle lamella. Pectin materials play important roles in fibre bundle integration since it is thought to be responsible for binding the cell wall layers together. Removal of pectin material allows the separation of the fibre bundles from the surrounding cells of the stem [15][21].

Wax

Most plants are covered with semi-crystalline wax consisting of mainly long-chain alkane, ester and alcohol waxes. Esters and fatty acids are common but minor components, while alcohols often comprise a major portion of the wax. The effect of the wax layer is to prevent water loss from a plant [15][21].

Minerals

The main plant fibre minerals include calcium (Ca), potassium (K), phosphors (P) and magnesium (Mg) [23]. Calcium in the cell wall exists mainly in pectin**,** forming calcium pectate to stabilize the structure of the cell wall. Calcium chelators can extract calcium ions from pectin in plant cell walls resulting in the pectin becoming soluble which leads to separation of fibre bundles [12].

2.2 Matrix

Both thermoplastic and thermoset polymers are currently used as matrices for composites. Thermoplastic polymers are long organic chains (either linear or branched) produced by joining together small molecules called monomers. There is no covalent bonding between these long chains of molecules, however weak secondary bonds provide some mechanical stiffness and strength. Thermoplastic materials can be remelted due to the fact that the bonds between molecules can be

easily broken. Thermosetting polymers are composed of long, rigid cross-linked chains or three dimensionally networked molecules, therefore, once polymerized; the polymers cannot be softened by heating without degrading some linkages of the polymers. Usually there are some performance differences between thermoplastic and thermosetting matrices. The cross-linked structure of thermoset polymers provides potential for higher Young's modulus and service temperatures than thermoplastics. On the other hand, thermoplastics often have very high failure strains compared to thermosets. This high failure strain capability also leads to high fracture toughness and high impact strength. However, in-plane mechanical properties of composites are generally strongly fibre-dominated, meaning that any difference in the mechanical properties of the matrix tends to be obscured.

Among the many issues that influence processability are matrix viscosity, processing requirements such as temperature, pressure and time, and worker health concerns. Low viscosity facilitates reinforcement impregnation, where each reinforcing fibre ideally should be surrounded by matrix without any voids. Fully polymerized thermoplastics have much higher melt viscosities than thermosets. The higher viscosity of thermoplastics means that higher pressures tend to be required to achieve the same degree of material flow as with thermosets, but in many cases this difference is not dramatic. Whereas thermoplastics only need to be melted, shaped, and then cooled to achieve dimensional stability in a matter of seconds at one extreme, thermosets may take several days to fully crosslink at the other extreme. The very nature of thermosets makes them unpleasant to work with since chemical reactions involving volatile and potentially toxic substances are involved. In contrast, the molecular structure of fully polymerized thermoplastics makes them chemically inert if processed correctly, meaning that no hazardous substances need to be considered.

In addition, the infinite shelf life of thermoplastics is also an advantage because some thermosets such as B-staged prepregs of epoxy and carbon have a limited shelf life prior to processing and often require subambient storage. Table 2.4 summarizes the advantages and disadvantages of thermosets and thermoplastic polymers [24], which clearly show why thermoplastic matrices are increasingly being used in preference to thermosets for industrially fabricated natural fibre composites.

Table 2.4: Summary of advantages and disadvantages of thermosets and thermoplastic polymer

Property	Thermoset	Thermoplastic
Recyclability	Limited	Good
Young's modulus	High	Medium
Service temperature	High	Medium
Toughness	Medium	High
Viscosity	Low	High
Processing pressure	Low	High
Processing temperature	Low	High
Cycle time	Long	Short
Health concern	More	Less
Shelf life	Short	Long

2.2.1 Polypropylene

Thermoplastic polymers to be used as matrices for natural fibre composites must meet several requirements including having a low melting temperature and low density, as well as being cheap and recyclable. The processing temperatures of natural fibre composites are limited below 200 ^{o}C to avoid fibre degradation, and so the first criterion for selecting a suitable composite matrix is that it melts below 200 ^{o}C. However, lower temperature processing also reduces processing costs and

is more environmentally friendly. Polypropylene (PP), high-density polyethylene (HDPE), low density polyethylene (LDPE) and polyvinylchloride (PVC) have suitably low melting temperatures. All of them are cheap and recyclable. PP and LDPE have the lowest densities and are therefore the most suitable in this respect (see Table 2.5).

A matrix with a low level of moisture absorption is also desirable. PP and LDPE are suitable as they have the lowest levels of moisture absorption. However, PP has a better combination of tensile strength and stiffness than LDPE. It can therefore be concluded that PP is the most suitable thermoplastic for use in natural fibre composites as it has the lowest density, lowest price, offers the best possible protection against water and has good mechanical properties. Due to these properties, PP is used in 90% of the glass mat thermoplastic (GMT) sheet material for compression molding [26].

Table 2.5: Price and physical properties of various polymers [25] [26]

Properties	PP	LDPE	HDPE	PVC
Price($/kg)	0.62	0.90	0.86	0.82
Density(g/cm^3)	0.920-0.899	0.925-0.910	1.000-0.941	1.30-1.58
W24h (%)*	0.02-0.01	0.015	0.2-0.01	0.40-0.04
T_g (°C)	-20	-90	-30	85
T_m (°C)	165	120	135	am*
Tensile strength((MPa)	22-41.9	8.3-32.1	22.1-31.4	40.7-52.4
Young's modulus(GPa)	1.15-1.57	0.17-0.70	1.08-1.10	2.44-4.19

*W24h (%) = water absorption after 24h immersion *am = amorphous

2.3 Interfacial Bonding

Using natural fibre as reinforcement in composites involves several challenges. The first and the most important problem is low fibre-matrix adhesion. The role of the matrix in a fibre reinforced composite is to transfer the load to the stiff fibres through shear stresses at the interface. This process requires good bonding between the polymeric matrix and the fibres. Poor adhesion at the interface means that the full capabilities of the composite cannot be exploited and leaves it vulnerable to environmental attack, thus reducing its life span. Natural fibres are hydrophilic and polar in nature, whereas common thermoplastic matrices are hydrophobic and non-polar. Natural fibres used in thermoplastic matrices are therefore dimensionally unstable and display insufficient adhesion between matrix and fibre, which results in poor composite mechanical properties. It is possible to improve bonding between the fibre and matrix by modifying the surface of the fibre, or by modifying the matrix with the addition of a coupling agent.

2.3.1 Wettability

A first condition required before the interfacial bonding can occur is that intimate contact between matrix and fibre can be obtained. In other words, good wetting of a surface is the prerequisite physical process required for good adhesion. Therefore, wettability of the fibre by the matrix would be one of the most important factors when predicting the matrix-fibre adhesion and the wettability can be evaluated from the surface energy of fibre and matrix.

2.3.2 Surface Energy

Surface energy is derived from the unsatisfied bonding potential of molecules at a surface. This is in contrast to molecules within a material which have less energy because they are subject to interactions with molecules which are satisfied in all

directions. Molecules at the surface will try to reduce this 'free energy' by interacting with molecules in an adjacent phase. When one of the bulk phases is a gas, the free energy per unit area is termed the surface energy for solids, and surface tension in liquids. One manifestation of surface energy is a state of tension at the surface of a liquid, as a consequence of which work is required to increase the surface area of a liquid. One definition of surface energy is the work required to increase the surface area of a substance by unit area. However, when both phases are condensed, (i.e. solid-solid, solid-liquid and immiscible liquid-liquid interfaces) the free energy per unit area of the interface is called the 'interfacial energy'.

Figure 2.10 shows the schematic detail of a droplet contact angle and its surface free energy components. When a liquid having a surface energy γ_{LV} is placed on a solid surface with surface energy γ_{SV}, the liquid will spontaneously form a droplet or spread out into a film. The surface free energy of the solid-liquid interface is labelled γ_{SL} and the equilibrium can be expressed as

$$\gamma_{SV} = \gamma_{SL} + \gamma_{LV} \cos\theta \quad (1)$$

Where θ is a contact angle measured between the solid-liquid interface.

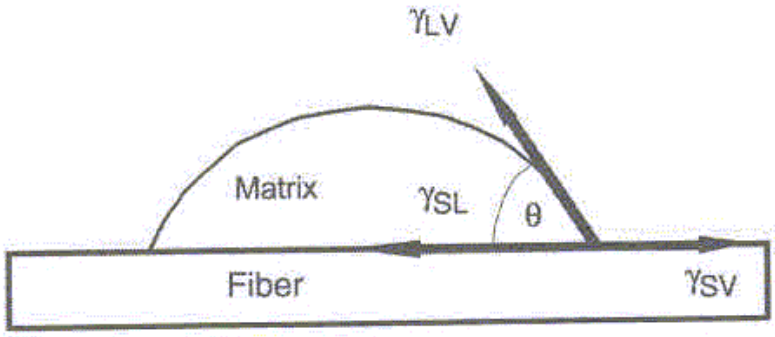

Figure 2.10: Schematic details of a droplet contact angle and its surface free energy components [27]

Liquids that form contact angles greater than 90^o are called "nonwetting" and liquid that forms a contact angle less than 90^o are termed "wetting". When the

contact angle is 0^o, the liquid wets the solid and spreads over the surface spontaneously. Hence the condition for spontaneous wetting to occur is:

$$\gamma_{SV}-\gamma_{SL} \geq \gamma_{LV} \quad (2)$$

The rule holds the higher the surface energy of the solid γ_{SV} relative to the surface energy of the liquid γ_{LV}, the better its wettability and the smaller the contact angle. That is, from a composite wetting process viewpoint, the surface energy of the fibre must be greater than that of the matrix.

Most polymers have low values of surface free energy (20 to 45 mJ/m^2) [27], which decrease slightly with increasing temperature. Fibre surfaces that have been exposed to the ambient environment act to minimize their surface free energy and, therefore, adsorb material to lower their surface free energy. In some cases, this surface can have a surface free energy lower than that of the polymer matrix. In order to increase the fibre surface free energy, surface treatment has been developed to enhance the wettability of a fibre surface.

2.3.3 Interfacial Bonding Mechanisms

Once two constituents come into contact, bonds can form at the interface. Mechanical interlocking, electrostatic bonding, chemical bonding and interdiffusion bonding are the common interfacial bonding mechanisms that can occur. Actually, each of these mechanisms may be valid to some extent, depending on the system chosen. These bonding mechanisms are described more fully in the following sections [28].

Mechanical Interlocking

Mechanical interlocking on the fibre/matrix interface occurs when the fibre surface is rough and jagged. Contraction of the matrix onto the fibre assists this process (see Figure 2.11). In addition, with good wetting, increased roughness

increases interlocking due to increasing of interfacial area. However, it should be noted that if insufficient wetting of the surface takes place, increased surface roughness may even lead to decreased adhesion due to the diminished contact area between matrix and fibre.

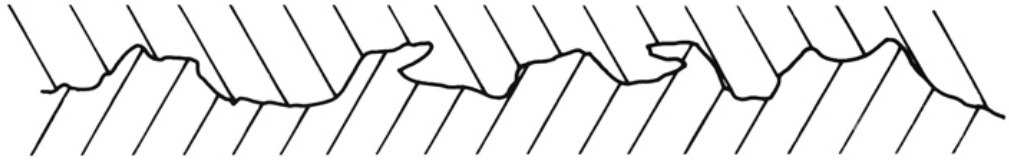

Figure 2.11: Schematic of mechanical interlocking [28].

Electrostatic Bonding

When one part is positively charged and the other is negatively charged, electrostatic bonding occurs (Figure 2.12). This only occurs over a short range and needs intimate contact, so contamination and entrapped gases will decrease the effectiveness of this bonding mechanism. In the case of polymer matrix-fibre systems, electrostatic mechanism will hardly be relevant, because contribution to adhesion by electrostatic forces may be noticeable only at the interface with a metal.

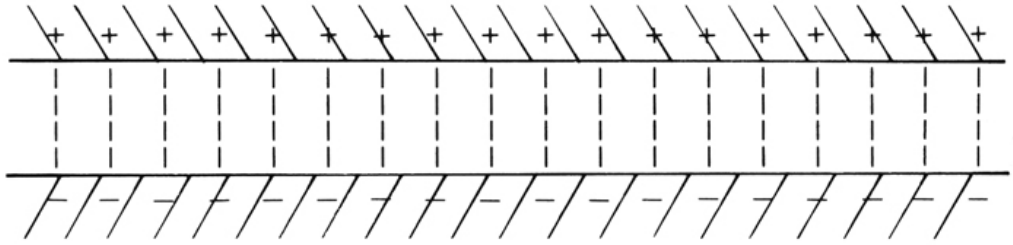

Figure 2.12: Schematic of electrostatic bonding [28].

Chemical Bonding

Fibre surface chemical groups can react with chemical groups in the matrix, forming chemical bonds (Figure 2.13). Van der Waals attractive forces, hydrogen bonds can also form, depending on the system. The strength of the bond will depend on the number of bonds per unit area and the type of bond. The most common chemical bonds and relative bond strengths are as follows:

- Covalent Bond: 200-800kJ mol $^{-1}$
- Hydrogen Bond: 10-40 kJ mol $^{-1}$
- Van der Waals: 1-20 kJ mol $^{-1}$

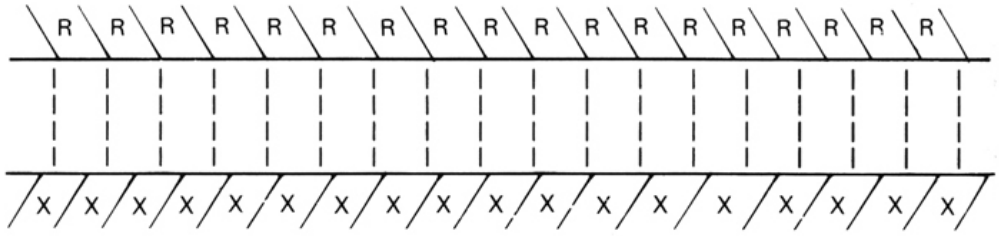

Figure 2.13: Schematic of chemical bonding, where R and X represent compatible chemical groups [28].

Reaction or Interdiffusion Bonding

Atoms and molecules of the fibre and matrix may interact or interdiffuse at the interface to give reaction or interdiffusion bonding. For interfaces involving polymers, reaction bonding may take place when polymer chains from each component entangle and intertwine together (Figure 2.14). The strength of this bonding mechanism depends on the distance over which the chains are entwined, the degree of entanglement and the number of chains per unit of area.

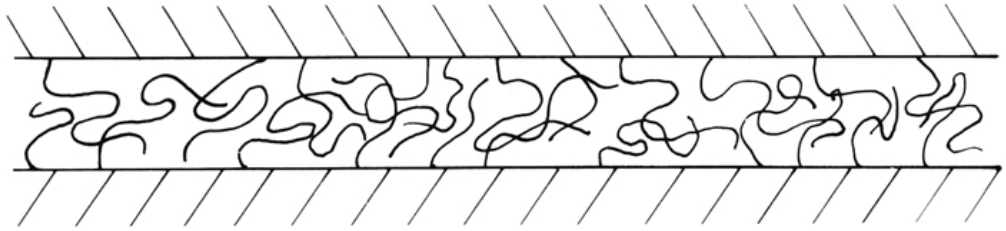

Figure 2.14: Schematic of reaction bonding involving polymers [28].

2.4 Treatments of Natural Fibre and Matrix

The natural fibre surface comprise of a complex heterogeneous arrangement of polymer including cellulose, hemicellulose and lignin and other non-cellulosic compounds. The natural fibre surface is influenced by polymer morphology, extractive chemicals and processing conditions. Natural fibre surface treatment generally involves imparting an altered surface chemistry and creates beneficial microtopographical features without a deliberate coating of the surface. In most cases, effective surface treatments not only remove native surface material and leave behind more active function group to promote wetting, but also roughen the surface to some degree, therefore increasing surface area [27], and potentially enhance mechanical interlocking. From a composite processing viewpoint, the use of a surface treatment is desirable to promote wettability and increase the interfacial bonding between matrix and fibre.

2.4.1 Hemp Fibre Treatment

Hemp fibre treatments are performed with the purpose of separating individual fibres from their fibre bundles, removing non-cellulosic compounds and increasing the fibre surface roughness [13][29]. Hemp fibre treatments used currently are described in the following sections.

2.4.1.1 Dew and Tank Retting

Dew and tank retting are commonly applied retting processes. During dew retting, hemp stalks should remain on the field for 3 to 6 weeks until microorganisms have separated the fibres from their bundles. Dew retting is a weather-dependent and time-consuming process resulting in variable fibre. The tank retting method utilizes anaerobic bacteria and fungi that break down the pectin of fibre bundles submerged in huge water tanks. Tank retting is a quicker method of retting (1 or 2 weeks) and produces uniform high-quality hemp fibres. However, the process results in waste water with a high oxygen demand and is therefore questionable from an ecological point of view. Both dew and tank retting are based on extensive manual work [29].

2.4.1.2 Bag Retting

It has been reported that separation of green decorticated hemp fibre bundles can be achieved by bag retting [8], in which fresh hemp fibre bundles are maintained in a closed plastic bag for a period of time. Bacteria and fungi already present in the fresh green hemp fibre produce enzymes which remove non-cellulosic compounds of hemp fibre and modify the surface of hemp fibre as well. An advantage of bag retting is that the fibres are protected from other environmental factors. A further advantage in the case of bag retting is that it produces high-quality hemp fibres. In addition, bag retting has the potential of significantly reduced water pollution compared to tank retting.

2.4.1.3 White Rot Fungi Treatment

Fungi can be classified into four groups, *basidiomycetes*, *ascomycetes*, *zygomcetes* and *deuteromycotes* based upon their reproduction structure. Only white rot fungi which belong to the *basidiomycetes* groups have the ability to selectively degrade lignin at a faster rate than they degrade cellulose [30]. White rot fungi produce

extracellular oxidases that act on the lignin molecule. This enzyme action enables these fungi to degrade not only lignin, but also an extensive range of other non-lignin related aromatic and non-aromatic compounds [30]. The most important lignin degrading enzymes are lignin peroxidases (LiP), manganese peroxidases (MnP) and laccases [31][32][33]. In addition, fungi produce an extensive system of hyphae (Figures 2.15), which possibly roughen the surface of hemp fibres. Therefore, there is the potential for white rot fungi to be selected to remove non-cellulosic components, and modify the hemp fibre wall and improve fibre/matrix interfacial boding.

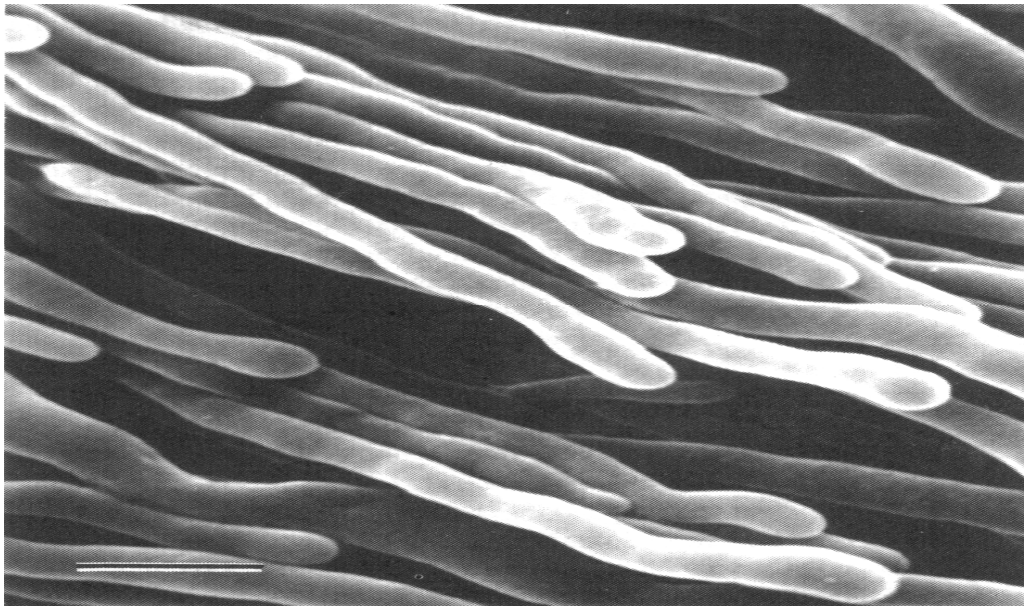

Figure 2.15: Scanning electron micrograph (SEM) of the tips of a number of hyphae[33]. Bar = 5μm

The important factors affecting white rot fungi growth are temperature, sources of carbon and nitrogen, oxygen, moisture and the pH. The majority of white rot fungi grow between 5°C and 37°C, with an optimum temperature of 25±30°C. White rot fungi require a carbon source and nitrogen for their growth. Carbon serves primarily as an energy source for the white rot fungi. Nitrogen is needed for

fungal growth because it is a component of the proteins, nucleic acids, and amino acids; however, the majority of white rot fungi grow at low nitrogen levels. White rot fungi are aerobic microorganisms, and thus need the presence of sufficient oxygen (aerobic conditions) to grow. White rot fungi are able to use organic molecules which dissolve in water. If the moisture content falls below a critical level, microbial activity will decrease and the microbes will become dormant. On the other hand, too high a moisture content can cause a lack of aeration and the leaching of nutrients. Most studies use a moisture content of 60-70% for white rot fungi growing on non-wood fibre. Although white rot fungi tolerate a wide range of pH, they prefer an acidic environment and do not grow well above pH 7.5. Table 2.6 shows the optimum conditions for white rot fungi growth [31][34][35][36][37].

Table 2.6: Summary of factors affecting white rot fungi growth on non-wood fibre

Factors	Optimum conditions
Temperature (^{0}C)	25-30
Carbon	Sufficient
Nitrogen	Low level
Oxygen	Sufficient
Moisture content (%)	60-70
pH value	Wide range, but prefer acidic environment

2.4.1.4 Alkali Treatments

Alkali treatment is one the most popularity applied chemical treatments. Alkali treatment can selectively degrade lignin, pectin and hemicellulose in the fibre wall, while having little effect on the cellulose components. Furthermore, alkali treatment also results in a rougher fibre topography, which improves interfacial bonding by mechanical interlocking [38][39]. However, alkali treatment is now

falling out of favour mainly on environmental grounds and the high cost of chemical. The cost of the fibre used for composites must be relatively low, which makes the use of chemical methods uneconomical.

2.4.1.5 Chelator/Enzyme Treatments

Some published reports have described the effect of enzymatic degradation of non-cellulosic compounds on hemp fibres [10][11]. Pectinases degrade pectin and laccases modify lignin. However, waxes and other non-cellulosic compounds can be a barrier to these enzymes. In order to achieve good results, these enzyme treatments have been preceded by pre-treatments such as chelator treatments with EDTA [12].

2.4.1.5.1 EDTA and EDTMPA

Chelating agents are organic compounds capable of forming covalent bonds with metals through two or more of their atoms. It has been reported that some chelators such as EDTA (Ethylene Diamine Tetra-acetic Acid) can remove calcium ions from pectin in plant cell walls such as in hemp fibres [12], resulting in the pectin becoming soluble in many liquids. This allows the hemp fibres to separate from their bundles. However, EDTA persists in the environment and due to its strong metal chelating properties, enhances the mobility and bioavailability of contaminant heavy metals. An alternative is EDTMPA (Ethylene Diamine Tetra Methylene Phosphonic Acid), a phosphonated analogue of EDTA. EDTMPA has a very strong interaction with all mineral surfaces [40], so it is easily removed from technical and natural systems. Due to this strong adsorption, little or no remobilization of metals occurs. Therefore, compared to EDTA, EDTMPA has less impact on the environment.

2.4.1.5.2 Pectinase Treatment

Pectinases can be broadly classified into acidic and alkaline pectinases based on their pH requirement for optimum enzymatic activity. Alkaline pectinases, which come mostly from bacterial sources, are capable of degrading pectin in the middle lamella of a fibre cell wall. They are widely used in the separation of bundles in crops such as flax, hemp and jute to obtain fibres [10].

2.4.1.5.3 Laccase Treatment

Laccases are one of most important lignin degrading enzymes. It has been reported that laccase alone cannot depolymerise lignin [11], but, when HBT (1-hydroxybenzotriazole hydrate) is used as a mediator, a degree of delignification up to 40% has been obtained. The mechanism of laccase-mediator systems, involves the oxidation of the mediator by laccase, followed by the oxidation of lignin by the low-molecular weight oxidized mediator, which can diffuse into the structure to oxidise the lignin molecule.

2.4.2 Matrix Treatment

Cellulose fibres are polar and inherently incompatible with hydrophobic polymers. There is the potential to increase compatibility by introducing a third material into the matrix that has properties intermediate between those of the other two [41]. Alternatives include coupling agents, compatibilizers and dispersing agents. Compatibilizers are chemicals that lower the surface energy of the fibre to reduce polarity and therefore increase compatibility with the thermoplastic matrix. Dispersing agents are used to improve the dispersibility of the fibres in the matrix. Coupling agents are used to improve the adhesion between the reinforcing fibres and the matrix. The most popular matrix treatments include the use of anhydrides and anhydride-modified copolymers and silane.

2.4.2.1 Maleic Anhydride Grafted Polypropylene (MAPP)

MAPP (shown in Figure 2.16) is a popular coupling agent in natural fibre reinforced plastic composites. Maleic anhydride contains one carbon-carbon double bond (-C=C-) and two carboxylate groups (-COO-). The MA functional group interacts strongly with the fibre surface through covalent and hydrogen bonding with the reactive OH groups on the surface of the cellulose and lignin (see Figure 2.17). The polymer chains of MAPP form a bond with the polypropylene matrix by means of chain entanglement. Therefore, MAPP acts as a bridge between the non-polar polypropylene matrix and the polar fibres [6]. Figure 2.18 shows the influence of MAPP in composite. Figure 2.18a shows poor bonding between fibre and matrix, while Figure 2.18b shows good interfacial bonding due to the addition of 3% MAPP for hemp fibre reinforced polypropylene composites [18].

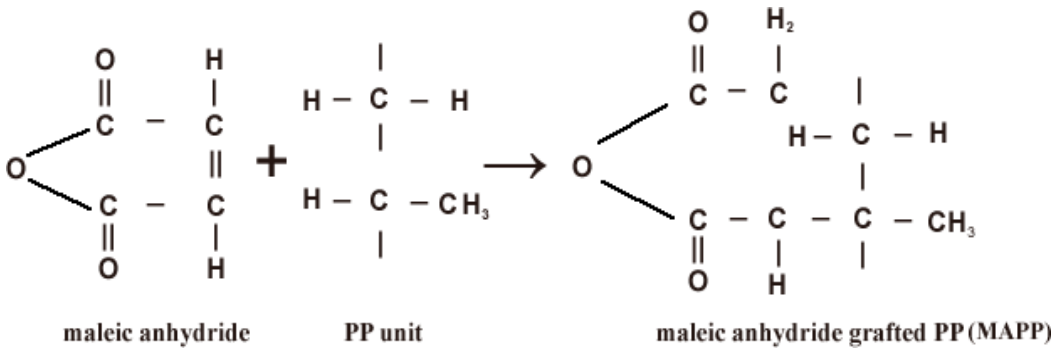

Figure 2.16: Maleic anhydride grafted PP

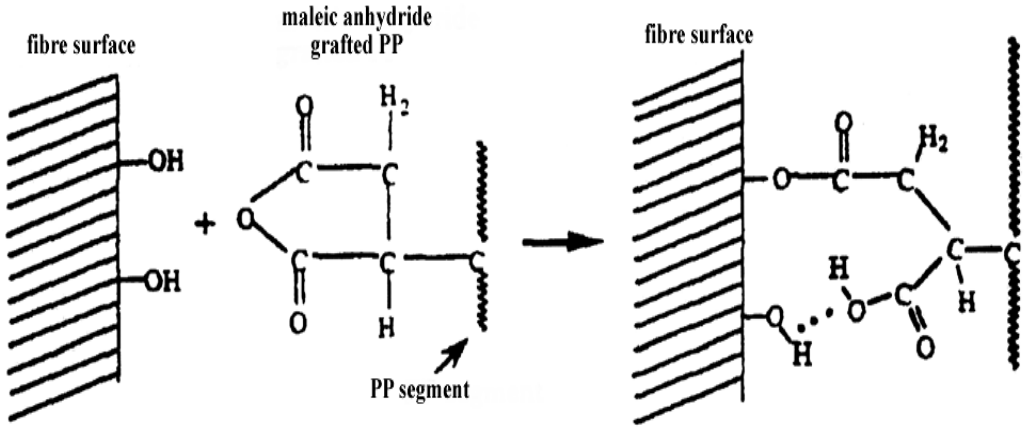

Figure 2.17: Reaction mechanisms of MAPP with the cellulose fibre surface

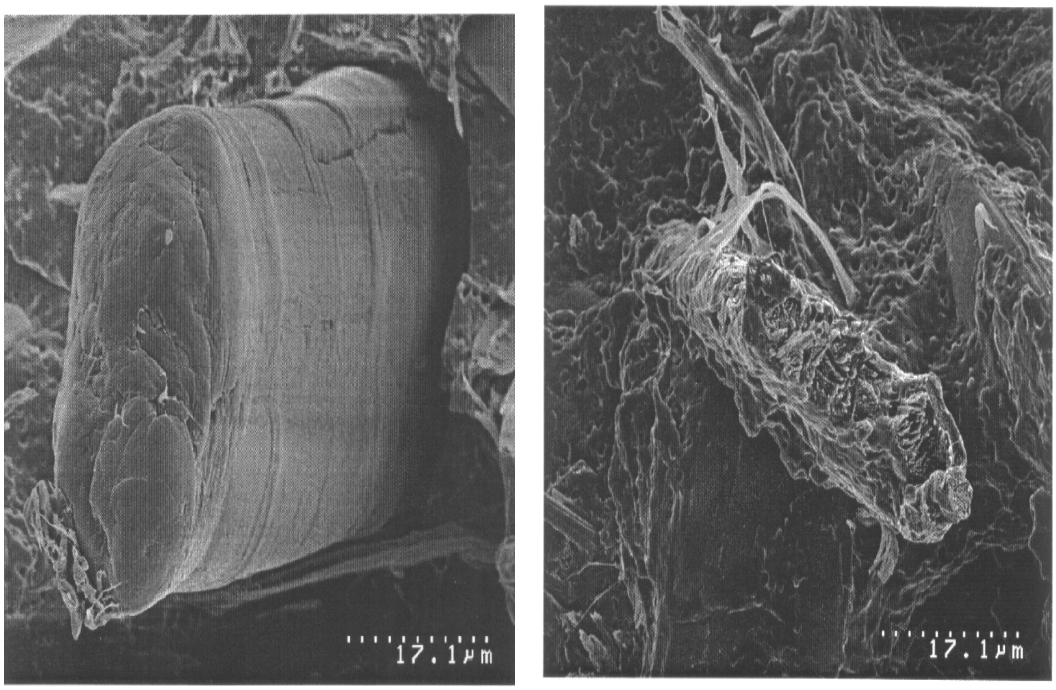

a. b.

Figure 2.18: Fracture surfaces showing the influence of MAPP in composites [18]

2.4.2.2 Silane Treatment

Several theories have been proposed to explain the interfacial bonding mechanisms of silane coupling agents. Among these, the most widely accepted is one based on chemical bonding. In this chemical bonding theory, the bifunctional silane molecules act as a link between the matrix and the cellulose by forming a chemical bond [7]. Silane-based coupling agents are hydrophilic compounds based on a silicon molecule with different organic groups attached. One group interacts with the hydrophilic cellulose fibres, while another group interacts with the hydrophobic thermoplastic matrix material. Therefore, hydrophilic and hydrophobic materials can be coupled together with the silane coupling agent acting as a bridge between them [42].

The reaction between cellulosic materials and silanes is not simple. It has been reported that application of alkyl-functional silanes did not lead to chemical bonds between the cellulose fibres and the polypropylene. However, it appeared that the long hydrocarbon chains caused by the silane application influence the wettability of the fibres and that the chemically affinity to the polypropylene is improved [41]. Hydrogen bonds as well as covalent bonding mechanisms have been found in the flax- silane system [41] hence influencing the strength of its composites.

2.5 Analytical Techniques for Natural Fibres

Due to the structural and chemical complexity of natural fibre, a combination of several destructive and non-destructive techniques each providing partial but complementary information are desirable in order to assess fibre modification. Several physical techniques, such as wet chemical analysis, FT-IR, SEM, lignin testing, XRD, thermal analysis, and zeta potential are suitable for analyzing natural fibre.

2.5.1 Wet Chemical Analysis of Hemp Fibre

There are several methods to measure the chemical compounds of bast fibre, amongst the GB 5881-86 (National Standard of China for Ramie Chemical Analysis) is one of most suitable methods to be used for hemp fibre chemical analysis. This gravimetric method involves the degradation and extraction of wax, water-soluble components, pectin and hemicellulose in the hemp fibres. The residual part is almost pure cellulose with a low content of minerals, which can be used as the amount of cellulose approximately. The wax is extracted in a benzene/ethanol (2:1) solution, water-soluble components in water, pectin in 5g/l ammonium oxalate solution and hemicellulose in 20g/l NaOH (sodium hydroxide) solution, consecutively. The loss of dry matter equals the removed content in the sample. The lignin analysis is carried out with sulphuric acid treatment; the residue after wax extraction is treated with 72% sulphuric acid for 24h, and then boiled in water, washed, filtered and dried. The remaining compound is assumed to be lignin.

2.5.2 Fourier-Transform Infrared (FT-IR) Analysis of Hemp Fibre

Fourier-transform infrared (FT-IR) can highlight changes in the main non-cellulosic compounds in cellulose fibres by characterizing the carboxyl acids and esters that are present in pectin, lignin, hemicellulose and waxes, which do not exist in the cellulose structure [43]. The absorbance intensity of the characteristic peaks at around 1736 cm^{-1} in the FT-IR spectrum of cellulose fibre is attributable to the presence of the carboxylic ester in pectin and wax and the peak at 1268cm^{-1} for COO stretching in lignin [43][44].

2.5.3 Scanning Electron Microscopy (SEM)

Composite properties are highly dependent on the surface state of fibres. Increased roughness of fibre surfaces has the potential to improve the bonding between the fibre and matrix. SEM is an excellent technique for the examination

of surface morphology of fibres and failure analysis due to its high depth of resolution. SEM can also indicate the presence of lignin, wax, oil and impurities on fibre surfaces. Removal of these from the surface that can occur with chemical treatments can be assessed [9]. The resolution of the conventional SEM is inadequate to detect fine holes caused by fungal hyphae attacking fibre walls on treated fibre surfaces. However, some researchers have used High-resolution Cryo-Field Emission Scanning Electron Microscopy (HR-Cryo-FE-SEM) to reveal fungal hyphae attacking fibre walls producing fine holes on the fibre surfaces (see Figure 2.19).

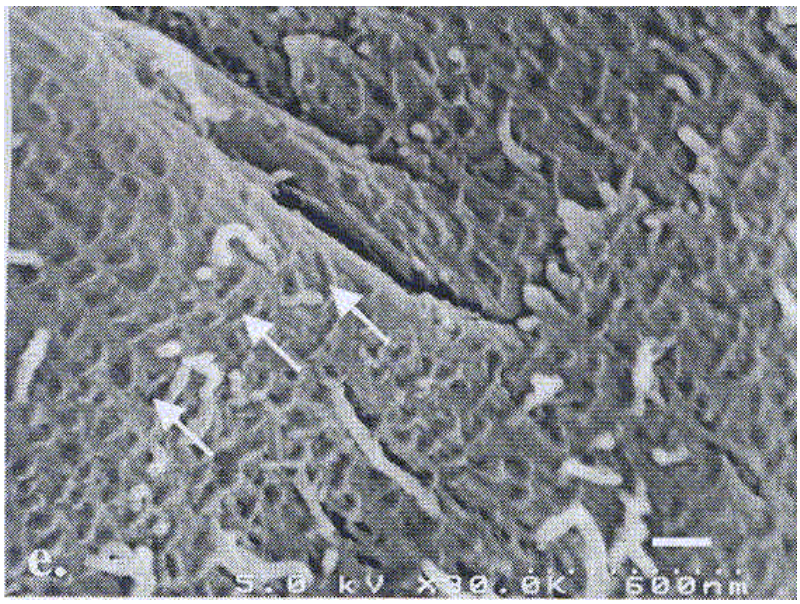

Figure 2.19: HR-Cryo-FE-SEM and TEM micrograph shows fungal hyphae make fine holes on the fibre surface [9]

2.5.4 X-ray Diffraction

X-ray diffraction (XRD) is an extremely powerful analytical technique for both qualitative and quantitative studies of structural properties of engineering materials. Figure 2.20 shows a typical X-ray system that is mainly comprised of an X-ray tube and two goniometers which are equipped with a scanning radiation

counter that monitors the diffracted beam intensity. Generally the material being analysed is converted into a powder from which the X-ray patterns or "powder patterns" are used for comparison against a large collection of known diffraction patterns (The Powder Diffraction File, including over 70,000 powder diffraction patterns catalogued by the International Centre for Diffraction Data-ICDD). The comparison of an experimental diffraction pattern with the database of known diffraction patterns can be done in a few seconds with "search/match" computer software and, through the unique relationship between such patterns and crystal structures, provides a chemical identification of powders.

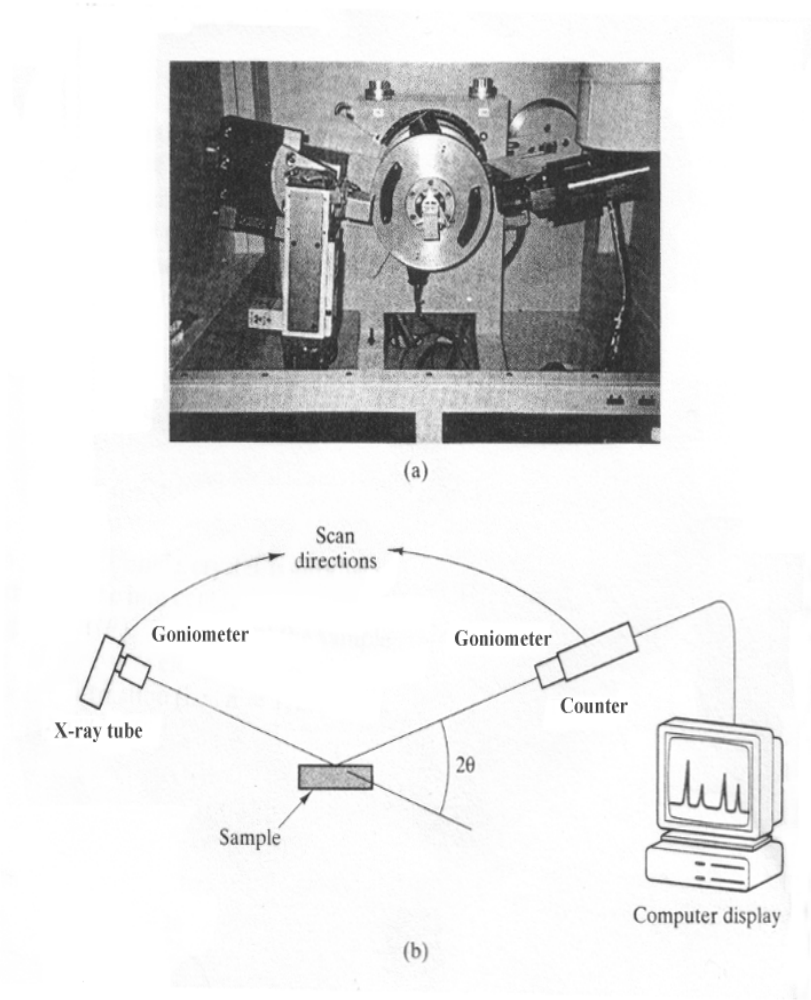

Figure 2.20: Typical X-ray system

2.5.4.1 Crystalline Cellulose

The chemical composition of hemp consists mainly of cellulose, hemicelluloses, lignin and pectin. Cellulose is usually composed of crystalline segments alternating with regions of amorphous cellulose. Most plant-derived cellulose is highly crystalline and may contain as much as 80% crystalline cellulose [46]. All the other components such as hemicelluloses, lignin and pectin are totally amorphous for which, therefore, X-ray analysis is unsuitable [45].

There are four types of crystalline cellulose, namely types I, II, III and IV, type I being unmodified native cellulose and the others forming on exposure to different chemical conditions. For cellulose I, the major diffraction planes are the $(1\bar{1}0)$, (110), and (200) planes with corresponding X-ray 2θ diffraction angles of 15.1, 16.88 and 22.82^{o} [47]. Treatment such as those using harsh alkali solutions can break down cellulose I to cellulose II (major diffraction planes at (110), $(1\bar{1}0)$, (012) and (020) for 2θ angle of 14.8, 16.7, 20.7 and 22.5^{o}) [48]. Cellulose III which can be obtained from cellulose I and II is formed after treating the cellulose with liquid ammonia. Cellulose IV which can be obtainable from Cellulose I, II and III is formed by treating stretched cellulose fibres in a hot bath [46] [49].

It has been mentioned that when the cellulose content is high, as is in the case of alkali treated fibres, two peaks (see Figure 2.21) can be observed at 2θ angles of 15.1 and 16.8, but when the fibres contain high amounts of amorphous materials such as lignin, hemicellulose, and amorphous cellulose, as for the untreated fibres, these two peaks are smeared, thus appearing as one broad peak [47].

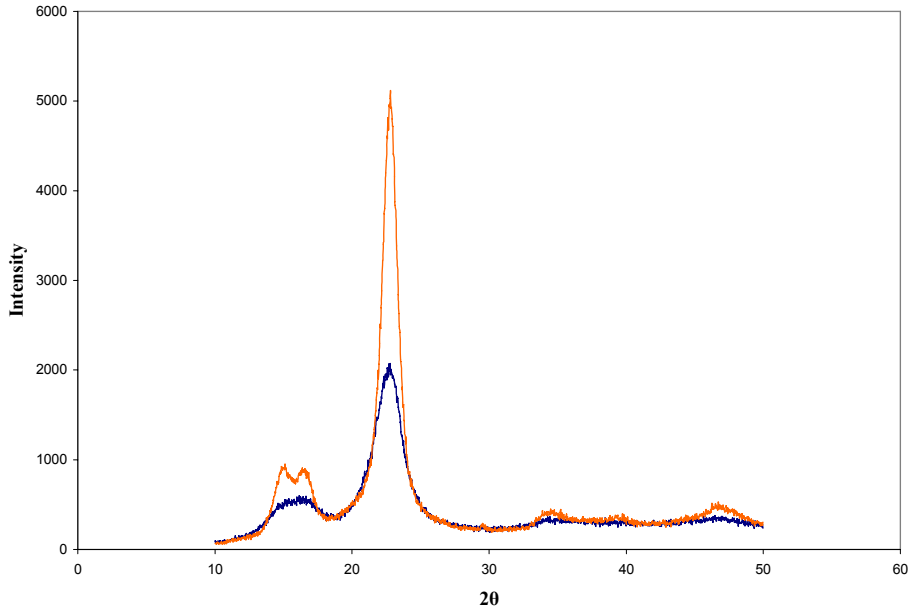

Figure 2.21: X-ray diffractograms of untreated and alkali treated fibre [47]

2.5.4.2 Crystallinity Index of Fibre

The crystallinity index (CrI) of the fibres can be calculated according to the Segal empirical method developed in 1959 for native cellulose, defined as:

$$CrI = \frac{I_{002} - I_{am}}{I_{002}} \times 100 \qquad (3)$$

where I_{002} is the intensity for the crystalline peak between 22^0 and 23^0 for cellulose I relating to the (200) plane, which is considered to represent the crystalline material in cellulose. I_{am} is the intensity between 18 and 19^o for cellulose I (and between 13 and 15^o for cellulose II) [50], which corresponds to the amorphous material in cellulose [51].

2.5.4.3 The Effect of Crystallinity on Fibre Properties

A number of properties are affected by fibre cellulose crystallinity. Amorphous cellulose is more accessible to chemicals and water than crystalline cellulose and so amorphous cellulose absorb more of these than crystalline cellulose [50]. The

mechanical properties of cellulose fibres are also related to their crystallinity. Tensile strength, Young's modulus and hardness increase whilst flexibility decreases with increasing crystallinity [52].

2.5.5 Measurement of Fibre Density

The density of matrix and composite samples can be readily determined because of their massive and solid forms, but the density of the fine and porous fibres is far more problematic to determine accurately. However, it has been reported that the Archimedes test using canola oil as an immersion fluid is a simple and effective method for measuring natural fibre density [53]. The published values of hemp fibre density are around 1.48g/cm^3 [3] with the density of crystalline cellulose (around 1.64g/cm^3) higher than the density of hemicellulose, lignin and amorphous cellulose (conservatively all assumed to be 1.40g/cm^3)[20].

2.5.6 Thermal Analysis

Most research into hemp fibre has been concerned with composite manufacture and structural characteristics, but little information is available about the properties of the fibre, especially its thermal stability, despite the fact that hemp fibres are subjected to extensive heat treatment during processing.

Thermal analysis is the term applied to a group of methods and techniques in which a physical property of a substance is measured as a function of temperature, whilst the substance is subjected to a controlled temperature programme.

2.5.6.1 DTA and TGA

Differential thermal analysis (DTA) and thermogravimetric analysis (TGA) are the most widely used thermal analysis techniques. DTA is a method which obtains information on temperature changes in a sample by heating or cooling it alongside an inert reference. TGA can be employed to monitor the weight loss of a material

as the material is heated, cooled, or held isothermally. Figure 2.22 is a schematic representation of the main parts of an instrument. The sample and reference are contained in the DTA/TGA cell. Temperature sensors and the means of heating the sample and reference are incorporated into the cell. A computer unit operates the various control functions, data capture and analysis. The term "differential" emphasizes an important feature of the techniques: two identical measuring sensors are used, one for the sample and one for the reference, and the signal from the instrument depends on the difference between the response of the two sensors in this way, the signal represents the thermal change to be studied free from diverse thermal effects which influence both sensors equally.

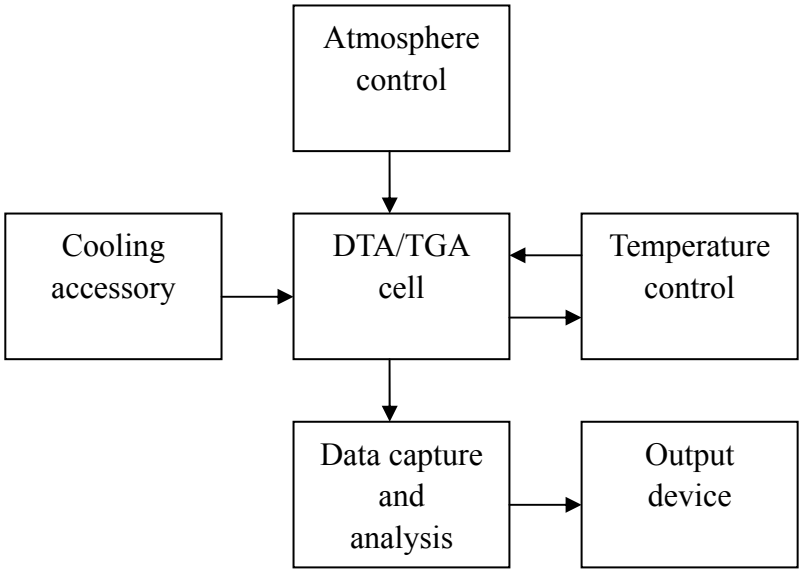

Figure 2.22: Schematic representation of a DTA/TGA instrument [54]

DTA finds application in the measurement of characteristic temperatures and in the qualitative identification of materials. This technique can be used reliably up to temperatures around 1600^{o}C. The results from DTA experiments are displayed as a thermal analysis curve in which the instrument signal is plotted against temperature – usually the sample temperature. Of particular importance is the

"extrapolated onset temperature" which is defined as the temperature of the intersection between the extrapolated initial base line and the tangent or line through the linear section of the leading edge of the peak. This temperature, rather than the peak maximum temperature is frequently used to characterise peaks because it is much less affected by the heating rate. [54]

TGA is one of the most widely used techniques to monitor the composition and structural dependence on the thermal degradation of natural cellulose fibre. This is because the different compositions and supramolecular structures of cellulose behave differently when undergoing thermal degradation. [48].

2.5.6.2 Activation Energy

The Broido method can be used to calculate kinetic parameters from TGA curves. The equation used is given below: [55][56]

$$\ln\left[\ln\left(\frac{1}{y}\right)\right] = -\frac{E}{R}\frac{1}{T} + \ln\left[\frac{R}{E}\frac{Z}{\beta}T_m^2\right] \tag{4}$$

where T is the temperature of maximum reaction velocity, β is the rate of heating (K min^{-1}), and T_m is the temperature at maximum reaction rate (temperatures all expressed in Kelvin). Z is the frequency factor, E the activation energy and y is the fraction of number of initial molecules not yet decomposed which can be determined from the expression

$$y = \frac{N}{N_0} = \frac{W_t - W_f}{W_0 - W_f} \tag{5}$$

where N_0 and N are the initial number of molecules, and the number at any time t respectively, W_0, W, and W_f are the weight initially, at any time t, and final weight respectively. Using the Broido equation, plots of $(\ln\ln 1/y)$ versus $1/T$ for various stages of thermal degradation can be plotted and the activation

energies calculated from the slopes of these plots.

2.5.6.3 Thermal Stability of Hemp Fibre

Bast hemp fibres have been found to contain a large amount of pectin and hemicelluloses with only a small amount of lignin [48]. These chemicals are not thermally stable and tend to degrade at an early stage of heating. It has been reported that hemicelluloses are less thermally stable than cellulose and lignin, therefore, their active degradation begins at a lower temperature [57] [58]. Lignin degrades at a temperature around 200°C while cellulose degrades at higher temperatures. Therefore, exothermic peaks in natural fibre higher than 200°C, indicate the decomposition of cellulose in the fibres [59] [60]. Decomposition reactions take place primarily in the amorphous regions of the cellulose [61]. Consequently, lower crystallinity of fibre leads to lower initial temperatures of decomposition, lower thermal stabilities and lower activation energies.

2.5.7 Zeta Potential

Zeta potential is an electrokinetic parameter giving information about the charge associated with surfaces. It can be used to assess chemical changes such as increased hydrophilicity or hydrophobicity. As the zeta potential cannot be directly measured, it has to be calculated from other measurable variables. The streaming potential method for determination of zeta potential is one of the most common methods used to characterise the surface of cellulose fibres. In order to understand zeta potential, the electric double layer has to be introduced.

2.5.7.1 The Electric Double Layer

The surfaces of materials have unsymmetrical or unbalanced molecular forces and are thus, much more reactive than their interiors. When particles of a solid are sufficiently small, they remain separated, and suspended in a liquid (a suspension). These particles are usually electrically charged to some extent, either positively or

negatively. This charge arises from the ionization of molecules on any surface, with separated ions going into the liquid, or by the capture or adsorption of positive ions (cations) or negative ions (anions) from the surrounding liquid [62].

When a solid is immersed in a liquid, the ions formed on the surface of the solid attract oppositely charged ions called counterions from the liquid. A layer of highly consolidated counterions, which may include adsorbed ions, form around the particle, but do not completely neutralize the charge of the particle. This compact layer is commonly called the Stern layer (see Figure 2.23). The plane through the centre of the Stern layer is called the Stern plane. Further away from the particle, there is a more diffuse region of charge called the diffuse layer which finally neutralizes the charge of the particle. Together the strongly attracted initial layer and the diffuse layer make up the double layer.

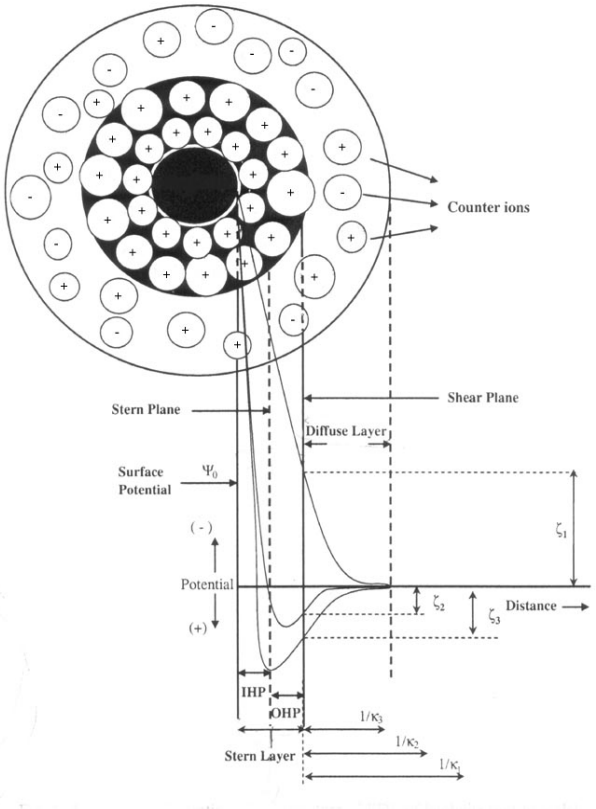

Figure 2.23: A schematic of the structure of the electric double layer [62]

2.5.7.2 Shear Plane, Zeta Potential and Isoelectric Point (IEP)

The Stern layer is generally considered to be rigidly attached to the solid, while the diffuse layer is not. When there is motion of the solution relative to the solid surface, shear is considered to occur at a plane close to the boundary between the Stern and diffuse layers [62]. In actual fact, the precise position of the shear plane in the diffuse double layer where this occurs has not yet been identified [63]; it is considered to be located somewhere between the Stern plane and the inner section of the diffuse layer. The zeta potential is the potential at the shear plane which is related to the mobility of the solid [64]. The zeta potential is also related to the pH of the surrounding medium. When acid is slowly added to a liquid in which a negatively charged solid is immersed, the outer surface of the positively charged layer moves nearer the surface of the solid, until the original electro-chemical charge is neutralized. Then the zeta potential becomes zero, and the pH is called the isoelectric point (IEP) [64].

The IEP, at which the zeta potential is 0, can be used to determine the surface chemistry by the shift in the IEP after a reaction. For example, a shift to a lower pH for cellulose indicates that more hydroxyl groups are available for bonding. Therefore, the IEP can indicate whether a material has become more hydrophilic or hydrophobic [64] [65]. A more negative zeta potential suggests increased hydrophilicity.

2.5.7.3 The Cellulose Fibre Surface

Cellulose fibres in an aqueous medium are negatively charged due to their characteristic hydroxyl groups. The hydroxyl groups enable the formation of hydrogen bonds in the interface region of composite materials; however, in order to get access to these hydroxyl groups, a cover of non-cellulosic compounds such as pectin and other waxy substances must be removed from the fibre surface. The degradation and removal of specific non-cellulosic compounds which cover the

primary wall of the cellulose polymer changes the surface charge. A typical plot of zeta potential for cellulose fibre is shown in Figure 2.24 [62]. Commonly there is a plateau at the higher end of the pH range. Removal of non-cellulosic compounds is clearly shown by a plateau with increasingly negative zeta potential [64]. The zeta potential is found to be mainly influenced by waxes, for which removal largely decreases the negative zeta potential [66].

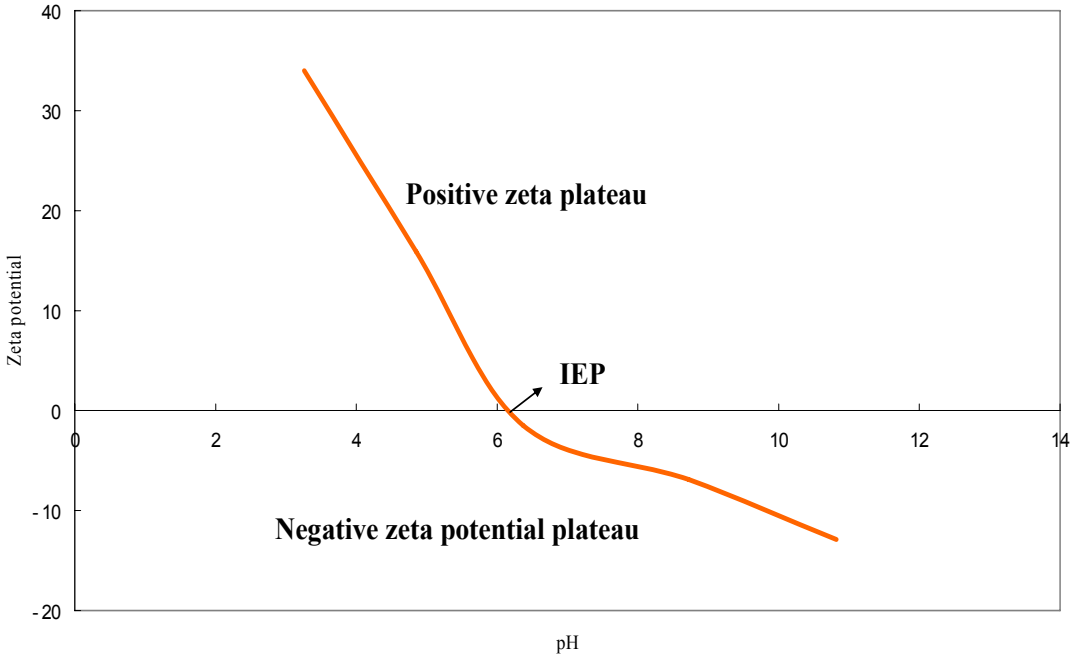

Figure 2.24: A typical plot of zeta potential versus pH for cellulose fibre

The characteristics of cellulose fibres, including reactivity as well as thermal and mechanical properties largely depend on the size of the cellulose crystallites and its amorphous regions, as well as surface morphology [65]. The amorphous cellulose regions have a lower frequency of linear-chain hydrogen bonding, thus exposing reactive inter-chain hydroxyl groups (OH) to bonding with water molecules. Crystalline cellulose on the other hand is highly packed, and very few accessible inter-chain OH groups are available for bonding with water and

therefore a higher tendency to bond with water. Amorphous cellulose can therefore be considered more hydrophilic than crystalline cellulose. Reduced degrees of crystallinity also allow increased swelling on exposure to water and which causes further reduction of the zeta potential [65]. Increased roughness associated with increased surface free energy tends to reduce the zeta potential.

2.5.7.4 Fungi Treated Cellulose Fibre

Fungi treatment can be used to remove non-cellulosic components due to the action of specific enzymes produced by the fungi. The degradation of waxes by the enzyme lipase has been seen to reduce zeta potential [64]. It has been reported that white rot fungi not only removes lignin but also waxes [23] which could cause a further reduction of zeta potential. It has also been reported that application of an enzyme mixture containing xylanase, pectinase, and lipase can lead to the most negative zeta potentials indicating the most complete removal of the non-cellulosic materials compound [66].

2.6 Processing of Fibre Thermoplastic Composites

The key problem with processing of thermoplastic composites lies in the effective impregnation of fibre with a thermoplastic matrix. Thermoplastic composite manufacturing processing can be grouped into short-fibre suspension methods and squeeze flow methods according to dominant flow processes (see figure 2.25)[67][68].

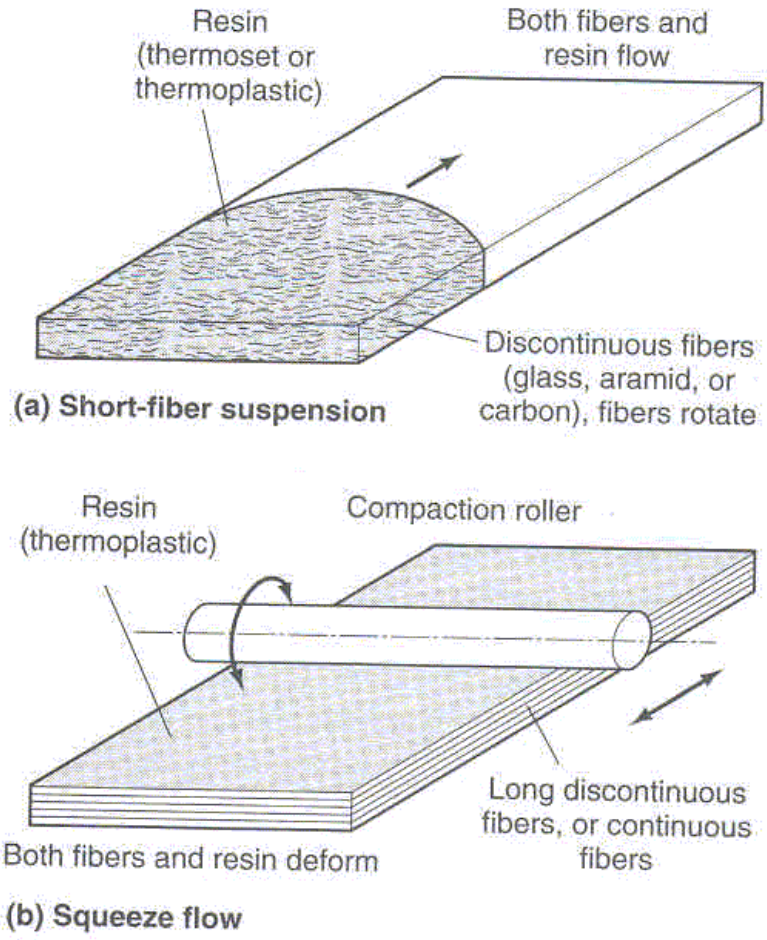

Figure 2.25: Types of flow in thermoplastic composites processing [68]

In the short fibre suspension method, the short fibres in the molten deforming matrix can travel large distances which allows them to obtain good impregnation. Fast and efficient moulding techniques such as extrusion and injection moulding have been commonly adopted by the plastics manufacturing industry to fabricate short fibre thermoplastic composites. In squeeze flow methods, the long or aligned fibre remains generally stationary and the matrix is introduced by flow or is dispersed in solid form prior to flow. Fabrication methods such as film-stacking and hot-pressing fall into this category.

2.6.1 Short Natural Fibre Reinforced Composites

Short fibre composites have lower mechanical properties, but are cheaper and easier to fabricate than their long fibre counterparts. The fibre length, fibre orientation and fibre volume fraction are important parameters that influence the mechanical behaviour of short cellulose fibre composites.

Fibre Length

In a composite, there is a critical fibre length required for the fibre to develop its fully stressed condition [69]. This length is not only determined by fibre and matrix properties, but also by the quality of the fibre/matrix interface. Load is transferred from the fibre to the matrix by shear along the interface. If the fibres are too short, the stress transfer area will be too small for them to offer effective reinforcement. However, if they are too long, they may get entangled resulting in clumping and reduced composite efficiency [69]. As fibre lengths are reduced during composite processing, the ultimate fibre lengths present in the composite are dependent on the type of compounding and moulding equipment used [28].

Fibre Orientation

Although the orientation effects for short fibre composites are not generally as marked as continuous fibres, they are not negligible. Short-fibre composites rarely consist of fibres oriented in a single direction. Fibre orientation changes during extrusion and injection moulding processes. These changes are complex, and are related to the size and concentration of fibres, the viscoelastic properties of the melted polymer matrix, the mould cavity and the processing conditions [70]. Figure 2.26 shows changes in fibre orientation during fibre suspension processing.

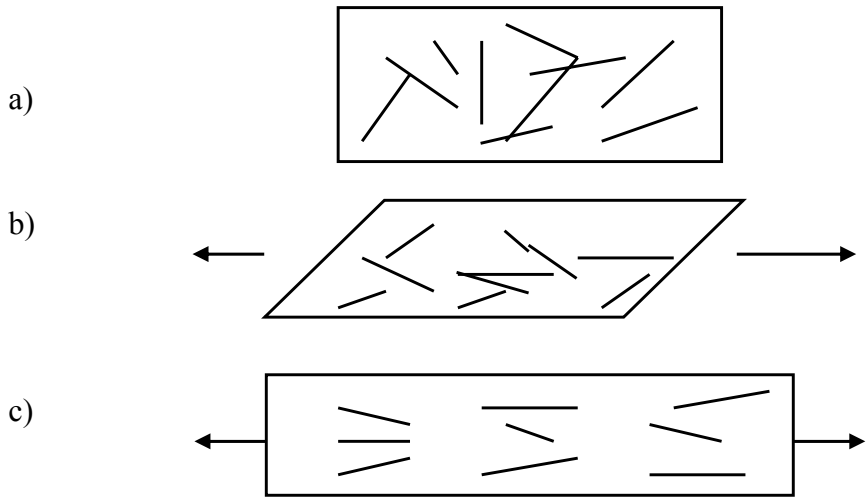

Figure 2.26: Changes in fibre orientation during processing [28] showing (a) Initial random distribution (b) Rotation during shear flow (c) Alignment during elongational flow

Fibre Volume Fraction

The fabrication and properties of fibre composites are strongly influenced by the proportions of the matrix and the fibre. The proportions can be expressed either via the weight fraction, which is relevant to fabrication, or via the volume fraction, which is commonly used in property calculations [28]. At low fibre fractions, a decrease in tensile strength compared to the matrix strength is usually observed. This is due to the introduction of flaws created by the fibre ends. These flaws act as stress concentrators, and cause the bonds between the fibre and matrix to break. At higher volume fractions, the matrix is sufficiently restrained and the stress is more evenly distributed. This results in the reinforcement effect outweighing the effects of the stress concentrations. As the fibre volume fraction is further increased, tensile properties gradually improve until they surpass those of the matrix [18]. Ductility falls with increasing fibre reinforcement. At very high fibre volume fractions, the material properties show greater variability due to fibre clumping [71].

2.6.1.1 Processing of Short Fibre Reinforced Thermoplastic Composites

The most commonly used technique for mixing short fibres with a thermoplastic polymer is extrusion. Injection moulding is the most commonly used composite forming technique, although extrusion is used in some instances.

Extrusion Compounding

Short reinforcing fibres and thermoplastic polymers are mixed and gravity–fed into a screw extruder. Matrix heating and impregnation all depend on the geometry of the screw. The extruder creates a uniform mixture from thermoplastic and short reinforcing fibres. Counter-rotating screws draw the composite melt forward through the extruder barrel. The material then exits the barrel through a shaped die (see Figure 2.27). Extrusion is a continuous process that can have high feed rates allowing the fast and efficient processing of materials. Extrusion using a twin-screw extruder is often carried out prior to injection moulding or compression moulding to achieve good fibre distribution within the matrix.

Processing temperature is an important parameter in extrusion that can affect the composite strength; insufficient wetting of fibre can occur if the temperature is too low, but fibre degradation can occur if the temperature is too high. Both situations result in a weaker composite. Other studies suggest an extrusion temperature of 165-175^{0}C for extruding hemp fibre/PP composites [18].

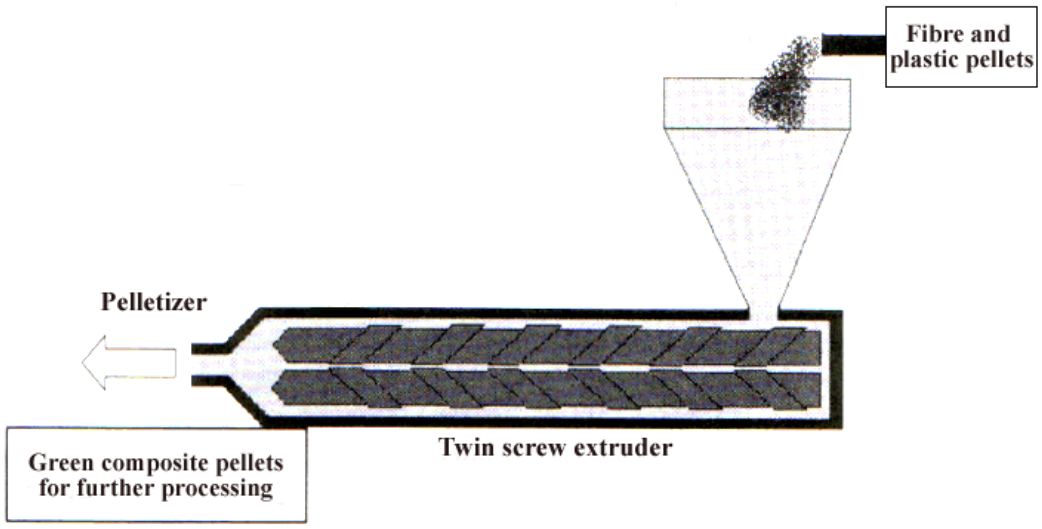

Figure 2.27: Schematic representation of twin screw extruder [4]

Injection Moulding

Injection moulding is one of the few manufacturing processes capable of producing net shape composite parts in high volumes. It is a high-pressure process with machine capital costs and tooling costs generally high compared to the processing routes of other composites. These costs can be recovered through inherent short cycle times, automation, and low labour costs. A recent forecast predicts that this process will be the most important technology for incorporating natural fibre composite materials [72]. Composite materials for injection moulding must be capable of flow under pressure. Therefore, short fibre reinforced thermoplastics with a relatively low fibre fraction (typically <50wt% or 30vol. %) are suitable for injection moulding as it is difficult for high volume fractions to be injection moulded [72][73]. However, too low a fibre fraction does not give sufficient property improvements.

Figure 2.28 shows a schematic diagram of a screw injection moulding machine.

The injection machine melts the pre-formed usually extruded and pelletized composite pellets, delivering a uniform material to the machine nozzle, and injects it into the closed mould. This process is followed by cooling after which the composite can be removed from the mould. Unlike extrusion, injection moulding generally does not significantly damage cellulose-reinforcing fibres [73][74]. Injection temperature can affect the composite property. If the temperature is too high, the fibre in the composite may be burnt, which generally degrades the composite properties. Previous work has highlighted a temperature of 165-175^{0}C for injecting hemp fibre/PP composites [18].

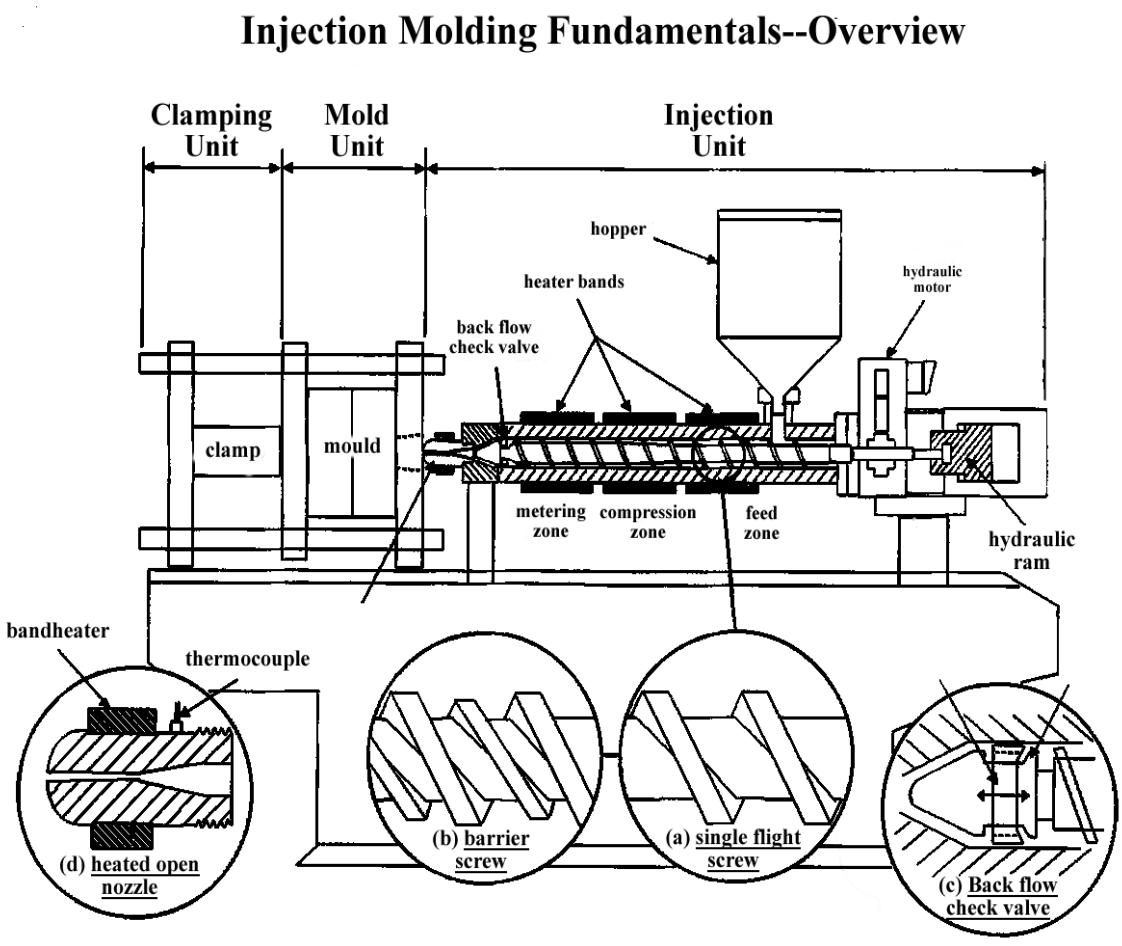

Figure 2.28: Schematic diagram of screw injection moulding machine [73]

2.6.2 Long Aligned Natural Fibre Composites

Long aligned fibre-reinforced composites contain reinforcements having lengths much greater than their cross-sectional dimensions [75][76]. Each layer of a long fibre composite typically has a specific fibre orientation direction. Therefore long fibre composites have high mechanical properties in the fibre direction, but can be very anisotropic depending on the arrangement of individual layers [75].

Fabrication of long fibre or aligned reinforced thermoplastic composites has proved difficult due to the lack of appropriate impregnation methods. However, some techniques have been adapted for processing long fibre thermoplastic composites. Hot-pressing is one of the best methods for manufacturing long fibre thermoplastic composite sheets, in which the fibre may either be completely impregnated with thermoplastic matrix through solvent impregnation, or just physically mixed with matrix through fibre commingling, and then processed by heat and pressure into composites. Solvent impregnation can lead to products of high impregnation quality. However, the main drawback of solvent impregnation is that most thermoplastics require expensive and toxic organic solvents which require removal by evaporation. Thus the process is slow, toxic and expensive. Fibre commingling can provide for effective impregnation, however, thermoplastic fibres represent an added cost [75, 76, and 77].

2.6.2.1 Film Stacking and Hot-Press Forming

A promising alternative for the production of long fibre thermoplastic composite sheet is film stacking and hot–press forming where fibres are stacked in between layers of thermoplastic film and consolidated between heated plates. In this process, most of the impregnation occurs via the flow of thermoplastic through the thickness, so minimizing the ply thickness enhances impregnation. This method is quite common in the use of research and development and could be both cost effective and environmentally friendly for larger scale manufacture [78].

The most important hot-press forming parameters are the forming temperature, forming pressure and heating time. High forming temperature and pressure may cause damage to the fibre as well as leading to matrix starvation due to a high degree of matrix bleed from the mechanically locked fibre. It is reported that the fibre/PP composite sheets can be successfully thermoformed at forming temperature within the range 120-150^{o}C, and forming pressure of 5-10 Pa. The length of the heating time influences the wetting between matrix and fibre. Longer heating time improves the quality of the wetting between matrix and fibre, thus results in the composites having better mechanical properties. Some studies use a 6-10 min heating time for hot pressing fibre/PP composites [77, 78 and 79].

2.7 Composite Interfacial Shear Strength

Since the interface plays a major role in transferring the stress from the matrix to the fibre, it is important to be able to characterise the level of interfacial adhesion to properly understand the performance of the composite. One common parameter for the description of interfacial strength is interfacial shear strength (IFSS). The most commonly used methods for determining IFSS are the single fibre pullout test and the single fibre fragmentation test.

2.7.1 The Single Fibre Pull-Out Test

The single fibre pull-out test is a commonly used technique to measure interfacial shear strength, in which the end of a fibre is embedded in block of matrix that is held as the fibre is pulled out whilst recording load versus displacement to give a "pullout curve"(see Figure 2.29). The single fibre pull-out test offers a number of important practical advantages: firstly, it is a direct measurement of interfacial strength, secondly, it requires only small amounts of fibre and matrix, and thirdly, the debonding force can be plotted as a function of displacement and information

about the failure process can be gained, e.g. a sudden drop in applied load indicates a brittle failure. However, the single fibre pull-out test is based on single fibre specimens and does not reflect the failure process within a composite. Overall though, the IFSS value from the pull-out test is considered to give a good indication of interfacial adhesion for natural fibre composites [80, 81 and 82].

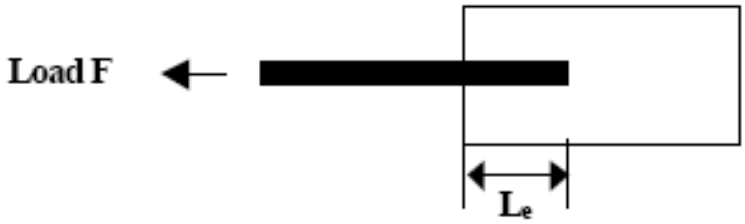

Figure 2.29: Schematic of the single fibre pullout test [18].

A typical force-displacement curve can be seen in Figure 2.30. This can be considered in three parts ($F< F_d$, $F_d < F< F_{max}$ and $F> F_{max}$) corresponding to the different stages involved in pull-out, where F is the applied force, F_d is the critical force at which debonding is initiated, and F_{max} is the peak load. During the first part ($0 < F< F_d$), the curve is considered to represent linear elastic behavior of the fibre-matrix system and the fibre-matrix interface remains intact. For the second stage ($F_d < F< F_{max}$), after initiation, debonding occurs by means of crack propagation along the embedded fibre length. The applied force continues to increase due to the remaining adhesion of the intact part of the interface and the presence of frictional forces between the fibre and matrix. After reaching a peak load (F_{max}), crack propagation becomes unstable and the whole embedded fibre length becomes fully debonded. The third part occurs after complete debonding has taken place, where the remaining force is due to frictional interactions between the fibre and the matrix (F_b). The apparent interfacial shear strength IFSS

(τ) can be calculated using the following equation:

$$\tau = \frac{F_{\max}}{\pi D L_e} \tag{6}$$

where D is the fibre diameter and L_e is the embedded length [80].

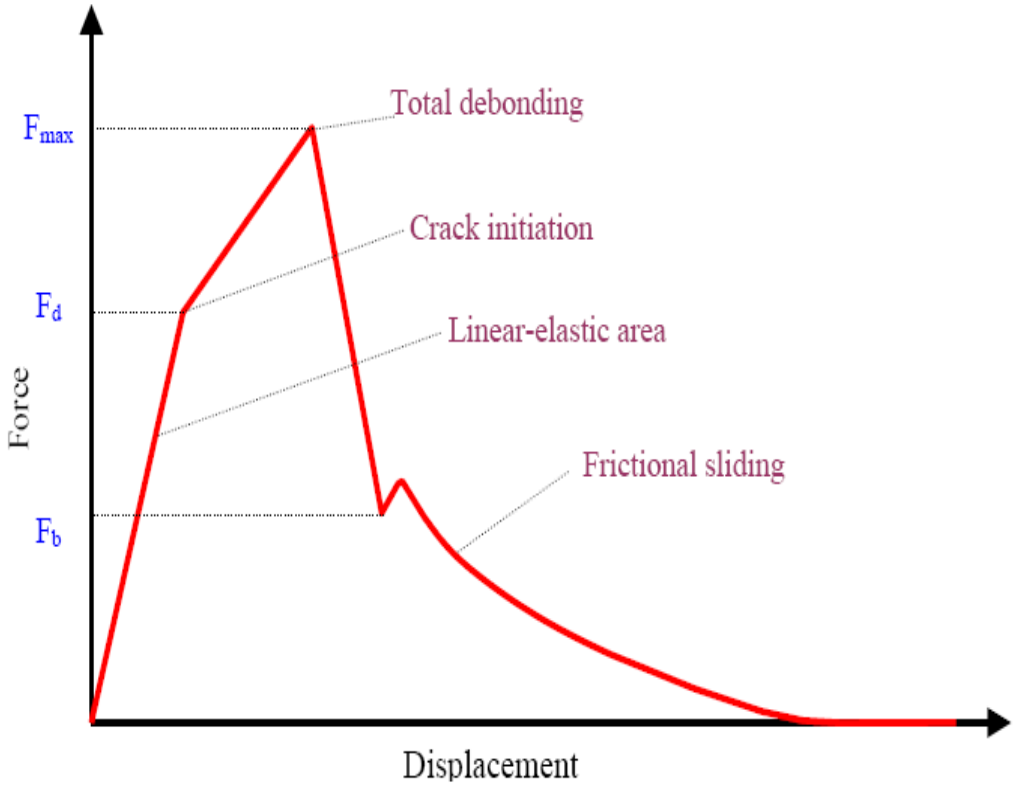

Figure 2.30: Typical force-displacement curve for the single fibre pull-out test [80].

In the single fibre pull-out test, the fibre is subjected to an axial force resulting in a Poisson contraction in the radial direction, leading to a reduction in the fibre cross sectional area. This phenomenon may reduce the normal radial stress induced on the fibre that results from matrix shrinkage during cooling of the matrix after elevated temperature. As a result, a decrease in the frictional

component of the interfacial strength is likely. This may facilitate the initiation and propagation of interfacial failure and reduce the measured IFSS [82]. Furthermore, one basic assumption of the single fibre pull-out test is that there is a constant shear stress at the fibre-matrix interface. In reality, non-linear shear stress occurs at the regions near the fibre ends. Additionally, the load in the pull-out test is an axial force, while the fibres in real composites are not oriented parallel to the applied loads. Therefore, the results obtained from the single fibre pull-out test are limited in their representation for a composite where fibre loading is more complex.

2.7.2 The Single Fibre Fragmentation Test

Another technique commonly used to calculate the IFSS is the single fibre fragmentation test. This test involves the application of increasing axial stress to a specimen containing a single fibre embedded in a polymer matrix (see Figure 2.31a). Load is transferred through the matrix into the fibre by means of shear stress at the interface, and stress transfer increases linearly from the tips of the fibre inwards to some maximum value (see Figure 2.31b). Fibre failure occurs when this transferred stress reaches the tensile strength of the fibre. This loading process continues until the fibre-fragment lengths are so small because the tensile stresses that are induced in the fibre can no longer reach the fibre tensile strength and the fibre fragmentation process ceases. This final fibre fragment length is referred to as the fibre critical length (L_c).

a

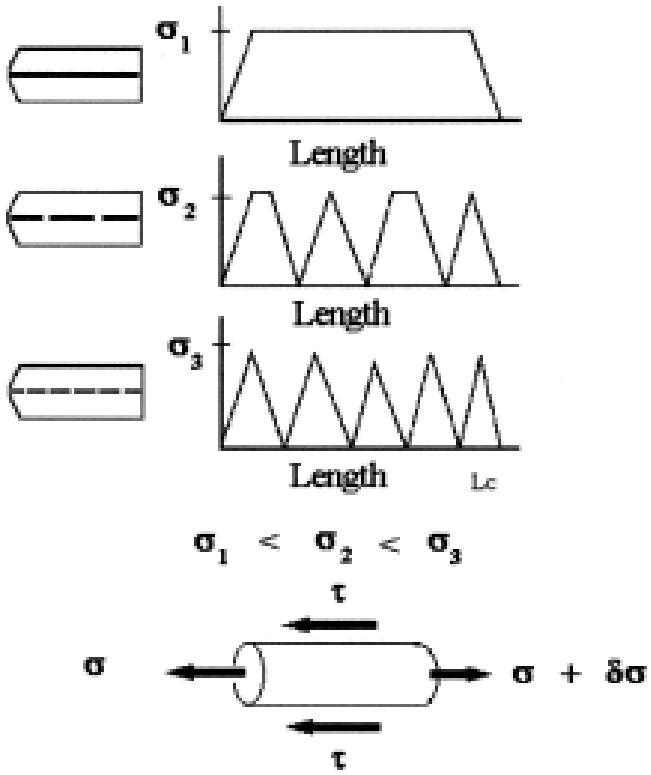

b

Figure 2.31: Schematic of the single fibre fragmentation test [82].

It is commonly accepted that L_c is a good indicator of the ability of the interface to transmit loads between the fibre and matrix. The IFSS can be estimated on the basis of the constant shear model proposed by Kelly and Tyson [82]

$$\tau = \frac{\sigma_{fc}}{2}\left(\frac{d}{L_c}\right) \tag{7}$$

where d is the diameter of the fiber, Lc is the critical length of the fibre and σ_{fc} is the fibre tensile strength at Lc. Early work by Ohsawa *et al*. (1978) provided the background for the semi-empirical analysis of the test data [84]. The critical fibre

length (*Lc*) is calculated by

$$L_c = \frac{4}{3} L_{ave} \tag{8}$$

where L_{ave} is the mean fragment length.

Drzal et al. [83] recognized that the distribution of fibre fragments fits a two-parameter Weibull distribution well and rearranged the Kelly and Tyson equation proposing the following modification to calculate IFSS:

$$\tau = \frac{\sigma_{fc}}{2\beta} \Gamma\left(1 - \frac{1}{\alpha}\right) \tag{9}$$

where α and β are the shape and scale parameters of the Weibull distribution, which are commonly estimated by means of the linear regression method (graphical method), or the maximum likelihood method. Γ is the gamma function.

In the single fibre fragmentation test, the tensile forces result in cross sectional area reductions for both the fibre and matrix due to the Poisson's effect during stressing of the composite [83][84]. If the Poisson's ratio of the matrix is greater than that of the fibre, the matrix will induce radial compressive stresses on the fibre, and the frictional component of the interfacial adhesion will be increased depending on the net cross-sectional reduction between the fibre and matrix [18]. Furthermore, thermal shrinkage arising in specimens during cool-down may also result in residual stresses that can greatly affect the fibre/matrix adhesion. Residual stresses may not always be evenly distributed in the composite. Therefore, it can be said that results obtained by the single fibre fragmentation test is an oversimplified representation of a uniform shear stress at the fibre-matrix interface.

2.8 Composite Strength Modeling

The tensile strength of composites is usually measured using ASTM test standards. However, creating and testing new material systems in this fashion is time-consuming and expensive. In practice, there is a desire to predict composite tensile strength based on properties of the individual constituent material such as fibre and matrix to save time and money during the development of composite material systems based on new fibre.

A range of mathematical models to predict the strength of composites has been developed in the last four decades. Most of the early strength prediction models are based on the assumption that reinforcing fibres are continuous and are aligned axially to the applied load. The strength prediction models of composites with discontinuous and off-axis fibre is far more complex than that of composites reinforced with continuous axially aligned fibres. Although none of the strength prediction models have been rigorously verified experimentally, some models have been shown to predict composite strength with some degree of accuracy [85] [86].

2.8.1 Rule of Mixtures Model (Parallel and Series Model)

Parallel Model

The rule of mixtures model, which was first proposed by Kelly and Tyson [87], can be used to predict the tensile strength of unidirectional, continuous fibre composites that are loaded parallel to the fibre. The parallel model is based on the assumptions of equal strain of the fibre and matrix in the composites, and states that:

$$\sigma_c = V_f \sigma_f + V_m \sigma_m \tag{10}$$

Series Model

The series model can be used to predict the tensile properties of unidirectional, continuous fibre composites that are loaded perpendicular to the fibre, based on the assumptions of equal stress of the fibre and matrix in the composites.

$$\sigma_c = \frac{\sigma_f \sigma_m}{\sigma_m V_f + \sigma_f V_m} \tag{11}$$

where V_f and V_m are the volume fractions of the fibre and matrix, respectively, σ_c is the composite tensile strength, σ_f is the mean fibre tensile strength of the fibre and σ_m is the matrix stress when the fibres reach their ultimate tensile stress in the composite. Alternatively, σ_m can also be taken as the matrix stress at the failure strain of the composite. The fibre and matrix volume fraction (V_f and $V_{m,}$) can be calculated from the fibre weight fraction (W_f) using the following equations [88]:

$$V_f = \left(1 + \frac{\rho_f}{\rho_m}\frac{1 - W_f}{W_f}\right)^{-1} \tag{12}$$

$$V_m = 1 - V_f \tag{13}$$

where ρ_f and ρ_m are density of fibre and matrix respectively.

2.8.2 Hirsch Model

This model is in fact a combination of the parallel and series models, and introduces a parameter (x), relating to the efficiency of the fibre-matrix interface [89]:

$$\sigma_c = x\left(\sigma_m V_m + \sigma_f V_f\right) + (1 - x)\frac{\sigma_f \sigma_m}{\sigma_m V_f + \sigma_f V_m} \tag{14}$$

It is assumed that x is determined mainly by fibre orientation, fibre length and stress amplification at the fibre ends. The efficiency factor x cannot be derived by mathematical means, and is instead empirically fitted to the model.

2.8.3 Modified Rule of Mixtures (Kelly-Tyson Model)

The rule of mixtures model was further modified by Kelly and Tyson [87] to predict the strength of axially aligned discontinuous fibre composites, taking into account the strength contribution of fibres and also whether the average fibre length (L) is greater than the critical fibre length ($L > L_\varepsilon$) or less than the critical fibre length ($L < L_\varepsilon$).

The critical fibre length (L_ε) can be calculated using the following equation Eq (15)

$$L_\varepsilon = \frac{E_f \varepsilon_c D}{2\tau} \tag{15a}$$

$$L_\varepsilon = \frac{\sigma_f D}{2\tau} \tag{15b}$$

where E_f is Young's modulus of fibres ε_c is composite strain, D is the mean fibre diameter (D), τ is the interfacial shear strength and σ_f is mean fibre tensile strength. Fibres shorter than L_ε carry an average stress $E_f\varepsilon_c L/2L_\varepsilon$ ($\sigma_f L/2L_\varepsilon$) and fibres longer than L_ε carry an average stress $E_f\varepsilon_c (1- L_\varepsilon /2L_\varepsilon)$. ($\sigma_f (1- L_\varepsilon /2L_\varepsilon)$).

Thus, the tensile strength (σ_c) of composites containing fibres shorter than L_ε ($L < L_\varepsilon$) is given by:

$$\sigma_c = V_f \sigma_f \left(\frac{L}{2L_\varepsilon} \right) + V_m \sigma_m \tag{16}$$

and the tensile strength of composites containing fibres longer than L_ε ($L \geq L_\varepsilon$) is given by:

$$\sigma_c = V_f \sigma_f \left(1 - \frac{L_\varepsilon}{2L} \right) + V_m \sigma_m \tag{17}$$

The Kelly-Tyson model only accounts for composites with all fibres aligned in the loading direction, and the equation cannot be integrated to give a factor which

accounts for the complex fibre orientations in many moulded thermoplastic composites.

2.8.4 Bowyer-Bader Model

Bowyer and Bader proposed a model based on the Kelly-Tyson modified rule of mixtures where the tensile strength of a composite with discontinuous off-axis fibre could be determined from the sum of sub-critical and super-critical fibre strength contributions (taking into account a fibre orientation) and the matrix contribution [90], as can be seen in Equation (18).

$$\sigma_c = K_1\left(X + Y\right) + Z \tag{18}$$

where X is the contribution from the subcritical fibres, Y is the contribution from the supercritical fibres, Z is from the matrix and K_1 is a fibre orientation factor. The individual terms can be expanded as follows:

$$X = \sum_{i}^{L_i<L_\varepsilon} \frac{\tau L_i V_i}{D} \tag{19a}$$

$$X = \sum_{i}^{L_i<L_\varepsilon} \frac{\sigma_f L_i V_i}{2L_\varepsilon} \tag{19b}$$

$$Y = \sum_{j}^{L_j>L_\varepsilon} E_f \varepsilon_c V_j \left(1 - \frac{E_f \varepsilon_c D}{4\tau L_j}\right) \tag{20a}$$

$$Y = \sum_{j}^{L_j>L_\varepsilon} \sigma_f V_j \left(1 - \frac{L_\varepsilon}{2L_j}\right) \tag{20b}$$

$$Z = E_m \varepsilon_c \left(1 - V_f\right) \tag{21a}$$

$$Z = \sigma_m \left(1 - V_f\right) \tag{21b}$$

where V is the volume fraction of the fibre lengths, L, subscripts i and j refer to the sub-critical and super-critical lengths, respectively. E_m is the Young's modulus of the matrix and V_f is the total fibre volume fraction.

2.8.4.1 Determination of Interfacial Strength (IFSS) and Orientation Factor (K_1) of Short Fibre Composites Using Bowyer-Bader Model

As well as prediction of tensile strength of short fibre composites the Bowyer and Bader model can be used to determine the micromechanical parameters of interfacial shear strength IFSS (τ) if the macromechanical tensile stress-strain curve and fibre length distribution are known. This model has an enormous attraction in that it utilizes data which are readily available from standard tensile testing of composites and requires only the extra determination of fibre length distribution. The basic premise of the Bowyer and Bader model is that at any value of composite strain, ε_c, there is a critical fibre length L_ε [88, 90, 91, and 92]

For a practical system, E_f, E_m, and D can be readily obtained. The fibre length distribution can be determined from direct measurements on the extracted fibres. Although K_1 and τ are not generally known, values for these factors can be obtained if the composite stress (σ_1 and σ_2) at two strain values (ε_1 and ε_2) are known. Values of two strains ε_1 and ε_2 need to be selected and the corresponding stresses σ_1 and σ_2 determined from the tensile stress-strain curve. The matrix contribution (Z) can be calculated from an independent matrix Young's modulus determination and used to calculate the ratio R of the fibre load bearing contributions at the two selected strain ε_1 and ε_2 strains:

$$R = \frac{\sigma_1 - Z_1}{\sigma_2 - Z_2} \tag{22}$$

which according to equation (13) should be equivalent to R' as follow:

$$R' = \frac{X_1 + Y_1}{X_2 + Y_2} \tag{23}$$

An assumed value of τ is initially taken and the corresponding value of $L_{\varepsilon 1}$ and $L_{\varepsilon 2}$ are calculated. The fibre contribution terms X and Y are evaluated using the assumed values of τ and the corresponding $L_{\varepsilon 1}$ and $L_{\varepsilon 2}$ for the measured fibre length distribution. The ratio of R' is calculated by Eq.(23). The assumed value of τ is adjusted until $R'=R$. This value of τ is assumed to be correct and K_1 is determined from Eq. (18).

2.8.4.2 Assumptions of Bowyer-Bader Model

Similar to all other models, the Bowyer and Bader model also involves a number of assumptions. These include [88]:

- Stress transfer at the interface increases linearly from zero at the fibre ends to a maximum value
- Fibre-matrix debonding does not occur
- K_1 is independent of strain and a constant for all fibre lengths
- Interfacial shear stress is independent of loading angle
- Porosity in the composite is negligible
- Fibre and matrix stress versus strain curves are linear

Strengths of this model include the consideration of an orientation factor, as well as the super-critical and sub-critical length distributions of fibres extracted from an actual composite.

2.8.5 Modified of Rule of Mixtures by Taking Account of Void Content

Prediction of composite strength requires knowledge of the content of different components in a composite. It is commonly based solely on the content of reinforcement fibre and matrix material as for the simple “rule of mixtures”.

However, a large amount of voids are commonly present in plant fibre composite laminates produced by commercial manufacturing processes, which should be expected to considerably influence tensile properties of the composites by introducing inhomogeneous stress concentrations in the loaded composites materials [93] Therefore, it would make sense to take account of void volume content, as well as fibre volume content and matrix volume content for predicting the tensile strength of composites. Based on a theoretical study adding spherical holes into materials, the effect of voids on an axially aligned long fibre composite tensile strength can be taken into account by the term $(1-V_p)^n$ [20,94,95] and the simply "rule of mixtures" (Eq 10) can be modified as follows:

$$\sigma_c = (V_f \sigma_f + V_m \sigma_m)(1 - V_p)^n \tag{24}$$

where σ_f is the mean fibre tensile strength of the fibre and σ_m is the matrix stress at the fibre failure strain. Alternatively, σ_m can also be taken as the matrix stress at the failure strain of the composite. V_f , V_m and V_p are the volume fractions of the fibre and matrix and void, respectively. n=0 relates to a homogeneous stress concentration, and n>0 is used when the inhomogeneous stress-concentration pattern decreases the composites strength σ_c. The correction factor for hemp fibre composites had been investigated elsewhere such that a value n=2.1 was found, giving [20, 94 and 96]:

$$\sigma_c = (V_f \sigma_f + V_m \sigma_m)(1 - V_p)^{2.1} \tag{25}$$

Void content can be determined using ASTM Standard Test Methods for Void Content of Reinforced Plastics [97] using the following equation:

$$V_p = 100 - \rho_c \left[\frac{w_m}{\rho_m} + \frac{w_f}{\rho_f} \right] \tag{26}$$

where V_p is void content of the composite (%), ρ_c is measured density of the composite (g/cm^3), w_m is matrix content (weight %), ρ_m is resin density (g/cm^3), w_f is fibre content (wt.%) and ρ_f is fibre density (g/cm^3). The value of V_f, V_m are calculated according the following Eqs (27, 28) [98].

$$V_f = \frac{\frac{w_f}{\rho_f}}{\frac{w_f}{\rho_f} + \frac{w_m}{\rho_m}}(1 - V_p) \tag{27}$$

$$V_m = \frac{\frac{w_m}{\rho_m}}{\frac{w_f}{\rho_f} + \frac{w_m}{\rho_m}}(1 - V_p) \tag{28}$$

For this method, density of fibre (ρ_f), matrix (ρ_m) and composite (ρ_c), weight fraction of fibre (w_f) and matrix (w_m) after processing are required to be accurately measured. The exact weight content of fibre (w_f) can be determined by dissolving the PP/MAPP matrix with xylene and applying gravimetric measurements [18]. The weight content of matrix (w_m) could be calculated using Eq (29) based on the weight content of fibre (w_f) as follows:

$$w_m = 100 - w_f \tag{29}$$

Chapter 3:
Materials and Methods

3.1 Introduction

The main objective of this research was to produce improved interfacial bonding between hemp fibre and polypropylene. In order to achieve this purpose, bag retting and white rot fungi treatments and chelator/enzyme treatments were performed on hemp fibre to improve fibre separation, remove noncellulosic compounds, and roughen the fibre surface (in the case of bag retting and white rot fungi treatments), therefore, improve fibre and matrix interfacial bonding and increase composite strength when the fibre was combined with a polypropylene matrix.

Characterization techniques, namely wet chemical analysis, visual inspection, FT-IR, scanning electron microscopy (SEM), X-ray diffraction (XRD), fibre density assessment, thermal analysis, zeta potential, and single fibre tensile testing were used to elucidate the effect of treatment on hemp fibres. Wet chemical analysis and FT-IR were used to assess the chemical compounds in the fibre and visual inspection was used to investigate the separation of the fibres. SEM provided a means of examination of the surface morphology of hemp fibres. XRD was used to show modification of the crystallinity of fibre. Fibre density assessment was used to monitor the change in density after treatments. Thermal analysis was used to obtain information about the thermal stability of the fibre. Zeta potential analysis was used to monitor the chemical surface properties of fibre. Single fibre tensile testing was used to obtain the tensile properties of untreated and treated fibres.

Chopped treated and untreated fibres, polypropylene and maleated polypropylene (MAPP) coupling agent were compounded using a twin-screw extruder, and then injection moulded into composite tensile test specimens. All composites were then tensile tested to determine their strength and stiffness. The single fibre pull-out test was used to assess the interfacial shear strength (IFSS) of short fibre composites. Fibre length distribution and fibre diameters after processing were measured in order to calculate IFSS of short fibre composite using the Bowyer and Bader model.

An improved composite manufacturing technique was investigated for fabricating long hemp fibre composite laminate specimens. Film stacking and hot-press forming was used, in which hemp fibres were layered on a PP film and PP and MAPP powder was spread over the hemp fibre layer. Layers of PP film, PP/MAPP powder and hemp fibre were stacked alternately, and then this stack was compressed in a hot-press. All composites sheets were analysed to evaluate their tensile strength and Young's modulus. Composite density and the exact fibre weight content after processing were measured in order to predict the tensile strength of long fibre composite sheets using a model taking account of void content.

3.2 Materials

Industrial hemp (*Cannabis sativa* L.) grown in Hamilton New Zealand was used in this investigation. The hemp had been initially planted at a density of 65 plants per square metre. After harvesting in 2007, green non-retted hemp bast fibres strips were separated from the stalk by hand and dried on shelves and prepared for fibre treatments.

White rot fungi *Phanerochaete sordida* (D2B), *Pycnoporus species* (Pyc) and *Schizophyllum commune* (S.com), which were used for fungal treatments, were kindly supplied by the Biology Department at the University of Waikato. For the chelator/enzyme treatments, EDTMP.Na5 (Ethylene Diamine Tetra (Methylene Phosphonic Acid Pentasodium salt), a sodium salt of EDTMP was kindly supplied by Taian Waste Water Treatment Factory in China**.** Pectinase (P2401) from Rhizopus, and laccase (53739) from Trametes versicolor, were purchased from Sigma. HBT (1-hydroxybenzotriazole hydrate), a mediator, was also purchased from Sigma.

Polypropylene (Icorene® PP CO14RM) with a density of 0.9g/cm^3, supplied by Aldrich Chemical was used as the composite matrix. The polypropylene film, which was used to fabricate long fibre composites sheets, kindly made by Sealed Air Company in Hamilton, New Zealand with the same polypropylene powder. A-C 950P, a high molecular weight maleated polypropylene (MAPP), supplied by Honeywell International Inc, USA, was used as the coupling agent.

3.3 Experimental Methods

3.3.1 Bag Retting and Fungal Treatments

For bag retting, the fresh green non retted hemp fibres were kept in a sealed plastic bag for one to two weeks to allow natural retting to occur under sealed conditions. For white rot fungi treatments, the dried non-retted hemp fibres were sterilised using gamma radiation of 26.0 kGy (kilogray) in sealed sterilisation bags. Irradiated hemp fibres were then inoculated with white rot fungi (D2B, Pyc and S.com) for two weeks, with fungi: hemp ratio of approximately 10mg fungi: 12g irradiated hemp. Water was added for all fungal treatments and bag retting to give a moisture content of 60wt%. Details of bag retting and fungal treatments are presented in Table 3.1. After bag retting and fungal treatments, treated fibres were

washed for 10 minutes in water and dried in an oven at 80°C until equilibrium moisture content was achieved.

Table 3.1: Description of bag retting and white-rot fungi treatments

Treatment (Ab.)	Description
Raw	Green non-retted hemp fibres separated by hand after harvesting and shelf drying
1 week ret	Fresh green non-retted hemp fibres with 60% moisture sealed in plastic bag for 1 week at room temperature
2 weeks ret	Fresh green non-retted hemp fibres with 60% moisture sealed in plastic bag for 2 weeks at room temperature
D2B	Irradiated hemp fibres with 60% moisture incubated with D2B for 2 weeks at 27°C
Pyc	Irradiated hemp fibres with 60% moisture incubated with Pyc for 2 weeks at 27°C
S.com	Irradiated hemp fibres with 60% moisture incubated with S.com for 2 weeks at 27°C

3.3.2 Chelator and Enzyme Treatments

Treatment of the green non-retted fibres was achieved by immersing the fibres in solutions (fibre: solution = 10g: 200ml) consisting of either EDTMP.Na5 or enzyme (see table 3.2). Fibres were then washed for 10 minutes in water and dried in an oven at 80°C until an equilibrium moisture content was achieved.

Table 3.2: Description of chelator/enzyme treatments

Treatment(Ab.)	Description
Raw	The green non-retted hemp fibres are separated by hand after harvesting and dried on the shelf
P	Pectinase (100 units) adjusted to a pH of 8 with NaOH at 50 ^{o}C for 6h at shake rate of 50 U/min
L	Laccase (100 units) with mediator HBT (300uM) adjusted to a pH of 4.5 with acetic acid at 50^{o}C for 6h at shake rate of 50 U/min
E	EDTMP.Na5 (5g/l) adjusted to a pH of 11 with NaOH at 60 ^{o}C for 6h
E2	EDTMP.Na5 (10g/l) adjusted to a pH of 11 with NaOH at 60 ^{o}C for 6h
E+P	Treatment E, washed, air-dried and then treatment P
E+L	Treatment E, washed, air-dried and then treatment L

3.3.3 Analytical Techniques for Natural Fibres

Several methods, such as wet chemical analysis, visual inspection, FT-IR, SEM, XRD, fibre density test, zeta potential, thermal analysis and single fibre tensile testing are suitable for analyzing natural fibre.

Wet Chemical Analysis of Fibre

The chemical analysis of the untreated and treated hemp fibres was carried out according to GB 5881-86 (National Standard of China for Ramie Chemical Analysis). This gravimetric method involved the degradation and extraction of wax, water-soluble components, pectin and hemicellulose in the hemp fibres. Following is the detailed explanation for chemical analysis.

1. Method for determination of wax content

The raw hemp sample of 5 g was weighed out and corrected for dry matter. Then the sample was extracted with 150ml benzene/ethanol (2:1) solution for 3 h in a soxhlet apparatus to remove waxes. After extraction the sample was dried overnight at 105°C and was weighed out again. Wax was determined by weight loss:

$$W_1(\%) = \frac{G_0 - G_1}{G_0} 100\% \quad (30)$$

$W_{1:}$ wax content (%)

$G_{0:}$ raw material (g)

$G_{1:}$ residue after wax extraction (g)

2. Method for determination of water soluble material

The residue after wax extraction was placed in a beaker and boiled for an hour in 150ml distilled water, after which the distilled water was replaced with fresh distilled water and boiled for another 2 hours. The sample was washed using a filter and dried overnight at 105°C before final weighing. The water soluble material determined by weight loss:

$$W_2(\%) = \frac{G_1 - G_2}{G_0} 100\% \quad (31)$$

W_2: water soluble material content (%)

G_2: residue after water soluble material extraction

3. Method for determination of pectin

The residue after water soluble material extraction was placed in a beaker and boiled for 3 h in 150ml, 5g/l ammonium oxalate solution, and then the sample was washed using a filter and dried overnight at 105^{o}C before final weighting. The pectin determined by weight loss:

$$W_3(\%) = \frac{G_2 - G_3}{G_0} 100\% \quad (32)$$

W_3: pectin content (%)

G_3: residue after pectin extraction

4. Method for determination of hemicellulose

The residue after pectin extraction was placed in a beaker and boiled for 3 h in 150ml, 20g/l NaOH (sodium hydroxide) solution, and then the sample was washed using a filter and dried overnight at 105^{o}C before final weighing. The hemicellulose determined by weight loss:

$$W_4(\%) = \frac{G_3 - G_4}{G_0} 100\% \quad (33)$$

W_4: hemicellulose content (%)

G_4: residue after hemicellulose extraction

5. Method for determination of lignin

The residue after wax extraction was cut into 1.5mm lengths. 1 g of sample was weighed and placed in a beaker. The sample was then treated with 72% sulphuric acid for 24h to destroy the cellulose, leaving a fraction comprised of lignin and ash. After sulphuric acid treatment, the sample was boiled for 1 h in 300ml

distilled water, and then the sample was washed using a filter and dried overnight at 105^{o}C before final weighing. The lignin was determined by weight loss:

$$W_5(\%) = \frac{G_5}{G_0} 100\% \quad (34)$$

W_5: lignin content (%)

G_5: residue after 72% sulphuric acid treatment

G_0: residue after wax extraction (1g)

FT-IR Spectra

Prior to FT-IR testing, sample discs were prepared by first mixing 2 mg of dried sample with 150 mg of KBr in an agate mortar and then pressing the resulting mixture successively at 8 tonnes /cm^2 for 5 min. FT-IR spectra for the untreated and treated fibres were then recorded between 4000 and 400 cm $^{-1}$ using a BIO-RAD FTS-40 FTIR instrument.

Scanning Electron Microscopy (SEM)

Prior to SEM evaluation, the sample was coated with using plasma sputtering to avoid the sample becoming charged under the electron beam. SEM micrographs of treated and untreated fibre surfaces and fracture surface of composite tensile test specimens were then taken using a Hitachi S-4100 field emission scanning electron microscope, operated at 5 kV.

X-Ray Diffraction

Fibre was cut finely to produce a powder, pressed into a disk and analysed using a Phillips X'Pert-MPD system over a range of 2θ values from 10 to 50^{o} at a scanning speed of 0.03 ^{o}/s.

Fibre Density Test

Hemp fibre density was measured in accordance with the ASTM Standard Test Method for Density of High-Modulus Fibers [99]. The Archimedes test using canola oil as an immersion fluid was chosen. Fibre was dried at 60^{o}C for 72 hours and a minimum of 0.5g of fibre sample was placed in a vacuum desiccator for 5 minutes to remove trapped air from between fibre cells. After determination of density of canola oil, the fibre was completely immersed in canola oil and a reading of mass was taken (see Figure 3.1). The difference in weight of the fibre sample in air and in canola oil is the buoyancy force. This force was converted to fibre sample volume by dividing it by canola oil density. The fibre sample weight in air divided by the sample volume equals the fibre sample density. The average fibre density was obtained based on 5 specimens for each fibre.

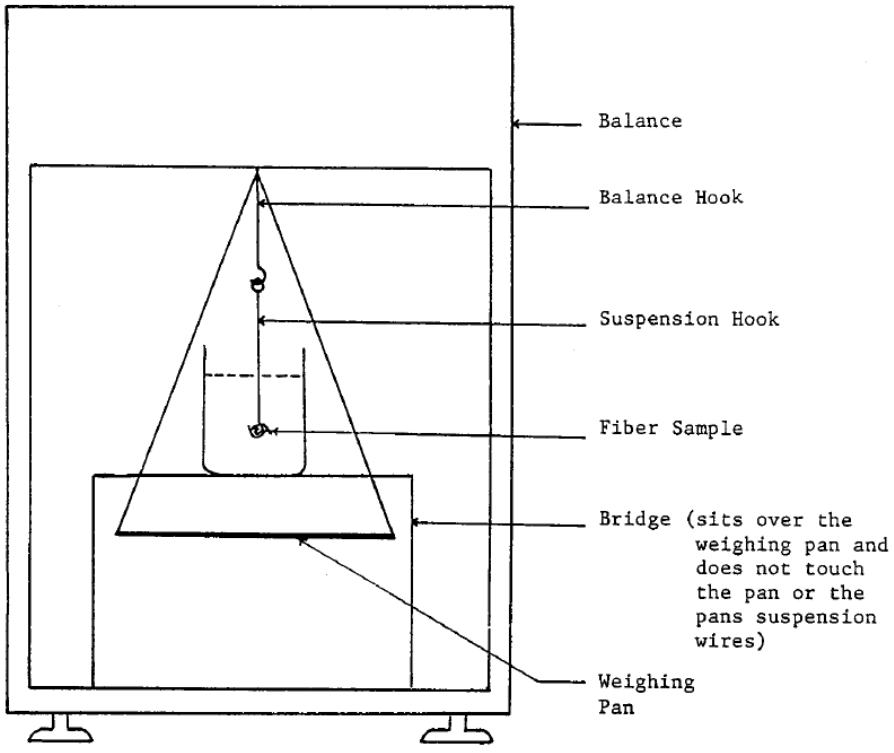

Figure 3.1: Density apparatus

Thermal Analysis

Untreated and treated fibre samples weighing between 6 and 13 mg were analysed using an Instruments SDT 2960 thermal analyzer (see Figure 3.2) operated in a dynamic mode, heating from ambient temperature to 773K at 10K/min in air purged at 150 ml/min with an empty pan used as a reference. Differential thermal analysis (DTA) curves and thermal gravimetric analysis (TGA) curves were obtained.

Figure 3.2: SDT 2960 Simultaneous DTA-TGA analyser

Zeta Potential

The SZP 06 streaming potential system was used to measure the zeta potential of hemp fibres. 5 g of fibre was added to 500 ml 0.001 mol/L KCl solution. The pH was varied by adding HCl or KOH to the fibre solution. The solution was placed in the electrophoresis cell and a voltage applied via the electrodes. Five readings were obtained at each pH value.

Single Fibre Tensile Testing

Single hemp fibres from each treatment were tensile tested in accordance with the ASTM Standard Test Method for Tensile Strength and Young's Modulus for High-Modulus Single Filament Materials [100]. Fibres were separated by hand and mounted on cardboard mounting–cards with 10mm holes. A small amount of PVA glue was applied to the two edges on either side of the hole to hold the fibres in place and allowed to dry for a few hours (see Figure 3.3).

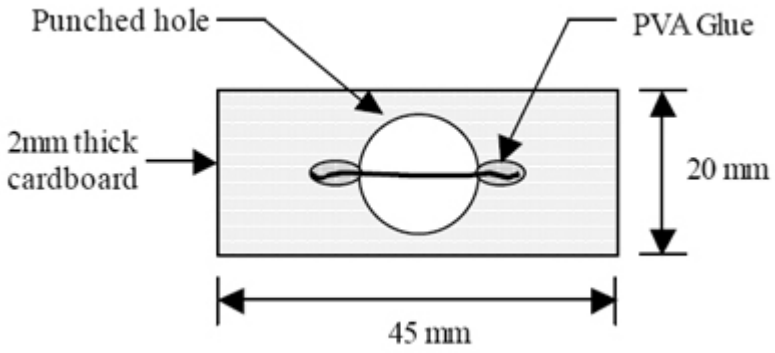

Figure 3.3: Single fibre mounting [18].

Fibre diameters were then measured (average of 6 reading equally spaced along fibre) using an optical microscope at 200x magnification. The mounted single fibres were then individually placed in the grips of an Instron-4204 tensile testing machine (see Figure 3.4) and the supporting sides of the mounting card cut using a hotwire cutter. The fibres were then tensile tested to failure at a rate of 0.5mm/min using a 10N-load cell. Average strength values were obtained using results from twenty specimens. The determination of Young's modulus of hemp fibres was obtained as described by Beckerman G [18], using a correction factor to determine the true displacement of the fibre, which, in turn, involves the calculation of the testing system compliance (*Cs*).

Figure 3.4: Instron-4204 tensile testing machine

The Single Fibre Pull-Out Test

A silicone rubber mould was made for preparing single fibre pull-out specimens. The mould was 12mm long, 10mm wide, and 3mm deep with a 6mm hole punched in the centre of the top face of the mould, with a slot cut to a depth of 2mm connecting from the centre of the outer length to the punched hole. White rot fungi treated and untreated fibres were separated from their fibre bundles by hand and then a single fibre was carefully placed in the slot of the mould (Figure 3.5). The single fibre diameter and the length inside the hole were measured by placing the silicone rubber mould under an optical microscope with a calibrated eyepiece. After measurement, the silicone rubber mould was place on a Teflon™

coated steel plate with PP powder and 3% MAPP added into the hole. The steel plate and mould was placed in an oven at 180°C for 10 minutes to ensure melting of the matrix. After cooling, the free end of the fibre was placed on a 2mm thick cardboard mounting card, and attached using PVA adhesive. The single fibre pull-out specimen was placed in the grips of an Instron-4204 tensile machine. The fibres were then loaded at a rate of 0.5 mm/min using a 10N-load cell. Average pull out forces were obtained based on twenty specimens.

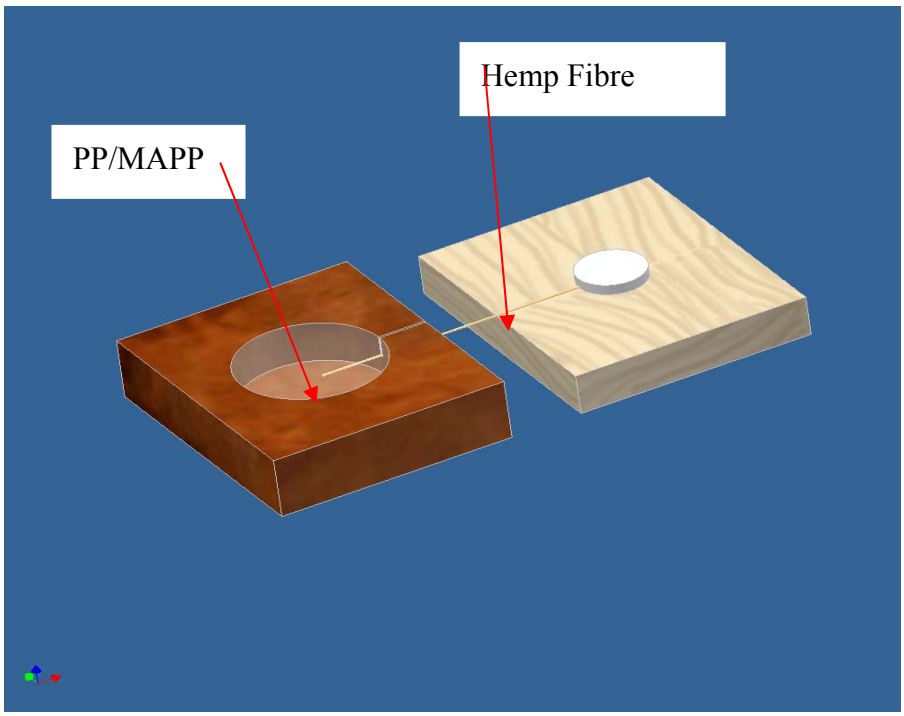

Figure 3.5: The single fibre pull-out specimen

3.3.4 Composite Fabrication

3.3.4.1 Extrusion and Injection Moulding of Short Fibre Composite

Fibre was guillotined into 10mm lengths. Fibre, polypropylene and maleated polypropylene (MAPP) coupling agent were dried at 70°C for 48 hours, and then compounded to give a content of 3wt% MAPP and 40wt% fibre using a ThermoPrism TSE-16-TC twin-screw extruder (Figure 3.6). The extruder barrel consisted of 5 heating zones, which were set at 80°C (barrel entrance), 110°C,

155°C, 180°C, and 175°C (barrel exit). The twin co-rotating screws were operated at 160 revolutions per minute (rpm). After air-cooling, the extruded composite material was pelletised to give dimension ranging from 1mm to 5mm, dried at 70°C for a further 48 hours and then injection moulded using a BOY 15-S injection moulder (Figure 3.7) into Type 1 tensile test specimens (as specified by the ASTM D638-91 standard).

Figure 3.6: ThermoPrism TSE-16-TC twin-screw extruder

Figure 3.7: BOY15-S injection-moulding machine

3.3.4.2 Film Stacking and Hot Press of Long Fibre Composite Sheet

Chelator EDTMP.Na5 (E2) and white rot fungi (S.com) treatments were applied to hemp fibre to separate its bundles and remove non-cellulosic compounds. After treatment, long untreated and treated hemp fibre composite laminate specimens, in which hand carded fibre ran through the entire test specimen length, were fabricated by film stacking and hot-press forming. Hemp fibres were oriented in the axial direction (0^o) on a PP film, and PP and MAPP powder was spread over the hemp fibre layer. Each stack consisted of four layers of PP film and three layers of hemp fibre with PP/MAPP powder distributed amongst the fibre as shown in Figure 1. Hemp and PP/MAPP layers were weighed using a precision balance to give a composition of 57wt% PP, 3wt% MAPP and 40wt% fibre. The stack was sandwiched between two aluminium plates, which were then compressed in a hot-press. A pressure of 10 Pa was applied for 10 minutes at a temperature of 170^oC. The resulting composite sheets were cut into tensile test specimens.

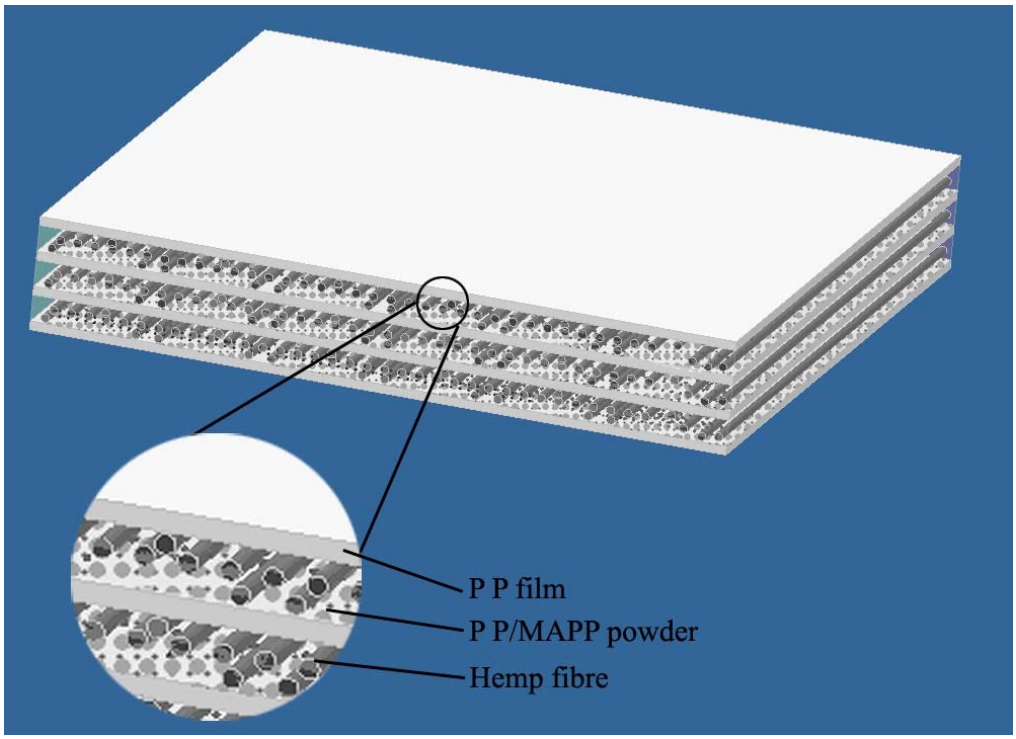

Figure 3.8: Layers of thermoplastic sheet, PP/MAPP powder and hemp fibre

3.3.5 Assessment of Composite

3.3.5.1 Composites Tensile Strength Testing

Short fibre and long fibre composite specimens were conditioned at 20^{o}C and 50% relative humidity for 48 hours prior to tensile testing. The composite specimens were then tested according to the ASTM Standard Test Method for Tensile Properties of Plastics [101] using an Instron-4204 tensile testing machine with a 5kN load cell, operated at a rate of 5mm/minute. An Instron 2630-112 extensometer was used to measure the strain for 12 specimens of each composite type.

3.3.5.2 Fibre Length Distribution and Fibre Diameter

To assess the fibre length distribution and fibre diameters after injection moulding, fibres were extracted from composites using boiling in xylene dissolve the matrix. Approximately 5g of composite was boiled in 150ml of xylene (135^{o}C) for 20 minutes to enable the extraction of the fibres from the composite. The extracted hemp fibres were separated by filtration, washed using 100ml of xylene, and dried in an oven. Dried fibres were dispersed on a glass slide for observation under an optical microscope. About 1000 fibres for each composite sample were examined and their measurements were statistically analyzed.

3.3.5.3 Composite Density

Composite density was measured in accordance with ASTM Standard Test Methods for Density and Specific Gravity (Relative Density) of Plastics by Displacement [102]. Distilled water was chosen as an immersion fluid and was rendered air-free by boiling and cooling. 2 g of long fibre composites specimen completely immerse in water and any bubbles adhering to the specimen, sample holder, or sinker were removed by rubbing them with a wire, and then a specimen mass reading was taken. The sample volume was calculated from the ratio of masses in air and in water. Composite density was then calculated from the

sample weight in air divided by the sample volume. Average composite density was obtained based on 5 specimens for each long fibre composite.

3.3.5.4 Fibre Weight Content

To assess the exact fibre content after hot-pressing, composites were extracted by boiling in xylene to dissolve the matrix. 5g of composite (w_1) was boiled in 150ml of xylene (135^{o}C) for 20 minutes to enable the extraction of the fibres from the composite. The extracted hemp fibres were separated by filtration, washed using 100ml of clean xylene, and dried in an oven. Dried fibres were applied gravimetric measurements (w_2) and the fibre weight fraction (w_f) was calculated by following equation:

$$w_f = \frac{w_2}{w_1} \times 100 \tag{35}$$

The average fibre content was obtained based on 3 specimens for each fibre composite.

Chapter 4

Results and Discussion

4.1 Bag Retting and White-Rot Fungi Treatments

Bag retting and white-rot fungi treatments were used to achieve the following objectives:

- Separation of hemp fibres from their fibre bundles
- Removal of non-cellulosic compounds in hemp fibres
- Roughening of the hemp fibre surface

4.1.1 Separation of Bag Retted and White Rot Fungi Treated Fibre

Figure 4.1.1 is the digital picture for untreated and bag retted and white rot fungi treated fibres, which shows that the untreated fibre exists in fibre bundles and the treated fibres show good fibre separation. This supported the removal of non-cellulosic compounds like pectin, which is responsible for bundling fibre together, leads to separate the fibres from their bundles. It should be noted that the treated fibre retained parallel orientation during the fungal treatment and bag retting and are thereby useful for composites with long and aligned fibres.

Figure 4.1.1: Digital pictures for untreated, bag retted (1 week and 2 weeks) and white-rot fungi treated fibre

4.1.2 Wet Chemical Analysis of Bag Retted and White Rot Fungi Treated Fibre

Table 4.1.1 shows the results of wet chemical analysis carried out on untreated and treated hemp fibres. All treatments reduced the amount of wax, pectin, hemicellulose and lignin in the fibre compared to the amounts in the untreated fibre. All the white rot fungi treatments appeared generally to remove more lignin than the bag retting treatments, which supported the ability of white rot fungi to selectively degrade lignin. All treated fibres were lighter in colour than the untreated fibre further supporting the removal of lignin as discussed in Section 2.1.6.

Table 4.1.1: Result of wet chemical analysis for untreated, bag retted and white-rot fungi treated fibre

Treatment(Ab.)	Wax (%)	Pectin (%)	Hemicellulose (%)	Lignin (%)	Colour of fibre
Raw	2.3	6.2	18.4	6.8	green
1 week	0.4	4.8	17.2	6.0	light
2 weeks	0.2	3.2	16.5	4.2	lighter
D2B	0.3	2.7	15.0	3.5	lighter
Pyc	0.4	3.4	13.8	3.5	lighter
S.com	0.3	1.8	13.5	4.1	lighter

4.1.3 FT-IR Spectra of Bag Retted and White Rot Fungi Treated Fibre

Figure 4.1.2 shows FT-IR spectra for untreated and treated fibres. The peak around 1736 cm^{-1}**,** which can be attributed to the presence of the carboxylic ester in pectin and wax, shows a significant reduction for the two week bag retting treatment and the white rot fungi treated fibres supporting removal of pectin and wax. Fibres from the one week bag retting treatment did not show significant reduction at the 1736 cm^{-1} peak, probably because the retting time was too short to allow bacteria and fungi to modify pectin effectively. The range from 3000cm^{-1} to 3600cm^{-1} corresponds to OH stretching vibrations, mainly attributed to cellulose and lignin; after treatment, the relative intensities at 3600-3000cm^{-1}decreased, which suggests the treatments have removed lignin. The peak around 1268 cm^{-1}, which represents the COO stretching in lignin, had disappeared in the 2 week bag retted and the white rot fungi treated fibres. This disappearance is likely to be due to the degradation of lignin. Thus, the change in the composition of treated fibre can be appreciated in the infrared spectra, which further supports the chemical analysis results.

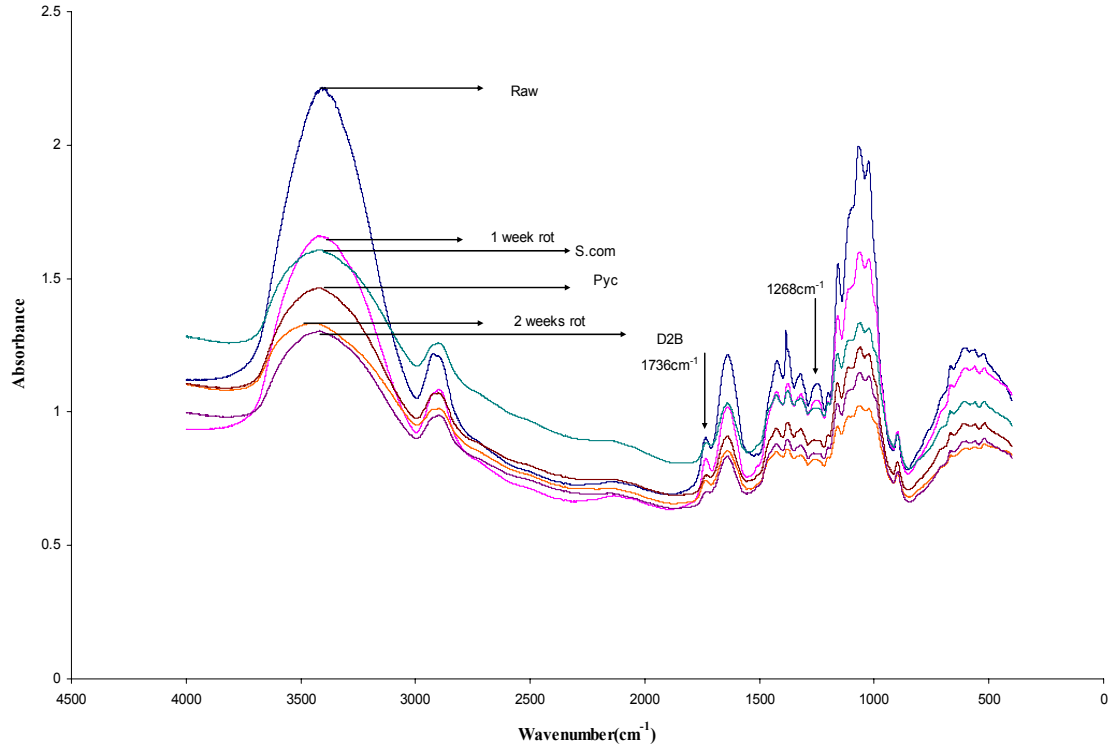

Figure 4.1.2: FT-IR spectra of untreated, bag retted and white-rot fungi treated fibre

4.1.4 Morphology of Bag Retted and White Rot Fungi Treated Fibre

The change in the surface morphology of the treated fibre was studied by scanning electron microscopy (SEM). Figure 4.1.3-4.1.8 present SEM micrographs of untreated and treated fibres. Examination of the untreated fibres (Figure 4.1.3) shows that they are coated with non-cellulosic material. Treatments with white rot fungi and bag retting led to relatively clean surfaces (see Figures 4.1.4-4.1.8) which supports the removal of wax, pectin, lignin and hemicelluloses as supported by FT-IR and chemical analysis. Unfortunately, the resolution of the available SEM was inadequate to detect fine holes caused by fungal hyphae attacking fibre walls on treated fibre surfaces, as seen with High-resolution Cryo-Field Emission Scanning Electron Microscopy (HR-Cryo-FE -SEM) elsewhere (see section 2.5.3).

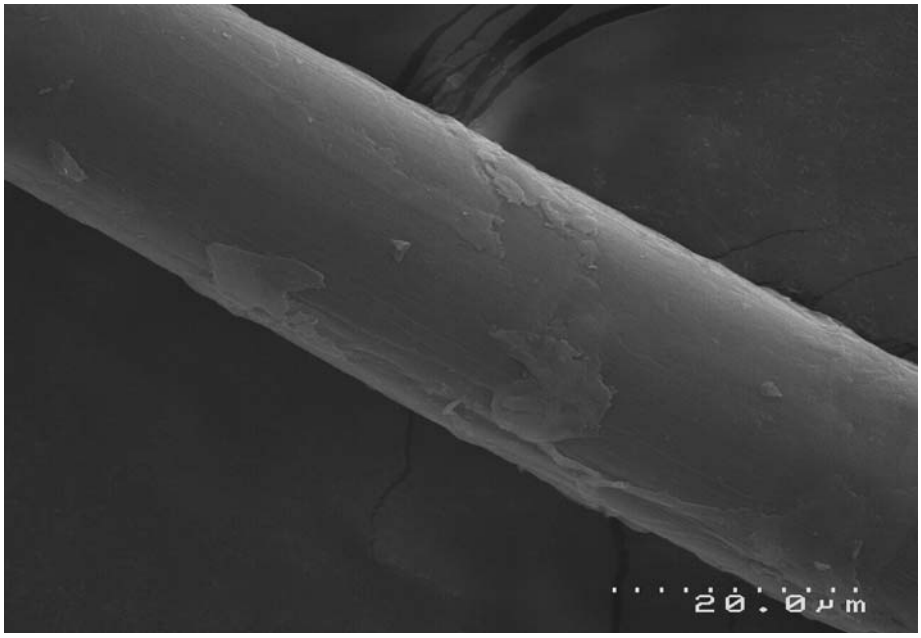

Figure 4.1.3: SEM of untreated hemp fibre

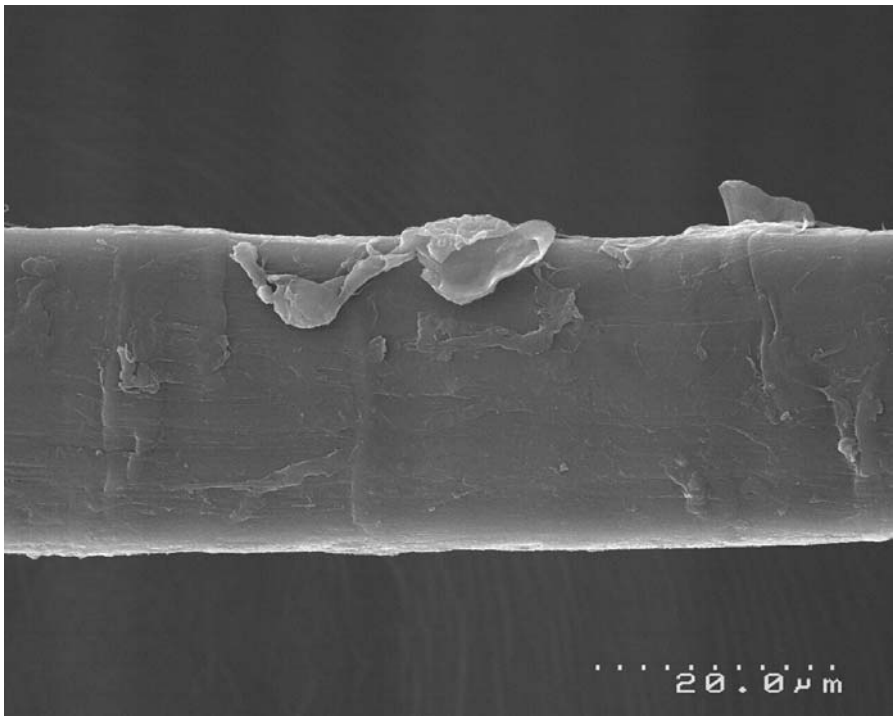

Figure 4.1.4: SEM of 1 week bag retted hemp fibre

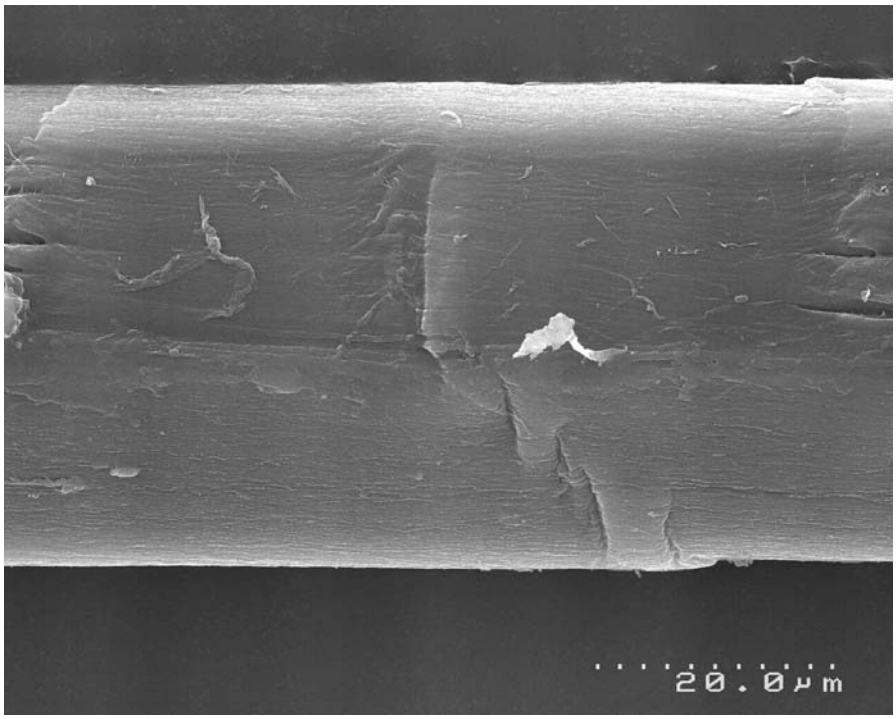

Figure 4.1.5: SEM of 2 weeks bag retted hemp fibre

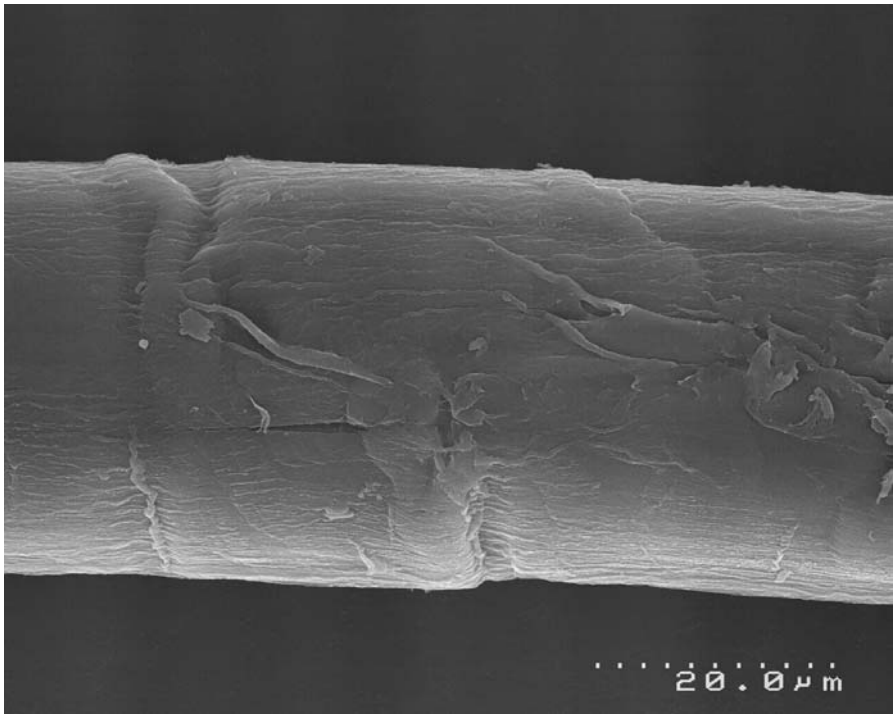

Figure 4.1.6: SEM of D2B treated hemp fibre

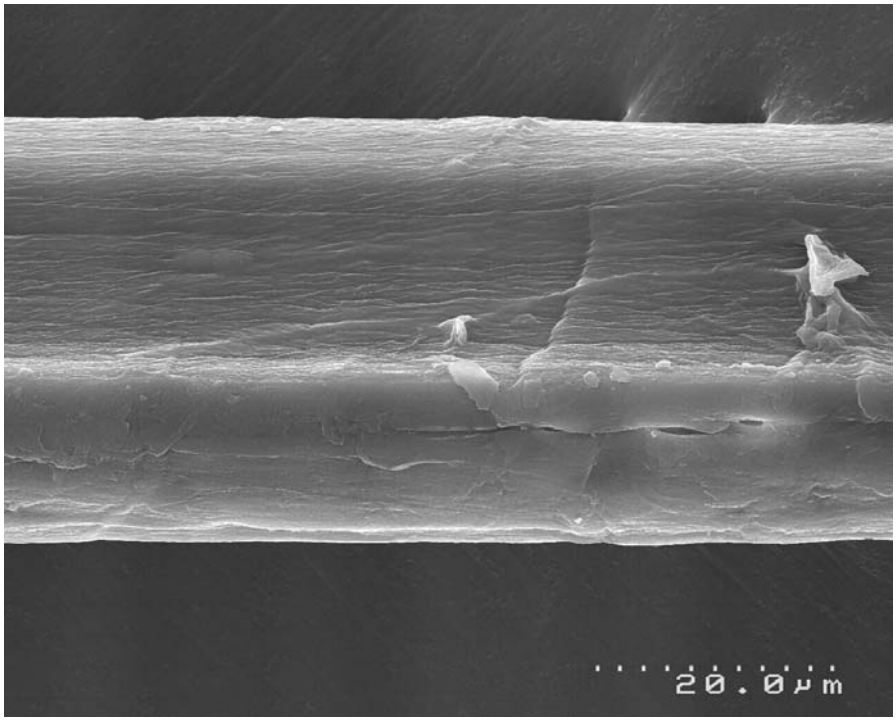

Figure 4.1.7: SEM of Pyc treated hemp fibre

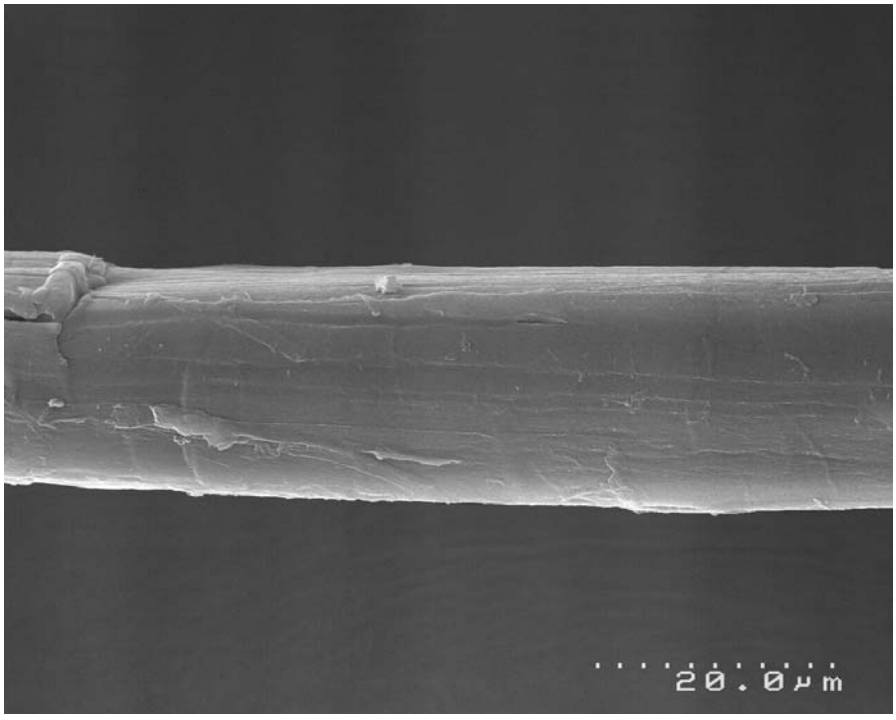

Figure 4.1.8: SEM of S.com treated hemp fibre

4.1.5 X-Ray Diffraction of Bag Retted and White Rot Fungi Treated Fibre

The X-ray diffraction patterns of green untreated and treated hemp fibre are given in Figure 4.1.9. The major peaks observed for all fibre samples are at 2θ diffraction angles of 15.1, 16.88 and 22.82° representing $(1\bar{1}0)$, (110) (merged in some cases) and (200) planes indicating the presence of Type I cellulose. Table 4.1.2 presents the crystallinity index calculated according to the Segal empirical method (Eq.3 in Section 2.5.4.2).The crystallinity index was found to increase for all fibre treatments, particularly for white rot fungi treatments. This increase could be related to the removal of non-cellulosic compounds, as supported by FT-IR and chemical analysis, which would allow better packing of the cellulose chains.

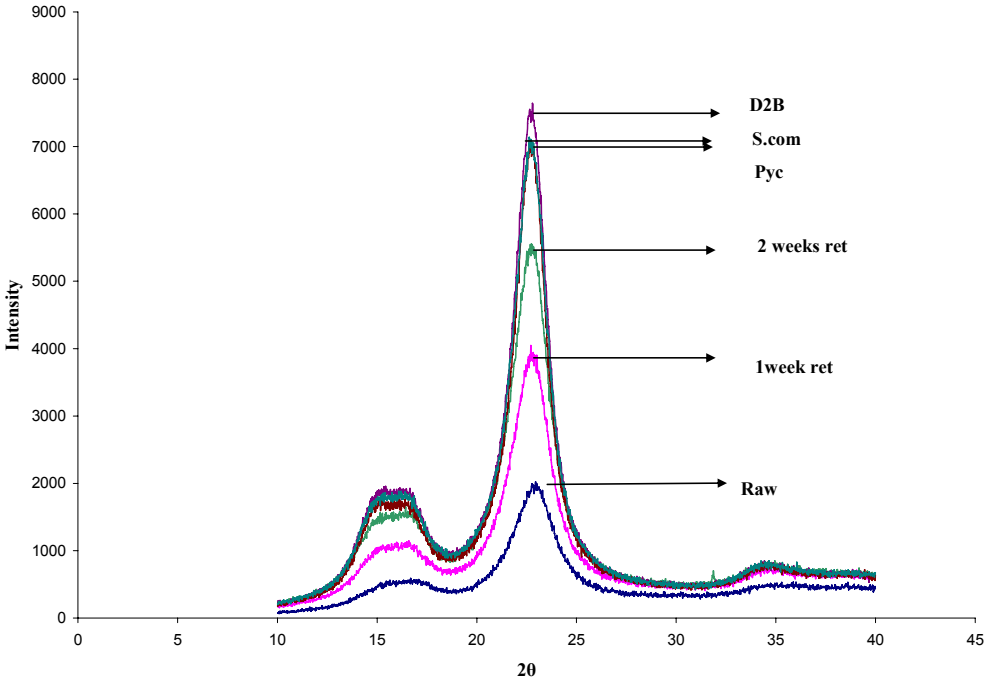

Figure 4.1.9: X-ray diffraction traces for untreated and bag retted and white rot fungi treated fibre

Table 4.1.2: Crystallinity index of untreated, bag retted and white-rot fungi treated fibre

Treatment(Ab.)	Crystallinity index (%)
Raw	66.56
1 week	84.34
2 weeks	85.27
D2B	88.45
Pyc	87.36
S.com	88.53

4.1.6 Density of Bag Retted and White Rot Fungi Treated Fibre

Densities of untreated and treated fibre were measured and the results are shown in Table 4.1.3. The density of untreated fibre was (1.525g/cm^3) lower than that of treated fibre, which is expected for untreated fibre contained less crystalline cellulose and more noncellulosic compounds than treated fibres as discussed in Section 2.5.5 and as supported by wet chemical analysis and FT-IR. However, it should be noted that the differences are not statistically significant.

Table 4.1.3: Density of untreated, bag retted and white-rot fungi treated fibre

Treatment(Ab.)	Fibre density (g/cm^3)
Raw	1.525±0.0156
1 week	1.530±0.0173
2 weeks	1.536±0.0148
D2B	1.529±0.0211
Pyc	1.534±0.0183
S.com	1.535±0.0103

4.1.7 Thermal Analysis of Bag Retted and White Rot Fungi Treated Fibre

The thermal properties of the treated and untreated hemp fibres were studied by thermogravimetric analysis (TGA) and differential scanning calorimetry (DTA). DTA curves were found to have three exothermic peaks coinciding with regions of weight loss observed using TGA as shown in Figures 4.1.10 and 4.1.11 for untreated and treated fibres. The initial temperature of decomposition and activation energy for different treatments are summarised in Table 4.1.4. The initial temperature of decomposition was obtained from the first exothermic peak, where the fibres begin to decompose. The activation energy was calculated for the first exothermic reaction, relating to the main fibre degradation step, by the Broido equation (Eq.4 and 5 in Section 2.5.6.2). The untreated hemp fibre started to degrade at about 523K, however, this value increased for all the treated fibres. The activation energy of untreated fibres was 106 kJ/mol, which increased for treated fibres to between from 111 to 127 kJ/mol, with D2B treated fibres having the highest activation energies (127 kJ/mol). The results suggested an increase in thermal stability for the treated fibres likely to be due to the reduced amount of non-cellulosic material and increased crystallinity.

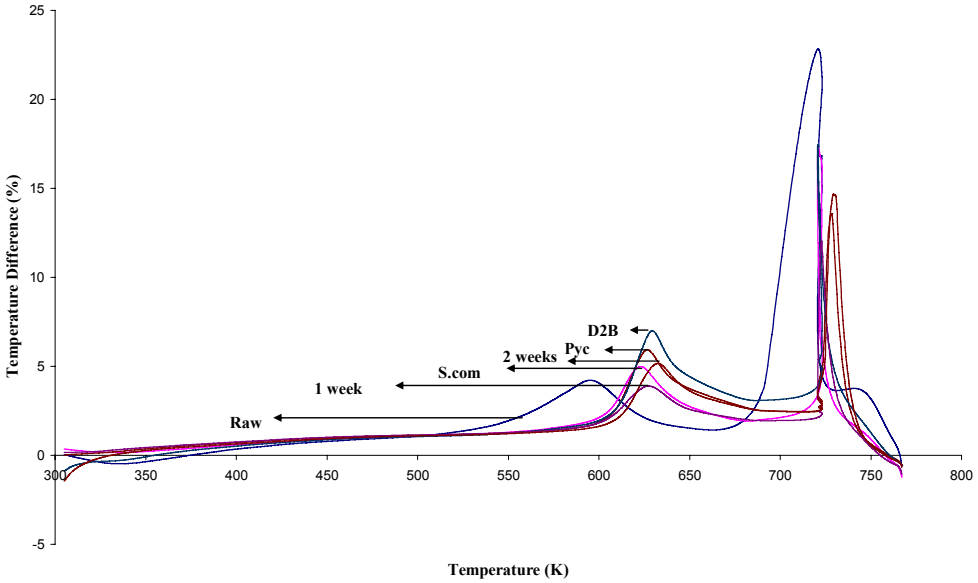

Figure 4.1.10: DTA curve of untreated, bag retted and white-rot fungi treated fibre showing exothermic peaks

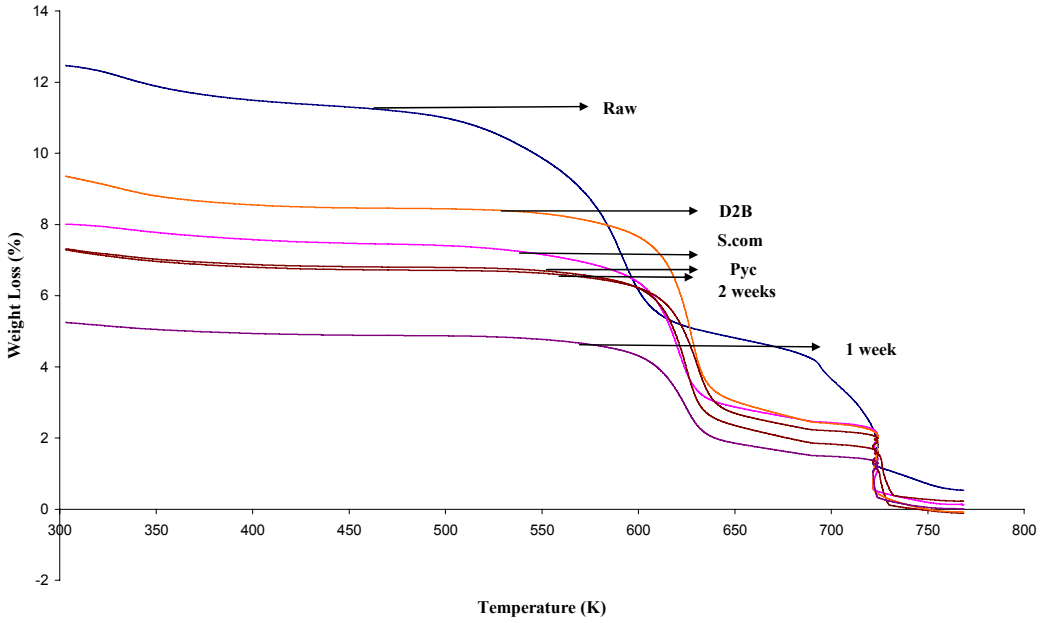

Figure 4.1.11: TGA curve of untreated, bag retted and white-rot fungi treated fibre showing three major weight loss regions

Table 4.1.4: Summary of thermal analysis for untreated, bag retted and white-rot fungi treated fibre

Treatment	Initial temperature of decomposition (K)	Activation energy(kJ/mol)
Raw	523	106
1 week	540	111
2 weeks	543	124
D2B	546	127
Pyc	542	125
S.com	547	125

4.1.8 Zeta Potential of Bag Retted and White Rot Fungi Treated Fibre

Zeta potential versus pH curves for untreated and treated fibres are shown in Figure 4.1.12. More negative values of zeta potential were generally obtained for treated fibres compared to the untreated fibre, suggesting they are more hydrophilic. Treatment of hemp fibre could affect the zeta potential through a number of competing processes which are discussed in Section 2.5.7. Removal of non-cellulosic material leading to exposure of more reactive hydroxyl sites would explain this increase of hydrophilicity. The action of fungal hyphae, which can produce fine holes in hemp fibre cell walls, would also be expected to make the fibre more susceptible to water absorption. On the other hand, an increase of the crystallinity index would be expected to reduce hydrophillicity and cause the zeta potential to become less negative. The fact that more negative values of zeta potential are obtained with fungal and bag rot treatments indicates that the influence of non-cellulosic compound removal and possible increased surface roughness is greater than the influence of higher crystallinity.

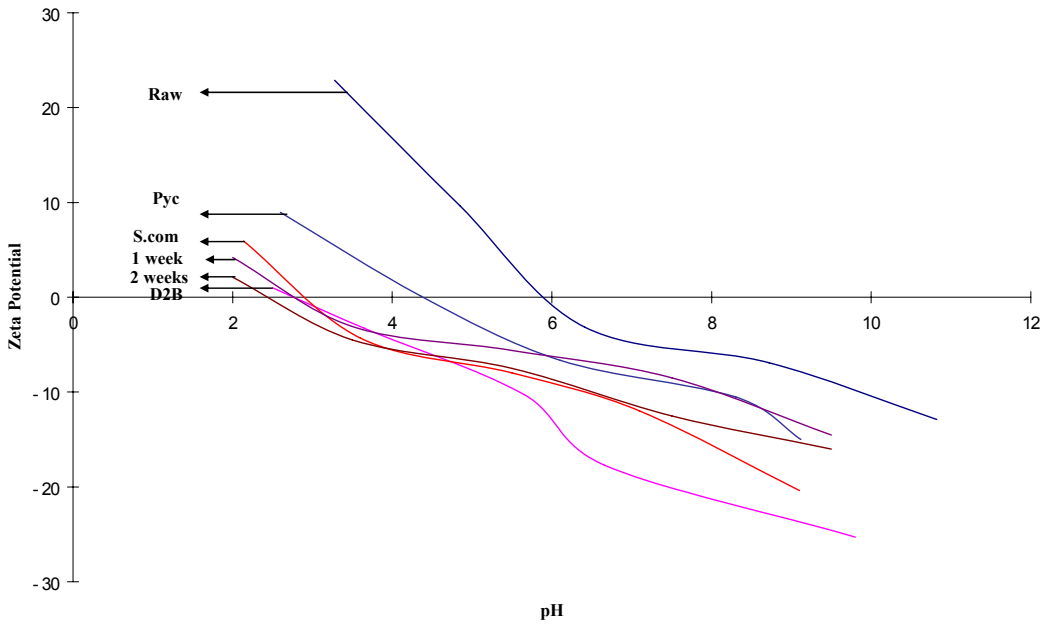

Figure 4.1.12: Zeta potential of untreated, bag retted and white-rot fungi treated fibre

4.1.9 Tensile Strength and Young's Modulus of Untreated, Bag Retted and White Rot Fungi treated Fibre

The tensile properties of white rot fungi and bag retted treated fibres decreased compared to untreated fibre as shown in Table 4.1.5 and Figure 4.1.13, in which the tensile strength from the two week retting treatment, was reduced the most (about 50%) to 342 MPa, followed by 402 MPa for the one week retting treatment, 410 MPa for S.com, 498 MPa for D2B and 512 MPa for Pyc. Hemp fibres can basically be considered as having rigid, crystalline cellulose microfibrils reinforcing an amorphous lignin and hemicellulose matrix; the tensile strength of hemp fibre is mainly influenced by its cellulose morphology. Removal of non-cellulosic compounds by fungal enzymes, which increases the fibre cellulose crystallinity as shown in XRD, has been reported to increase tensile strength (see Section 2.5.4.3). However, fungal hyphae can also break into the plant fibres, and

make fine holes as they pass through the cell wall to bring about structural degradation of cellulose, although this effect was not observed with the available SEM as previously discussed. The reduction of tensile strength of the treated fibre indicates that the influence of degradation is greater than that of the increase in crystallinity for cellulose.

Although, the Young's modulus of treated and untreated fibres is invariant within experimental uncertainty, the trend suggests a slight decrease in fibre Young's modulus for treated fibres (Table 4.1.5 and Figure 4.1.14). Highly cross-linking or branched lignin, pectin and hemicellulose provide a degree of structural integrity and rigidity, the removal of which could cause some reduction in fibre stiffness.

Table 4.1.5: Tensile strength and Young's modulus of untreated, bag retted and white-rot fungi treated fibre

Treatment(Ab)	Fibre tensile strength (MPa)	Young's modulus (MPa)
Raw	666±84	24000±9300
1 week	402±103	18200±9200
2 weeks	342±122	17900±7800
D2B	498±132	21600±8700
Pyc	512±97	20300±9400
S.com	410±110	22000±8500

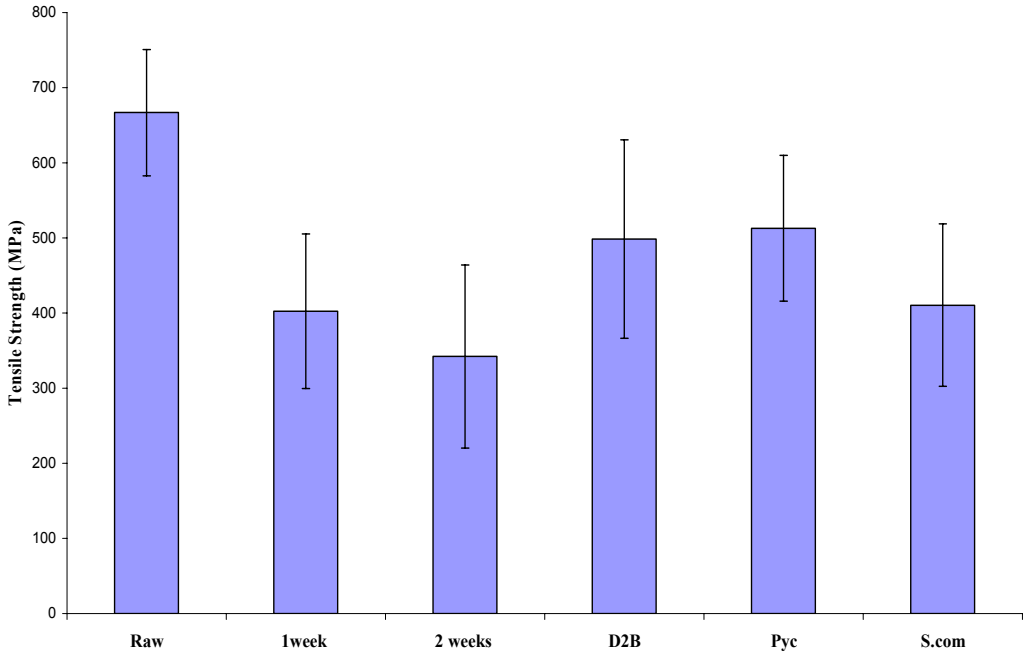

Figure 4.1.13: Single fibre tensile strength of untreated, bag retted and white-rot fungi treated fibre

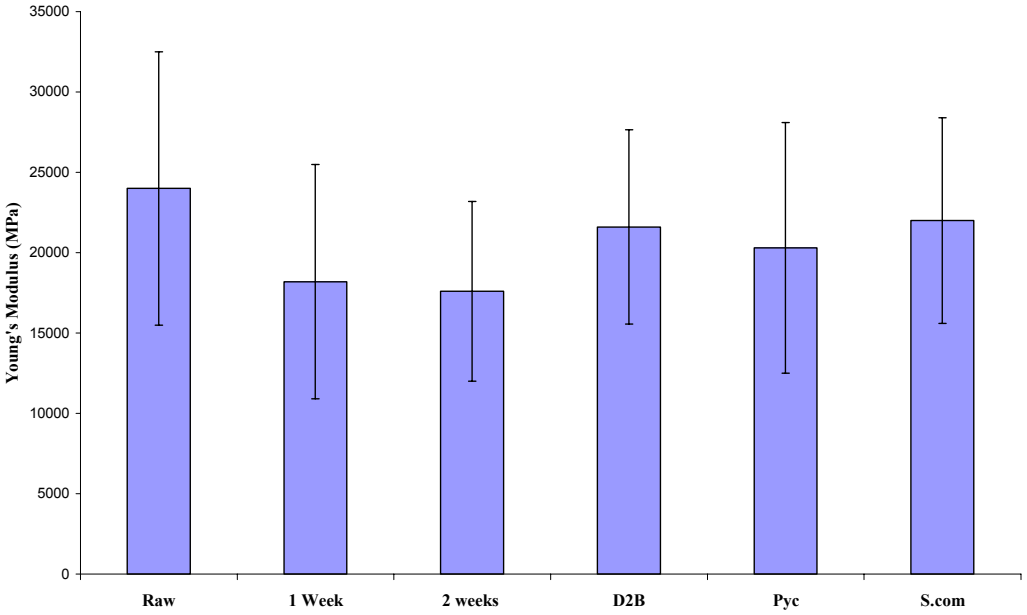

Figure 4.1.14: Young's modulus of untreated, bag retted and white-rot fungi treated fibre

4.2 Chelator/enzyme Treatments

Chelator/enzyme treatments were carried with the following purposes:

- Separation of hemp fibres from their fibre bundles
- Removal of non-cellulosic compounds in hemp fibres

4.2.1 Separation of Chelator/enzyme Treated Fibre

Visual inspection highlighted that the untreated fibre existed in fibre bundles. The enzyme-only treated fibres (P and L) remained in their bundles, whereas E, E2, E+L and E+P treated fibres showed good fibre separation (see Figure 4.2.1). The lack of significant separation for the enzyme-only treatments indicates that the enzymes are too specific in their activity. It appears that neither the pectinase nor the laccase can break down the waxy layer to remove pectin in the middle lamella and lignin in the secondary wall. Therefore the current project did not investigate the enzyme-only treatments further. Good separation with EDTMP.Na5 treatments and the combined EDTMP.Na5 and enzyme treatments was believed to be likely to have occurred due to the removal of calcium ions in the pectin as discussed in Section 2.1.6 and Section 2.4.1.5.1. Aligned fibres were easily produced by EDTMP.Na5 treatments and the combined EDTMP.Na5 and enzyme treatments and such fibres are considered useful for composites with long and aligned fibres.

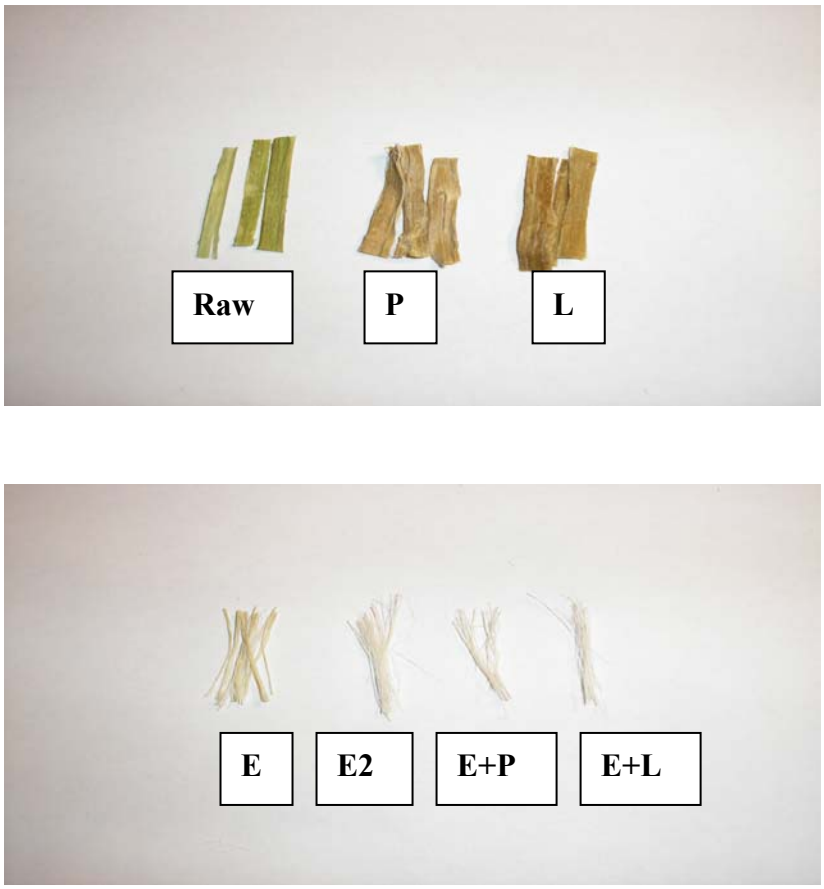

Figure 4.2.1: Digital pictures for untreated and chelator/enzyme treated fibres

4.2.2 Wet Chemical Analysis of Chelator/enzyme Treated Fibre

Table 4.2.1 shows the results of wet chemical analysis carried out on untreated and treated hemp fibres. Treatments with E and E2 were found to reduce the amount of wax, pectin hemicellulose and lignin in the fibre compared to the amounts in the untreated fibre. It was noted that E2 with higher EDTMP.Na5 concentration removed more pectin than E. The combined EDTMP.Na5 and enzyme treatments (E+P and E+L) reduced a little more of the non-cellulosic compounds than the EDTMP.Na5 treatment only (E, E2). Evidence of lignin removal was also obtained by a change in fibre colour; fibres with E, E2, E+P and E+L treatments were lighter in colour than the untreated fibre (see Table 4.2.1).

Table 4.2.1: Wet chemical analysis of untreated and chelator/enzyme treated fibres

Treatment	Wax (%)	Pectin (%)	Hemicellulose (%)	Lignin (%)	Colour of fibre	Separate
Raw	2.30	6.17	18.42	6.77	green	no
E	0.27	4.37	14.56	4.13	light	yes
E2	0.22	1.87	14.12	3.57	lighter	yes
E+P	0.22	3.52	13.95	4.01	lighter	yes
E+L	0.23	4.05	14.10	3.36	lighter	yes

4.2.3 FT-IR Spectra of Chelator/enzyme Treated Fibre

FT-IR spectra revealing the classical peaks for all samples are presented in Figure 4.2.2. Qualitatively, they appear similar; however, the peaks with distinct differences are around 1736 cm^{-1} and 1268 cm^{-1}. The peak around 1736 cm^{-1} can be attributed to the presence of the carboxylic ester in the pectin and wax, and the peak at 1268 cm^{-1} to the COO stretching in lignin. The peak around 1736 cm^{-1} shows a significant reduction for treated fibres indicating removal of pectin and wax. The range from 3000cm^{-1} to 3600cm^{-1} corresponds to OH stretching vibrations, mainly attributed to cellulose and lignin; after treatment, the relative intensities at 3600-3000cm^{-1}decreased, which suggests the treatments have removed lignin. The peak around 1268 cm^{-1} seen in untreated fibres, no longer exists in the treated fibres, which is considered to be due to the degradation of lignin.

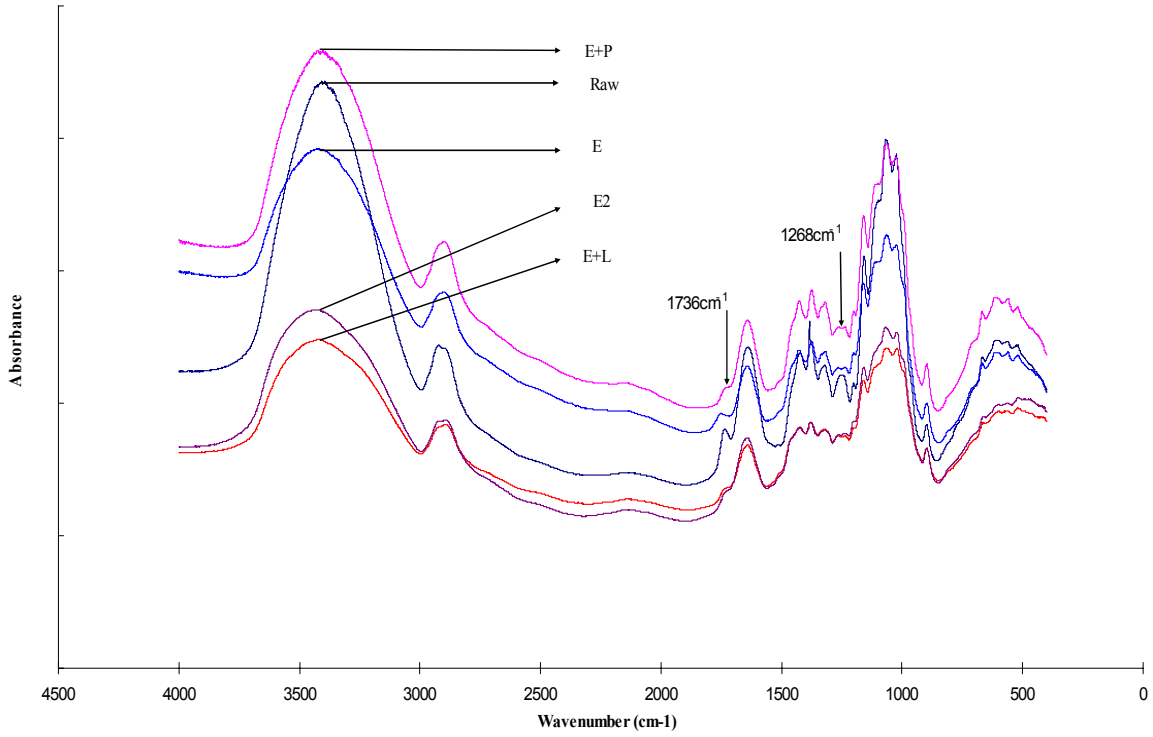

Figure 4.2.2: FT-IR spectra of untreated fibre and chelator/enzyme treated fibres

4.2.4 Morphology of Chelator/enzyme Treated Fibre

SEM micrographs of the surfaces of chelator/enzyme treated fibre are shown in Figures 4.2.3-4.2.6. Compared to untreated fibre, treated fibres show relatively clean surface which supports the removal of wax, pectin, lignin and hemicelluloses as supported by FT-IR and chemical analysis.

Figure 4.2.3: SEM of E treated hemp fibre

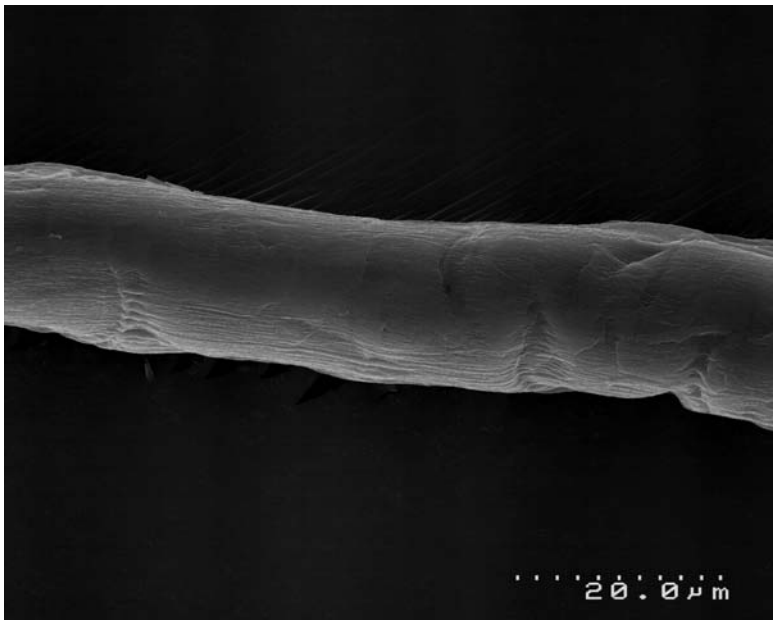

Figure 4.2.4: SEM of E2 treated hemp fibre

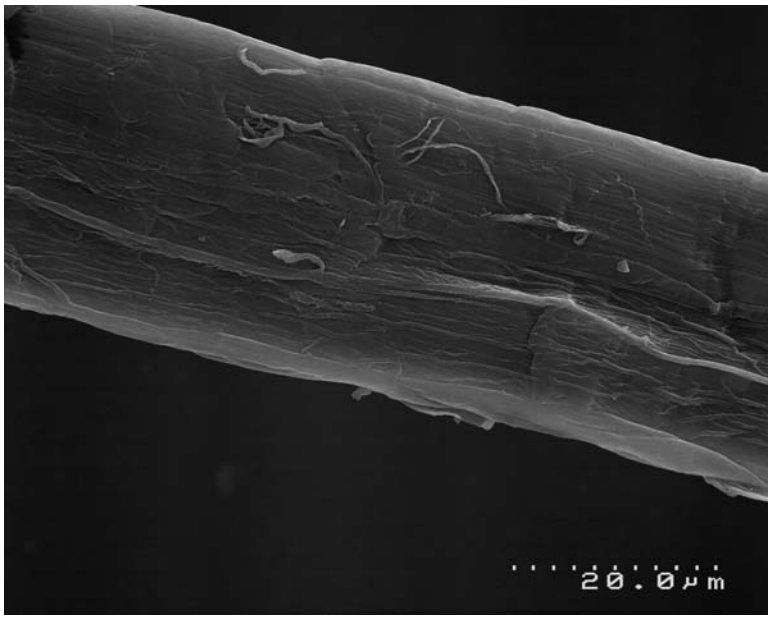

Figure 4.2.5: SEM of E+P treated hemp fibre

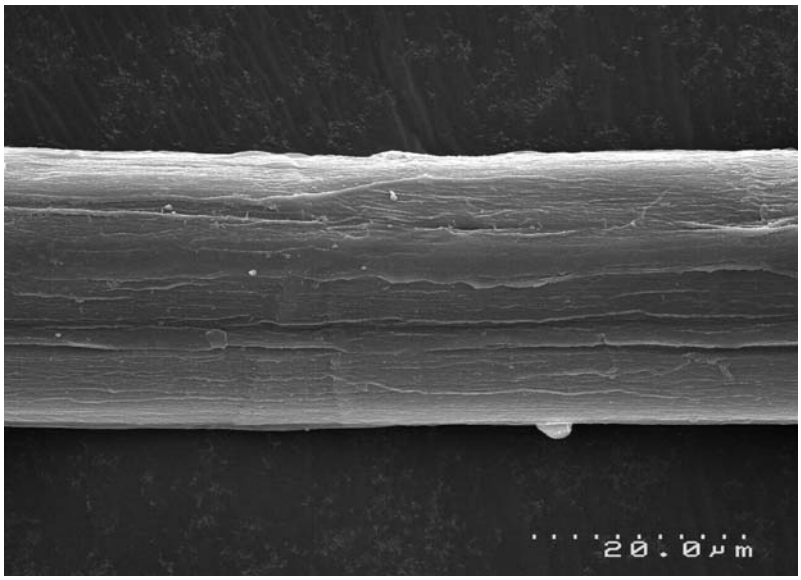

Figure 4.2.6: SEM of E+L treated hemp fibre

4.2.5 X-Ray Diffraction of Chelator/enzyme Treated Fibre

The crystallinity of chelator/enzyme treated hemp fibres increased as shown in Figure 4.2.7. The crystallinity index of the chelator/enzyme treated fibres (see Table 4.2.2) gives more evidence to support increased crystallinity of their fibre, for the crystallinity index of the treated fibre was around 86, a lot higher than the untreated fibre index which was 66.3. This increase could be due to the removal of amorphous non-cellulosic or amorphous cellulose compounds, as seen by chemical analysis and FT-IR, which would allow better packing of the cellulose chains; the trend of crystallinity was generally found to match the degree of non-cellulosic material removal.

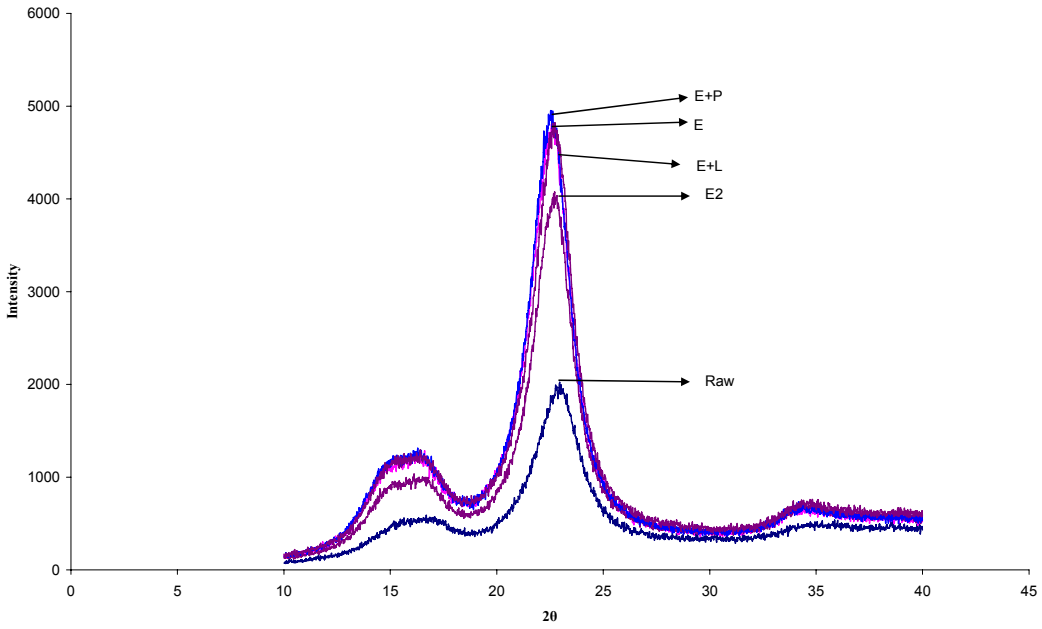

Figure 4.2.7: X-ray diffraction traces for untreated and chelator/enzyme treated fibres

Table 4.2.2: Crystallinity index of untreated and chelator/enzyme treated fibres

Treatment	Crystallinity index (%)
Raw	66.32
E	85.86
E2	86.35
E+P	86.14
E+L	85.82

4.2.6 Density of Chelator/enzyme Treated Fibre

The densities of treated fibre were higher than that of untreated fibre as shown in Table 4.2.3, which supports for treated fibre containing more crystalline cellulose and less noncellulosic compounds than untreated fibre. However, it should be noted that the differences are not statistically significant.

Table 4.2.3: Density of untreated, chelator/enzyme treated fibre

Treatment	Fibre density (g/cm^3)
Raw	1.525±0.0156
E	1.528±0.0106
E2	1.530±0.0129
E+P	1.532±0.0140
E+L	1.531±0.0178

4.2.7 Thermal Analysis of Chelator/enzyme Treated Fibre

Figures 4.2.8 and 4.2.9 show the DTA and TGA curves of untreated and treated fibres. A summary of the initial decomposition temperature for treated fibres is given in Table 4.2.4. The activation energies calculated from the slopes of TGA curves (see Section 2.7.4.2) are also tabulated in Table 4.2.4. The higher initial

temperature and higher activation energy values of the treated fibres support that highly crystalline cellulose leads to increased thermal stability.

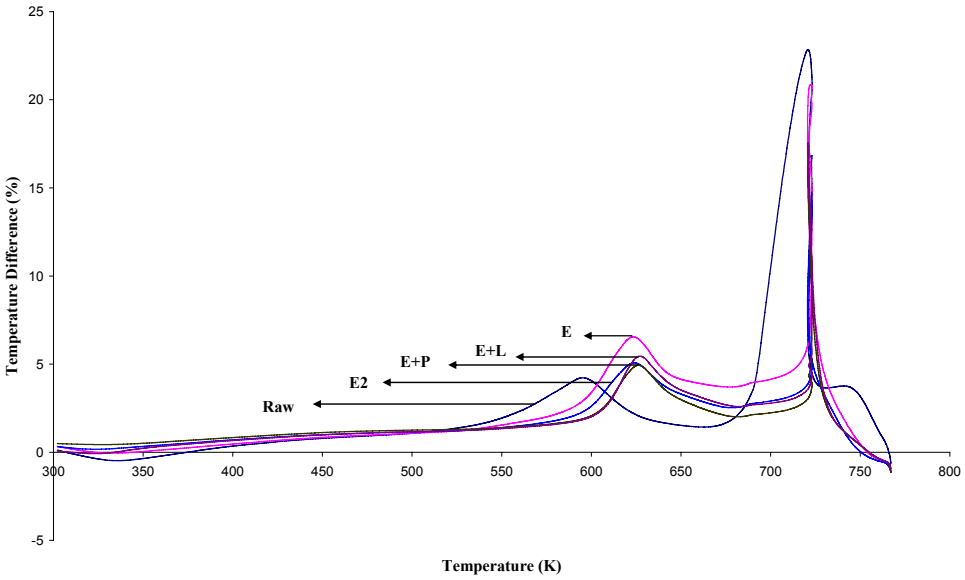

Figure 4.2.8: DTA curve of chelator/enzyme treated fibre

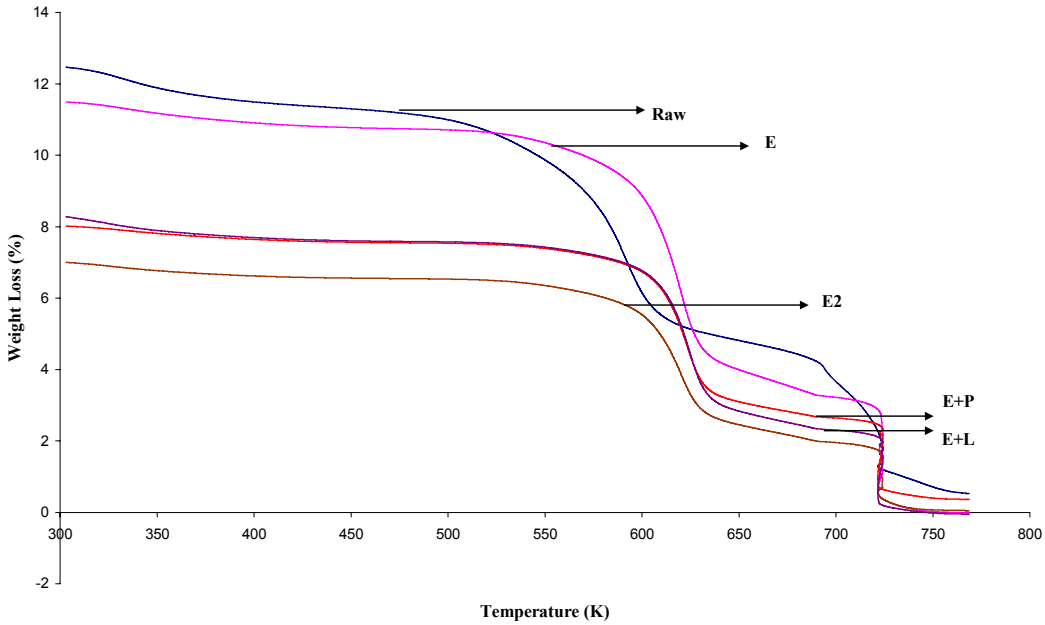

Figure 4.2.9: TGA curve of chelator/enzyme treated fibre

Table 4.2.4: Summary of thermal analysis of chelator/enzyme treated fibre

Treatment	Initial temperature of decomposition (K)	Activation energy(kJ/mol)
Raw	523	106
E	543	137
E2	571	162
E+P	578	164
E+L	581	153

4.2.8 Zeta Potential of Chelator/enzyme Treated Fibre

Zeta potential versus pH curves for untreated and treated fibres are shown in Figure 4.2.10, in which treated fibres gave more negative values of zeta potential then untreated fibre. Removal of non-cellulosic material leading to exposure of more reactive hydroxyl sites would tend to increase hydrophilicity which would result in a larger negative zeta potential. On the other hand, an increase of the crystallinity index would reduce hydrophillicity and cause the zeta potential to become less negative. From the results shown in Figure 4.2.10, the larger negative zeta potential values obtained all the other treatments indicates that removal non-cellulosic compounds have more influence than increased crystallinity.

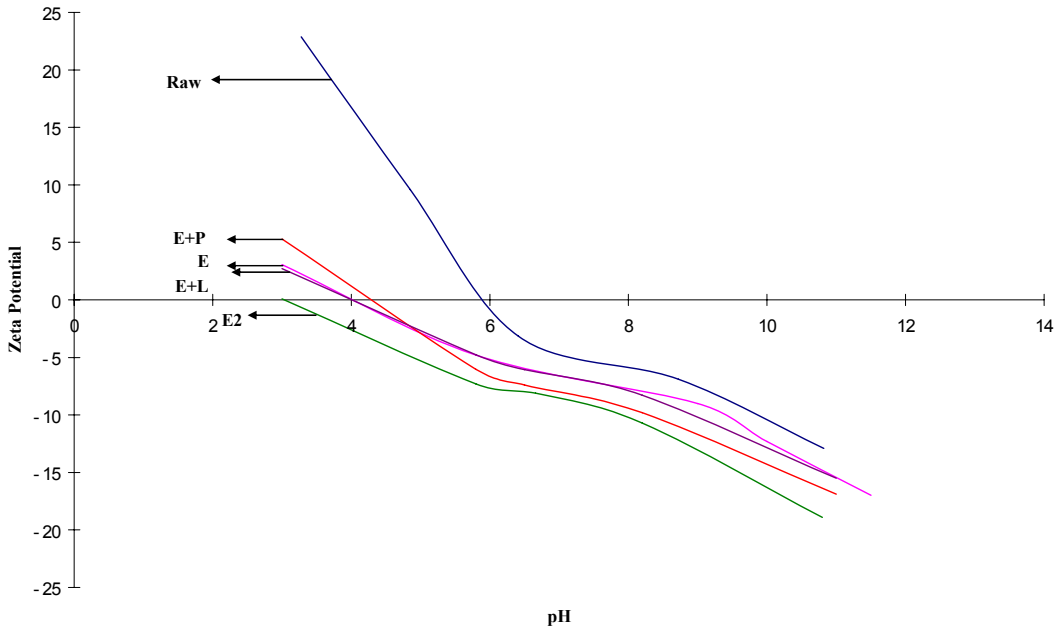

Figure 4.2.10: Zeta potential of chelator/enzyme treated fibre

4.2.9 Tensile Strength and Young's Modulus of Chelator/enzyme Treated Fibre

The tensile strengths and stiffness of fibres were slightly reduced for all treatments compared to untreated fibre as shown in Figure 4.2.11-12 and Table 4.2.5. As relatively weaker compared to cellulose coupled with the resulting of increased crystallinity, lignin, pectin and hemicelluloses removal would be expected to result in increased fibre tensile strength. However, cellulose degradation could occur (supported by SEM of treated fibre, in which striations become visible along the fibre length) during the treatments which would be expected to decrease the fibre tensile strength. The slight reduction of tensile strength of treated fibre indicates that the influence of cellulose degradation is larger than the influence of the higher crystallinity index. Although, the Young's modulus of treated and untreated fibres is invariant within experimental uncertainty, slight decreases in Young's modulus for treated fibres could be

caused by removal of highly cross-linking or branched lignin, pectin and hemicellulose.

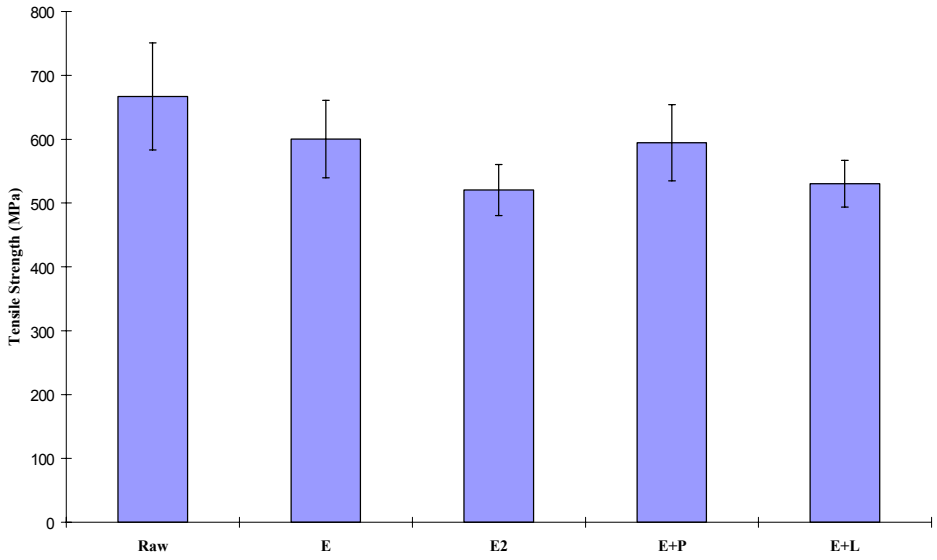

Figure 4.2.11: Single fibre tensile strength of untreated and chelator/enzyme treated fibres

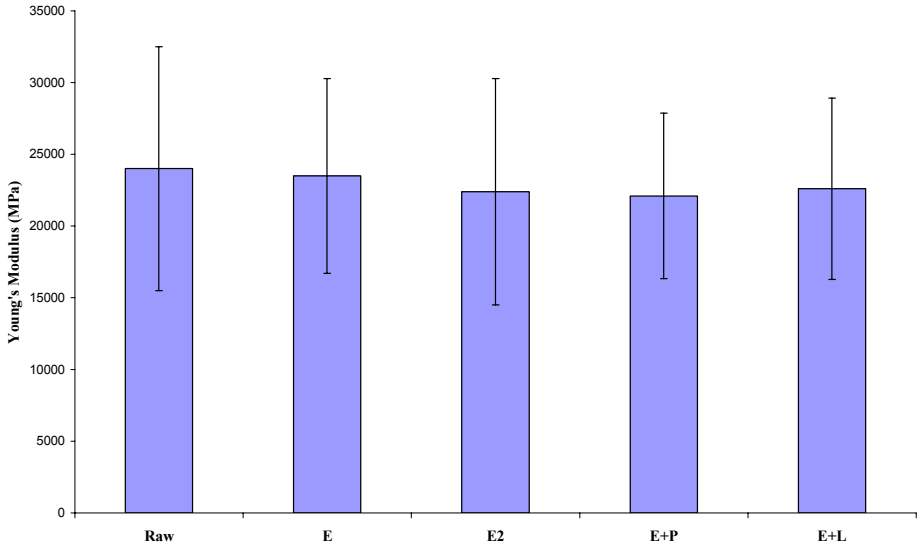

Figure 4.2.12: Young's modulus of untreated and chelator/enzyme treated fibres

Table 4.2.5: Tensile strength and Young's modulus of chelator/enzyme treated and untreated fibres

Treatment (Ab.)	Tensile strength(MPa)	Young's modulus (MPa)
Raw	667±84	24000±9300
E	600±61	23500±8700
E2	520±40	22400±8900
E+P	594±60	22100±6200
E+L	530±37	22600±8500

4.3 Composites Results

Short fibre composites were produced by extrusion and injection moulding. Fibres, polypropylene (PP) and a maleated polypropylene (MAPP) coupling agent were compounded using a twin-screw extruder, and then injection moulded into composite tensile test specimens. Long hemp fibre composite sheets were fabricated by film stacking and hot-press forming. Layers of PP film, PP/MAPP powder and hemp fibre were stacked alternately and the stack then was compressed in a hot press. The assessment of treatment effect on the tensile strength of short fibre composites and long aligned fibre composites is shown in the following section

4.3.1 Tensile Strength and Young's Modulus of Untreated, Bag Retted and White Rot Fungi Treated Short Fibre Composite

All white rot fungi treatments and bag retting treatments improved the tensile strength of composites (see Table 4.3.1 and Figure 4.3.1), despite treatment reducing single fibre strength. This suggested that improved strength for treated

fibre composites was achieved through improved interfacial bonding. Removal of non-cellulosic compounds (supported by chemical analysis, FT-IR and XRD results) and increased surface roughness (see fibre morphology section) would be expected to improve interfacial bonding between the fibre and matrix by exposing more effective contact area, increasing mechanical interlocking and increasing the potential for interaction between the hydroxyl sites and the MAPP coupling agent (see zeta potential results).

The stiffness of all treated fibre composites increase when compared with untreated fibre composites(see Table 4.3.1 and Figure 4.3.2), which could be assumed to be due to improved interfacial bonding giving good transfer of fibre stiffness into the composites, leading to higher composite stiffness than for untreated fibre, despite untreated fibre resulting in higher stiffness fibres.

Table 4.3.1: Tensile strength and Young's modulus of untreated, bag retted and white-rot fungi treated short fibre composites

Treatment(Ab)	Tensile strength (MPa)	Young's modulus (MPa)
PP	23.00±0.10	1260±30
Raw	35.46±0.70	4300±416
1 week	37.54±0.76	4860±623
2 weeks	43.69±1.18	6554±516
D2B	42.42±1.19	6236±627
Pyc	43.98±2.16	6450±421
S.com	45.33±3.01	6969±537

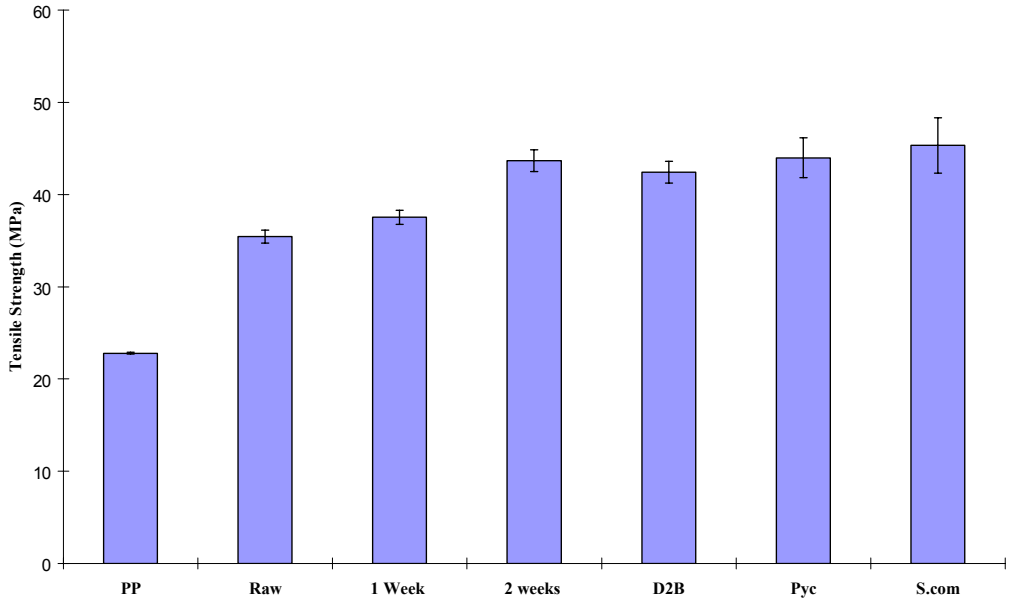

Figure 4.3.1: Tensile strength of untreated, bag retted and white-rot fungi treated short fibre composites

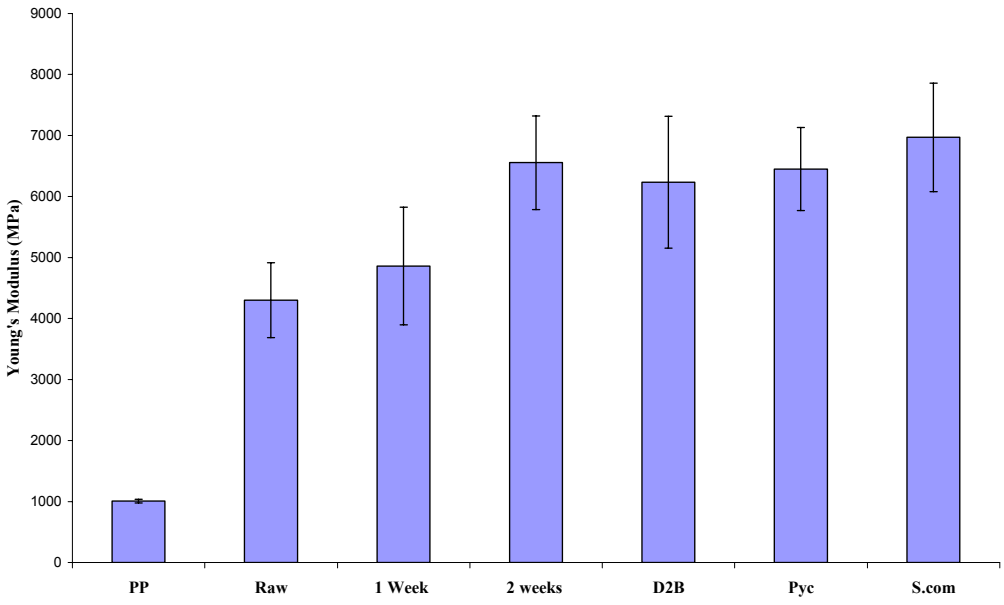

Figure 4.3.2: Young's modulus of untreated, bag retted and white-rot fungi treated short fibre composites

Evidence of improved interfacial bonding for treated fibres was obtained from examining composite fracture surfaces. Fracture surfaces of weaker untreated fibre composites (see Figure 4.3.3) generally showed debonding between fibre and the matrix. The stronger composites shown in Figure 4.3.4 for S.com treated fibre were observed to have better interfacial bonding between the fibre and matrix.

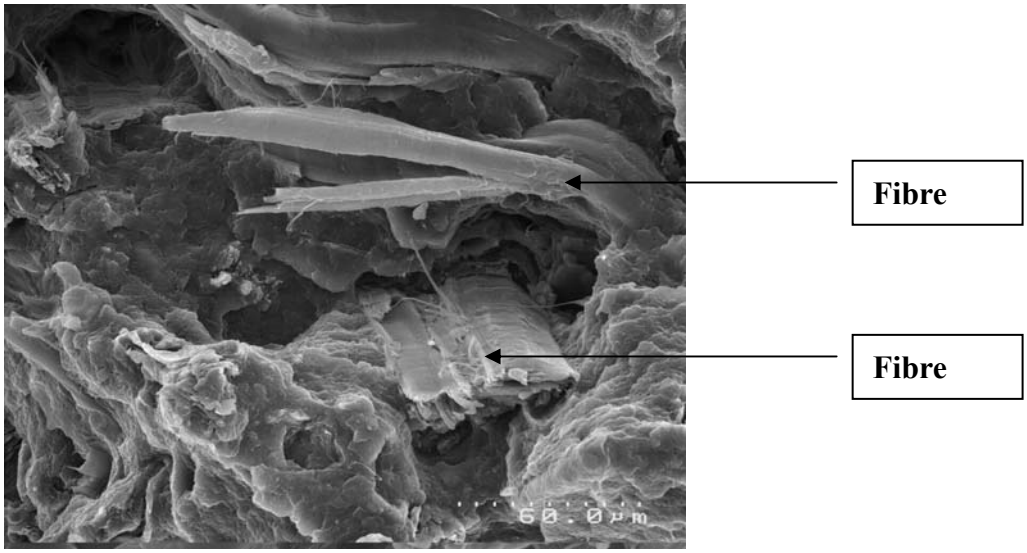

Figure 4.3.3: SEM of untreated short fibre composite fracture surface

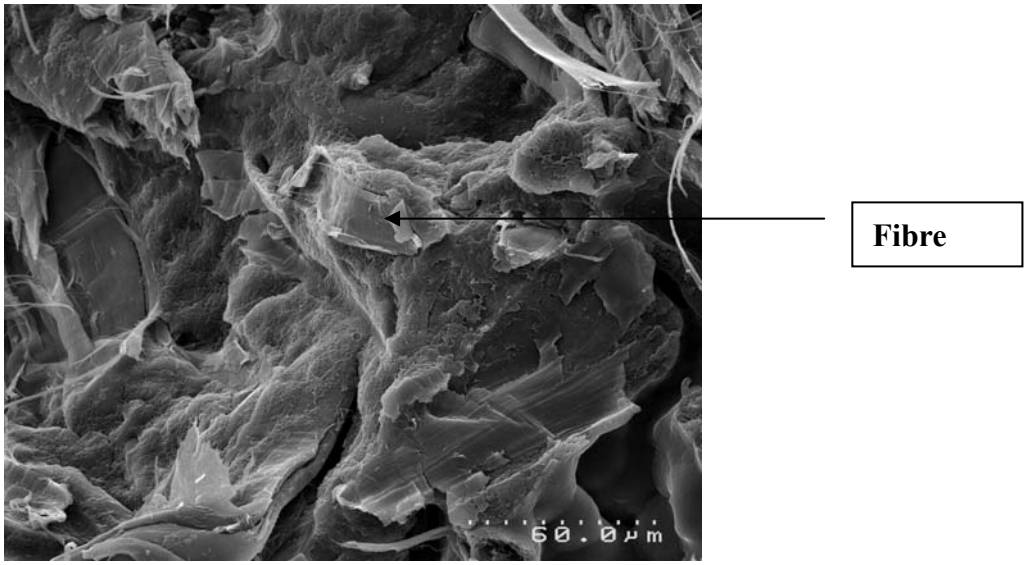

Figure 4.3.4: SEM of S.com treated short fibre composite fracture surface

4.3.2 Tensile Strength and Young's Modulus of Chelator/enzyme Treated Short Fibre Composites

Composite tensile strength and Young's modulus can be seen graphically in Figure 4.3.5-6 and is tabulated in Table 4.3.2. All treatments produced an improvement in composite strength and stiffness. The untreated hemp fibres were bundled together which would limit the effective surface area and fibre surfaces were covered non-cellulosic compounds such as wax, pectin and lignin, which would hinder chemical fibre-matrix bonding. Removal of these during treatment would separate fibre bundles and expose hydroxyl groups on the fibre surface. This would increase the interfacial bonding between the matrix and fibre with the MAPP coupling agent, resulting in improved composite strength despite the slightly lower single fibre strength for treated fibres. Improved interfacial bonding gave good transfer of fibre stiffness into the composites, leading to higher composite stiffness than for untreated fibre.

Table 4.3.2: Tensile strength and Young's modulus of chelator/enzyme treated short fibre composites

Treatment	Tensile strength(MPa)	Young's modulus (MPa)
PP	23±0.10	1260±30
Raw	35.46±0.70	4300±416
E	41.55±1.21	5230±404
E2	42.30±1.02	6270±476
E+P	41.73±0.92	6120±746
E+L	41.41±1.26	5900±369

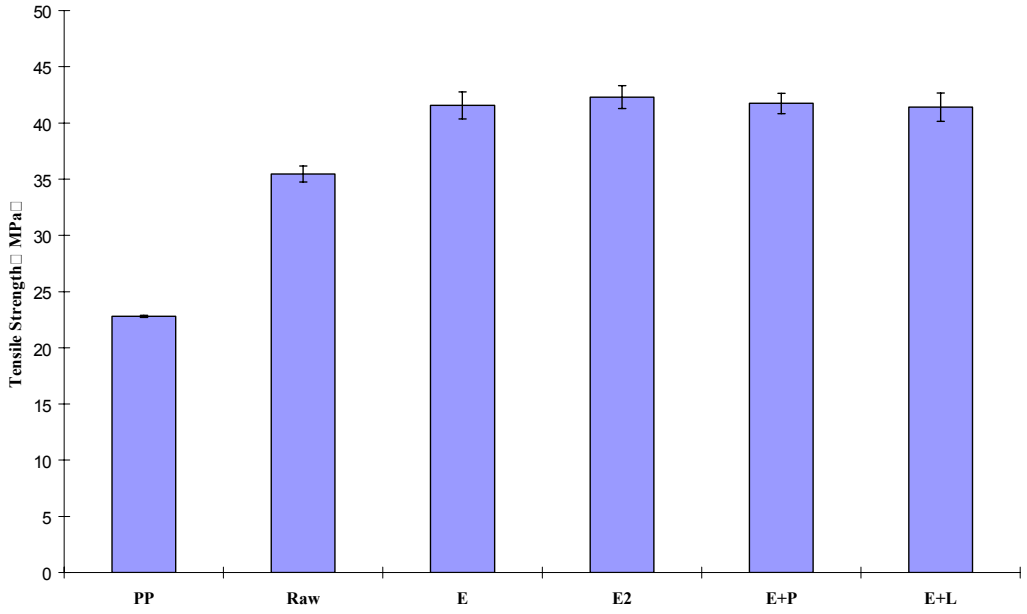

Figure 4.3.5: Tensile strength of chelator /enzyme treated short fibre composites

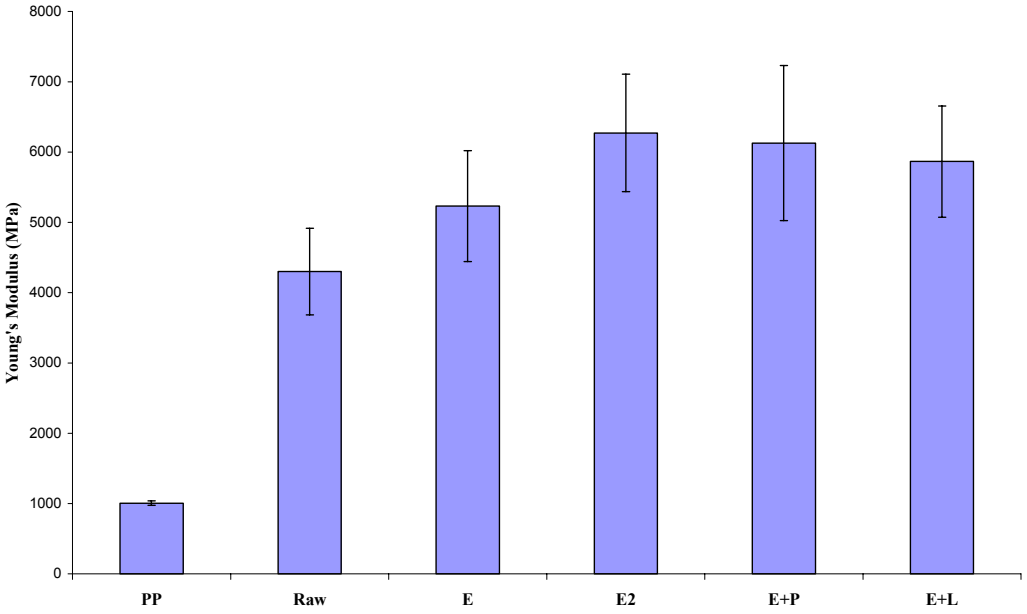

Figure 4.3.6: Young's modulus of chelator /enzyme treated short fibre composites

SEM photographs of untreated and treated fibre composite fracture surfaces are shown in Figure 4.3.3 and 4.3.7. Fracture surfaces for untreated fibre (see Figure 4.3.3) generally showed debonding between fibre and matrix, whereas, it was difficult to discern the actual interface between the fibre and matrix for the stronger composites as shown in Figure 4.3.7 for E2 treatment. This supports that higher tensile strength of composites is obtained through improved interfacial bonding between the fibre and the matrix.

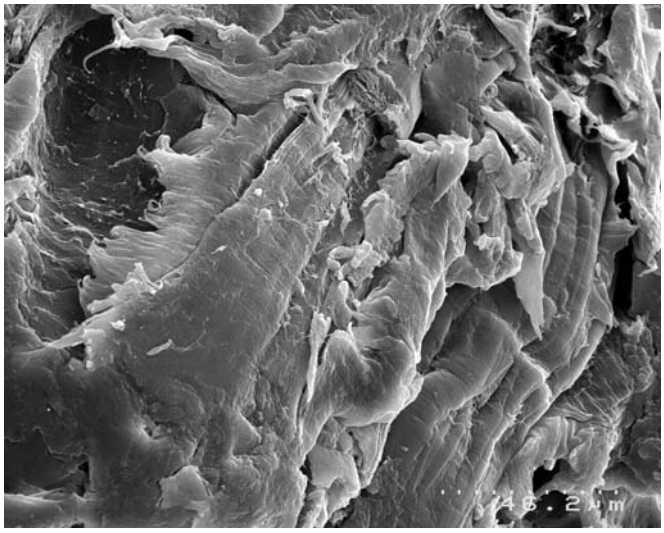

Figure 4.3.7: SEM of E2 treated short fibre composite fracture surface

4.3.3 Environmental and Economic Consideration of Chelator/enzyme Treatment

Environmental as well as economic factors must be considered when hemp fibre treatments are used on an industrial scale. Table 4.2.7 gives a relative assessment of environmental and economic factors with composite strength for each treatment. From an environmental perspective, EDTMP.Na5 (E) and the combined EDTMP.Na5 and enzymes treatments (E+P, E+L) have relatively low environmental impact. From an economic point of view (see Table 7), E would be the cheapest treatment, followed by E2. E+P and E+L were the least cost

effective, with no justification for use in terms of performance. Overall E and E2 treatments would achieve a good balance between economics, environmental and composite strength.

Table 4.3.3: Relative environmental, economic and composite strength summary for each chelator/enzyme treatment

Treatment	Environmental impact	Treatment costs				Composite strength(MPa)
		Chemical	Energy	Equipment	Processing	
E	Low	lowest	lowest	lowest	lowest	41.55
E2	Low	low	lowest	lowest	lowest	42.30
E+P	Low	higher	higher	higher	higher	41.73
E+L	Low	higher	higher	higher	higher	41.41

4.3.4 Assessment of Chelator and White Rot Fungi Treatment Effect on the Tensile Strength of Long Aligned Fibre Composite

The tensile strength of the long aligned fibre composites, which were fabricated using film-stacking and hot-pressing, was measured in order to assess the treatment effect. Chelator (E2) and white rot fungi (S.com) treatments improved the tensile strength of the composites as seen in Table 4.3.4. Both white rot fungi (S.com) as well as chelator (E2) treatments have been shown to remove non-cellulosic compounds, leading to fibre separation from its bundles. Separation would increase the effective surface, area of fibre allowing it to intermingle with the matrix. Removal of non-cellulosic compounds would also expose the hydroxyl groups on the fibre, and increase the potential for interaction between the hydroxyl sites and the MAPP coupling agent. In addition, the rougher surface of

the white rot fungi (S.com) treated fibre and the presence of holes in the cell walls may have improved the mechanical interlocking. This could explain the observed higher tensile strength of the fungi treated fibre composites.

SEM photographs of untreated and treated fibre composite fracture surfaces are shown in Figures 4.3.8 and 4.3.9. Fracture surfaces for untreated fibre (see Figure 4.3.8) generally showed fibre bonded together with a high degree of pull-out. Fracture surfaces for the strongest composite (Figure 4.3.9 for S.com treated fibre composite) showed more fibre separation and short length of pulled out fibre indicating better interfacial bonding. This further indicated that high tensile strength of composites can be obtained through improved interfacial bonding between fibre and matrix.

The tensile strength of long aligned fibre composites was generally higher than those of short fibre reinforced composite fabricating through injection moulding (Table 4.3.4), supporting that film-stacking and hot-pressing could be a suitable method to fabricate long fibre thermoplastic composites.

Table 4.3.4: Tensile strength of short and long aligned fibre composites

Treatment	Fibre tensile strength (MPa)	Short fibre composite tensile strength (MPa)	Long fibre composite tensile strength (MPa)
Raw	666±83.37	35.46±0.70	50.88±8.73
E2	520±45.26	42.30±1.02	67.45±10.39
S.com	410±68.78	45.33±3.01	73.12±10.23

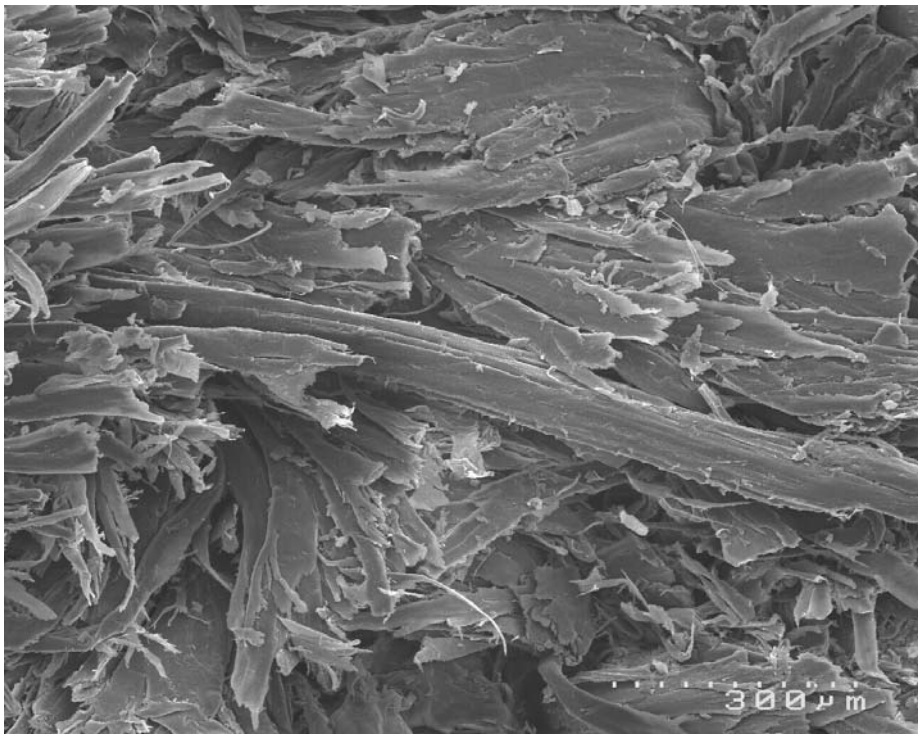

Figure 4.3.8: SEM of untreated long aligned fibre composite fracture surface

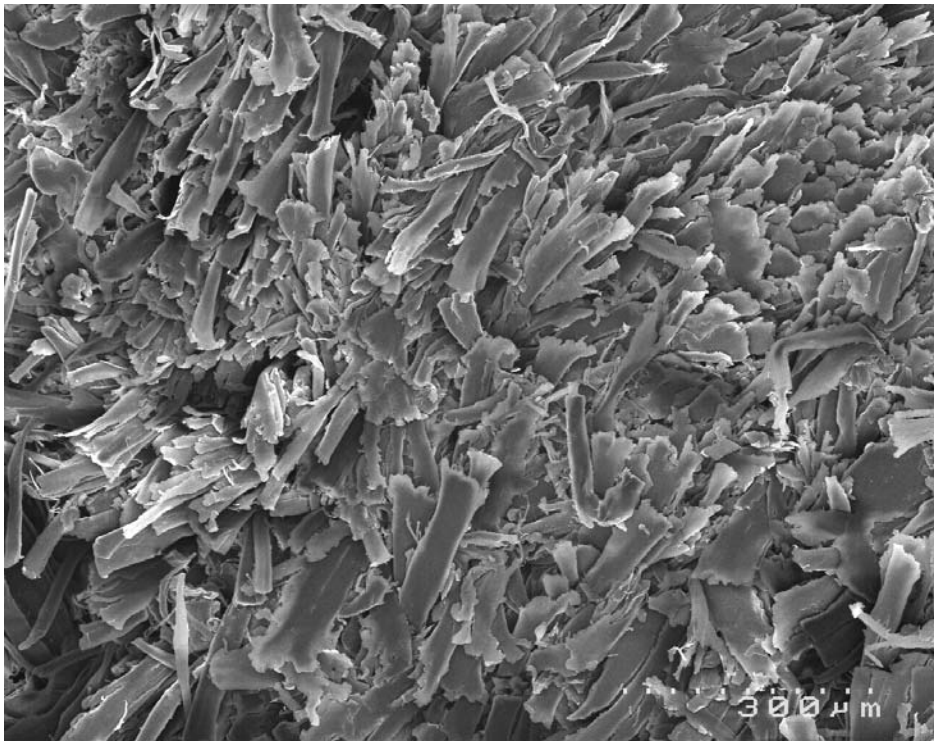

Figure 4.3.9: SEM of S.com treated long aligned fibre composite fracture surface

4.4 Composite Tensile Strength Modelling

4.4.1 Modelling for Short Fibre Composite

The Bowyer-Bader model was selected for this study as it takes into consideration the super-critical and sub-critical length distributions of fibres extracted from an actual composite (see section 2). In the case of Bowyer and Bader model, the tensile strength of a composite with short off-axis fibre could be determined from the sum of sub-critical and super-critical fibre strength contributions (taking into account fibre orientation) and the matrix contribution.

4.4.1.1 Fibre Contribution to Composite Strength

To obtain the tensile strength of a fibre-reinforced composite, it is necessary to investigate fibre and matrix properties, as well as the stress transfer that takes place at the interface between the fibre and matrix, which is usually characterised by the interfacial shear strength (IFSS). Therefore, in order to assess the fibre contribution to strength of short fibre composites, it is necessary to obtain the IFSS value of this composite. Single fibre pull-out testing and the Bowyer and Bader model were used in this study to assess the IFSS of short fibre composites and results from both methods have been compared.

4.4.1.1.1 Determination of IFSS Using the Single Fibre Pull-Out Test

Typical force-displacement curves for white rot fungi (S.com) treated and untreated hemp fibre PP specimens are shown in Figure 4.4.1. During the pull-out process, the force increased approximately linearly until failure of the interface, after which the load decreased while the fibre was extracted in a controlled way. The pull-out force for white rot fungi treated fibre PP specimens is higher than

that of untreated fibre PP specimen. The average IFSS (τ) of untreated and treated fibre PP specimens was calculated using Eq.6 and the results are presented in Table 4.4.1. The IFSS of white rot fungi treated fibre in PP was found to be 40% higher than untreated fibre in PP. It is likely that this can be credited to the removal of non-cellulosic compounds and increased surface roughness leading to increased exposure of more surface area, increasing potential for interaction between hydroxyl sites and the MAPP coupling agent, as well as increased mechanical interlocking providing better interfacial bonding.

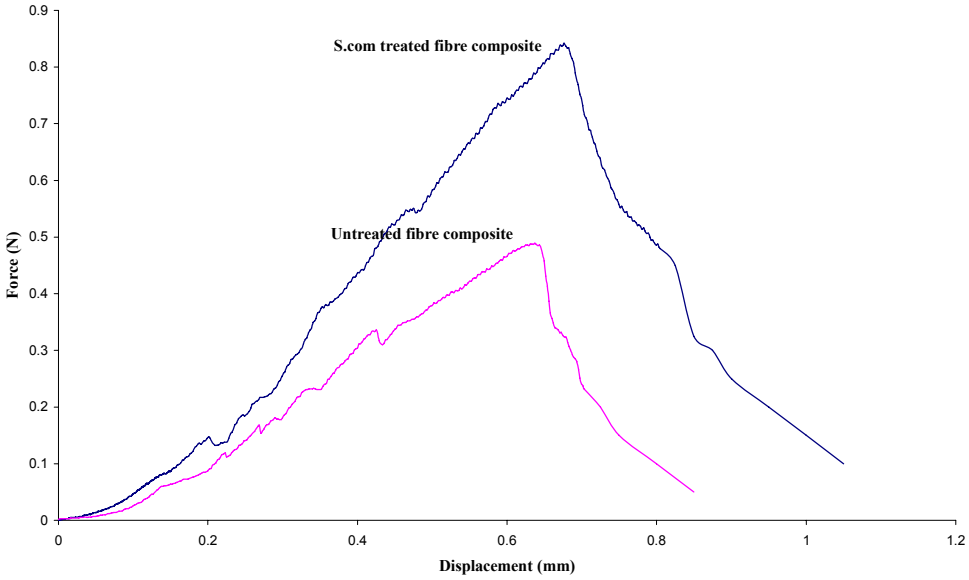

Figure 4.4.1: Single fibre pull-out test force –displacement curve for untreated and S.com treated fibre specimens

Table 4.4.1: IFSS from single fibre pull-out test for untreated and S.com treated fibre specimens

	Untreated fibre	White rot fungi(S.com) treated fibre
IFSS (τ) pull-out (MPa)	3.26	5.84

4.4.1.1.2 Determination of IFSS and Orientation Factor (K_1) Using the Bowyer and Bader Model

Factors required to calculate IFSS and orientation factor (K_1) using the Bowyer and Bader model include the tensile strength and Young's modulus of the fibre, matrix and composite, fibre volume fraction, fibre length distribution, sub-critical and super-critical fibre lengths and the volume fraction of sub-critical and super-critical fibre lengths. The tensile properties of fibre, matrix and composites were used from the previously described tensile tests (Table 4.1.5, and 4.3.1). The methods for obtaining the remaining factors are described in following sections.

Fibre Volume Fraction

The fibre volume fraction (V_f) can be calculated from the fibre weight fraction (W_f) using the Eq.12. Using a value of untreated fibre density (1.525g/cm^3) and white rot fungi treated fibre density (1.535g/cm^3), the fibre volume fraction obtained for the hemp fibre PP composites containing 40wt% hemp fibre was 0.282 for untreated fibre composite and 0.281 for white rot fungi (S.com) treated fibre composite. It is noted that this value has assumed an absence of voids; however, given the high pressure involved in extrusion and injection moulding processing, this is assumed sufficient in the current work. Where lower pressures are involved accurate calculation of V_f based on the void contents of composites, composite density, matrix weight content and fibre weight content would be recommended.

Fibre Length Distribution and Fibre Diameter

It is widely known that the compounding and moulding of composites leads to large reductions in the fibre length. Therefore, it was necessary to obtain the length distributions and average diameter of the fibres inside the composites after processing. Table 4.4.2 shows the average fibre length for treated fibre composites. It indicates that fibres, originally chopped to 10mm, were significantly shorter as a

result of processing. Figure 4.4.2 and 4.4.3 shows the fibre length distribution in untreated and treated fibre composites. It can be seen that both the treated and untreated fibre composites appeared to have very similar fibre length distributions.

Table 4.4.2: Average length and diameter of fibre in composites

	Untreated fibre	White rot fungi treated fibre
Average fibre length (mm) after processing	0.515	0.512
Average fibre diameter (μm) after processing	30	29

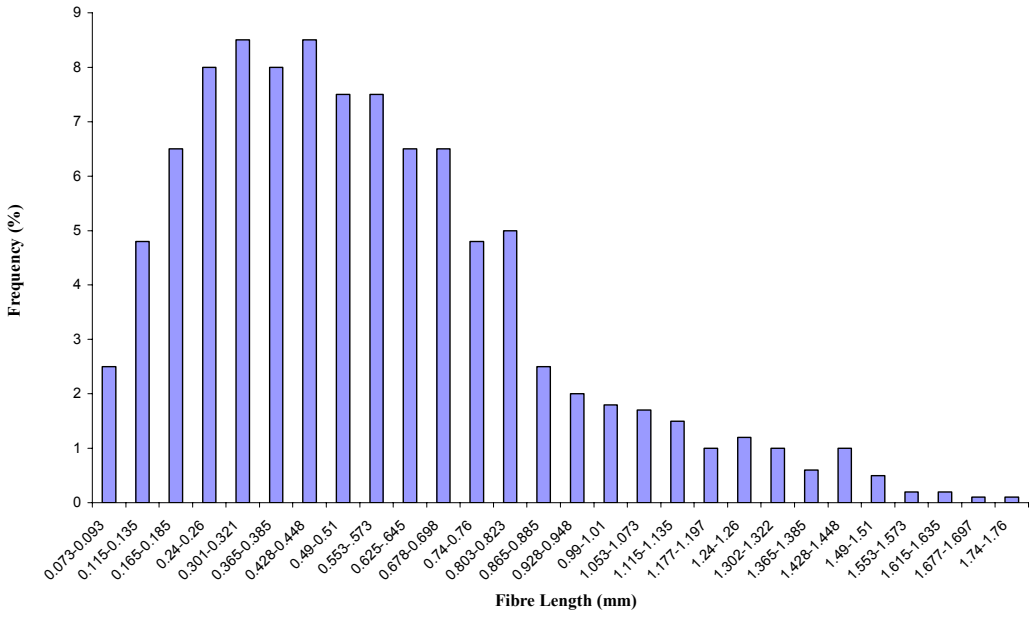

Figure 4.4.2: Fibre length distribution in untreated short fibre composite

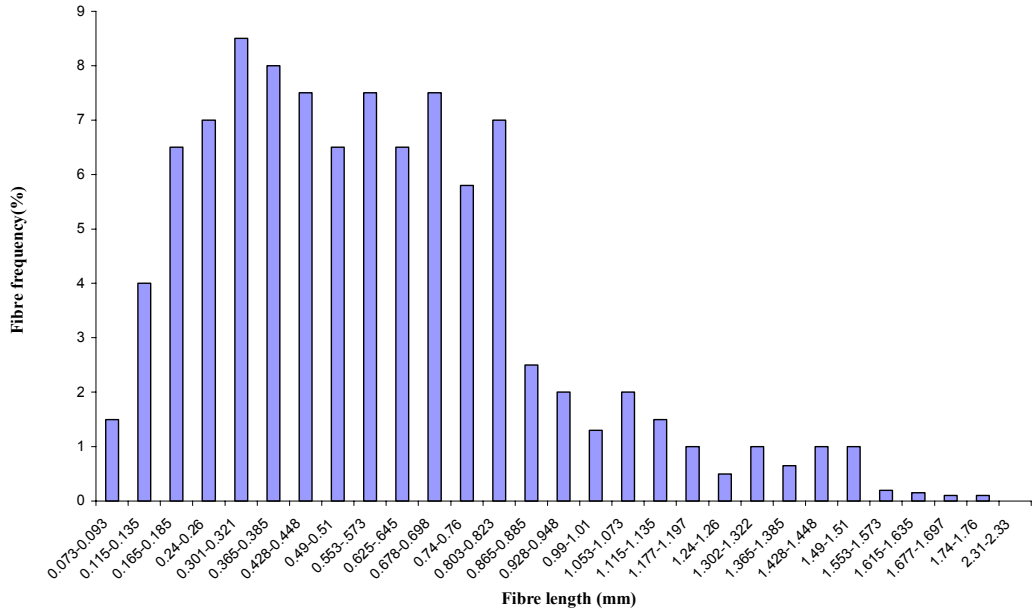

Figure 4.4.3: Fibre length distribution in white rot fungi (S.com) treated short fibre composite

Critical Fibre Length at ε_1 and ε_2 ($L_{\varepsilon 1}$ and $L_{\varepsilon 2}$)

A typical tensile stress-strain curve for treated fibre composites is shown in Figure 4.4.4. All untreated and treated fibre composites failed at a strain of more than 0.03. For this reason, strains of 0.01 and 0.02 were selected for ε_1 and ε_2 respectively, and then the composite stress (σ_{c1} and σ_{c2}) at these two strain values was obtained according to the stress-strain curve. An assumed value of τ was taken and the corresponding critical fibre lengths $L_{\varepsilon 1}$ and $L_{\varepsilon 2}$ at the two levels of strain were calculated from Eq.15a.

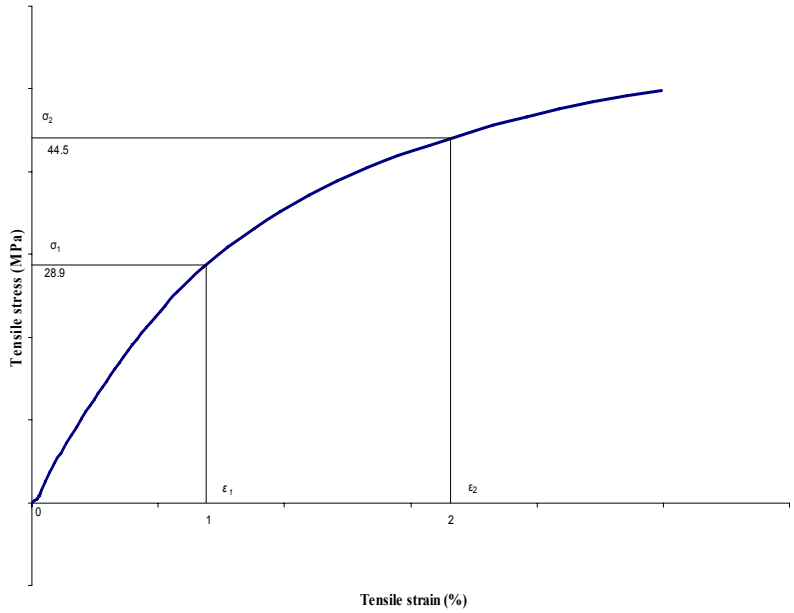

Figure 4.4.4: A typical tensile stress-strain curves of white rot fungi treated hemp fibre composites

Sub-critical and Super-critical Fibre length Volume Fraction

The volume fraction of the sub-critical fibre lengths (V_i) and the volume fraction of super-critical fibre lengths (V_j) were obtained according to the follow steps:

- The volume of each individual fibre was calculated by multiplying the fibre cross-sectional area by the fibre length.
- Summation of all the fibre volumes.
- Determination of volume fraction of each fibre in the fibre distribution, by dividing the volume of each fibre by the sum of all the fibre volume.
- Determination of the volume fraction of each fibre in the composites (V_i, V_j) by multiplying the fibre volume fraction in the sample by V_f

Interfacial Shear Strength (IFSS) and Orientation Factor (K_1)

Taking into account E_f , E_m, V_f , ε_{c1} ,$\varepsilon_{c2,}$ $\sigma_{c1,}$ $\sigma_{c2,}$ D and combining all the fibre length distributions obtained via direct measurements from each composite, IFSS(τ) and K_1 were obtained according the Bowyer and Bader method (using Eq.15a,18,19a,20a,21a,22,23) and the results are shown in Table 4.4.3. It can be seen that IFSS for white rot fungi treated fibre composites was higher than that for untreated fibre composites, supporting improved interfacial bonding between the matrix and fibre.

Table 4.4.3: IFSS of untreated and white rot fungi (S.com) treated fibre composites obtained according the Bowyer and Bader model

	Untreated fibre composite	S.com treated fibre composite
Young's modulus of fibre: E_f(MPa)	24,000	22,000
Young's modulus of matrix: E_m (MPa)	1,260	1,260
Volume fraction of fibre: V_f (%)	28.2	28.1
Strain in composites at point 1: ε_{c1}(%)	1	1
Strain in composites at point 2: ε_{c2}(%)	2	2
Stress in the composites at $\varepsilon_{c1;}$ σ_{c1}(MPa)	25.5	28.9
Stress in the composites at ε_{c2} ;σ_{c2}(MPa)	34.7	44.5
Fibre diameter: D (μm)	30	29
Interfacial shear strength: τ (MPa)	6.68	8.92
Fibre orientation factor : K_1	0.43	0.46

Although, results from both the single fibre pull-out test and the Bowyer and Bader model indicate that the white rot fungi treatment increased IFSS, results

from the pull-out test are lower than those from the Bowyer and Bader model. This raises the need to consider the assumptions made for these two methods, which had been discussed in Section 2.7.1 and 2.8.4.2. Overall it could be considered that, in particular, due to Poisson contraction and axial loading in the pull-out test, the IFSS would be expected to be lower for this test than for the Bowyer and Bader model as observed experimentally. Therefore, in a composite material, the Bowyer and Bader model can be considered to give a more relevant value for IFSS.

4.4.1.1.3 Determination of Critical Fibre Length for Short Fibre Composites

The critical fibre length (L_ε) can be calculated using the mean fibre strength (σ_f), the mean fibre diameter (D) and the interfacial shear strength (IFSS) (τ). Taking into account IFSS (τ) obtained according to the Bowyer and Bader model, critical fibre length (L_ε) for untreated and S.com treated fibre composites were calculated using Eq (15b). The critical fibre length (L_ε) of untreated short fibre composites was found to be 1.49 mm , while the critical fibre length (L_ε) of S.com treated short fibre composites was 0.67 mm (Table 4.4.4).

In untreated short fibre composites, based on the Bowyer-Bader model (Eq 19b, 20b), fibres shorter than L_ε make up 97% of the total fibre volume, and yet account for only 88.5% of the fibre contribution to composite strength; fibres longer than L_ε make up 3% of the total fibre volume and account for 11.5% of the fibre contribution to composite strength. For S.com treated short fibre composite, fibres shorter than L_ε make up 43% of the total fibre volume, and yet account for 28% of the fibre contribution to composite strength; fibres longer than L_ε make up 57% of the total fibre volume and account for 72% of the fibre contribution to composite strength. It can be seen that the super-critical length fibres are more

effective in contributing to the overall composite strength compared to sub-critical length fibres.

4.4.1.1.4 Fibre Orientation of Injection Moulded Composites

In the case of the Bowyer and Bader model, good agreement between the theoretical and experimental values have been observed for axially aligned fibre composites when K_1=1, and for randomly oriented fibre composites when K_1=0.2 [18]. Assuming all the fibres are perfectly aligned in the axial direction (K_1=1), in the case of untreated short fibre composites, fibre contribution to the composite strength would have a theoretical tensile strength of 48.83 MPa, while S.com treated short fibre composite would have a theoretical tensile strength of 62.12 MPa.

The value of K_1=0.43 for untreated short fibre composite and K_1=0.46 for S.com treated short fibre composite suggest that the fibre orientation in those composites is slightly better than a typical random fibre orientation. Taking into account of K_1, fibre contribution to the tensile strength of untreated short fibre composite is 21 MPa, while fibre contribution to the tensile strength of S.com treated short fibre composite is 28.58 MPa(Table 4.4.4), which indicates that only a small fraction of the fibre effectively contribute to the strength of the composites.

4.4.1.2 Matrix Contribution to Composite Strength

Matrix contribution to composite strength was determined according Eq(21b), in which σ_m is the matrix stress at the failure strain of composites, which is 22 MPa for untreated short fibre composite and 22.2 MPa for S.com treated short fibre composite, respectively; the matrix contribution to the tensile strength of untreated fibre composite is therefore 15.8MPa, and the matrix contribution to the tensile strength of S.com treated fibre composite is 15.9MPa.

Table 4.4.4: Tensile strength of untreated and white rot fungi (S.com) treated short fibre composites obtained according to the Bowyer and Bader model

	Untreated fibre composite	S.com treated fibre composite
Fibre tensile strength :σ_f(MPa)	666	410
Fibre diameter: D (μm)	30	29
Interfacial shear strength: τ (MPa)	6.68	8.92
Critical fibre length: L_ε (mm)	1.49	0.67
The total fibre volume of fibres shorter than L_ε	97%	43%
The total fibre volume of fibres longer than L_ε	3%	57%
Fibre contribution to composite strength (fibre shorter than L_ε)	89%	28%
Fibre contribution to composite strength (fibre longer than L_ε)	12%	72%
Theoretical fibre contribution to tensile strength of composites when assuming all the fibres are perfectly aligned in the axial direction (K_1 = 1)	48.8	62.1
Fibre orientation factor : K_1	0.43	0.46
Theoretical fibre contribution to tensile strength of composites when taking into account of K_1	21	29
The matrix stress at the failure of composites (MPa)	22	22
The strength contribution of the matrix (MPa)	15.8	15.9
Tensile strength of short fibre composite according to the Bowyer-Bader model (MPa)	36.8	44.5
Experimental tensile strength of short fibre composite (MPa)	35.5	45.3

4.4.1.3 Total Predicted Composite Strength

Summed the fibre contribution and matrix contribution to the tensile strength of a composites, the tensile strength of untreated short fibre composite was found to be 36.8MPa, and the tensile strength of S.com treated short fibre composite was 44.5MPa (Table 4.4.4), which closely match the experimentally values (35.5MPa for untreated short fibre composite and 45.3 MPa for S.com treated short fibre composite).

It can thus be concluded that in order to produce a strong composite material, as well as the need to use strong fibre, the good fibre-matrix interfacial adhesion is essential as great a proportion of the fibres as possible need to be longer than the critical fibre length (L_ε), fibres need to be oriented as well as possible in the loading direction and matrix strength is also important.

4.4.2 Modelling for the Tensile Strength of Long Aligned Fibre Composite

The modified model based on the simple "rule of mixture" by taking account of void content was used to predict the tensile strength of composites, and the results obtained experimentally and mathematically were compared.

4.4.2.1 Composite Density (ρ_c)

Density of untreated, white rot fungi (S.com) treated and E2 treated fibre were used from the previously described density tests (Table 4.1.3 and 4.2.3) and density of composites were measured and the results are shown in Table 4.4.5. For composites, the density with untreated fibre was the lowest (0.918g/cm^3), which suggests that its void content was high. The density of white rot fungi (S.com) treated fibre composites was the highest (1.074g/cm^3) suggesting a lower void content.

Table 4.4.5: Density of fibre and composite

Treatment	Fibre density (g/cm^3)	Composite density (g/cm^3)

Raw	1.525±0.0156	0.918±0.0188
E2	1.530±0.0129	0.998±0.0234
S.com	1.535±0.0103	1.074±0.0304

4.4.2.2 Fibre Weight Content, Void Volume Content (V_p), Fibre Volume Content (V_f) and Matrix Volume Content (V_m) of Composite

The fibre content (w_f) obtained via direct measurement from each composite and the matrix content (w_m) calculated according to Eq (29) is shown in Table 4.4.6. Taking into account ρ_f, ρ_m, ρ_c, and w_f, w_m, void (V_p), fibre (V_f), and matrix (V_m) contents of composites were determined using Eq (26,27,28) and the results are shown in Table 4.4.6. A higher void content in untreated fibre composites could be explained by the existence of much larger fibre bundles with more wax and other non-cellulosic compounds on the fibre bundle surfaces, which could be expected to reduce impregnation, resulting in a higher void content than for treated fibre composites. Conversely, for composites with chelator (E2) treated fibre, where the fibre bundles had been separated and non-cellulosic compounds removed, better impregnation appears to have resulted in a lower void content. Based on void content, composites with white rot fungi (S.com) treated fibre appeared to have the best impregnation.

Table 4.4.6: The weight content of fibre and matrix, the volume content of void, fibre and matrix

Treatment	w_f (%)	w_m (%)	V_p (%)	V_f (%)	V_m (%)
Raw	43	57	16	26	58
E2	43	57	9	28	63
S.com	44	56	2	31	67

4.4.2.3 Comparison of Composite Strength with Models

The matrix stress at the failure strain of the composite was determined from a stress-strain curve for polypropylene (see Figure 4.4.5) and the results are presented in Table 4.4.7. The tensile strength of composites was calculated according to the simple "rule of mixtures" using Equations 10, 12, and 13 and the results are shown in Table 4.4.8. Unfortunately, the simple "rule of mixtures", which neglects the void content, predicts that the tensile strength of untreated fibre composites should be higher than those of treated fibre composites, an opposite trend to that obtained experimentally.

Alternatively, the modified model based on the simple "rule of mixtures" taking account of voids was used to calculate composite tensile strength. The results calculated according to the modified model (Eq.25) are given in Table 4.4.5 and it can be seen that tensile strength calculated for treated fibre composites is higher than that for untreated fibre composites, and the trend (125.17MPa for untreated, 128.12MPa for E2 treated and 130.16MPa for S.com treated) matches the experimental trend (58.88, 67.45 and 73.12). However, results from the modified model are higher than those from the experiments. This is not surprising when the assumptions of the modified model are considered. The modified model used to predict the theoretical tensile strength of composites has assumed that the reinforcing fibres in the composites are perfectly aligned in the axial direction. In reality, however, the actual fibres were not all aligned in the axial direction perfectly; off-axis fibre would be expected dramatically to reduce the composite tensile strength dramatically. In addition, fibre can be damaged during composite processing, which can account for deviations in composite experimental properties from the theoretical prediction. Moreover, the failure criterion of the composite was the failure of the fibre. A mean fibre tensile strength was taken as the failure strength of the fibre. However, plant fibres are naturally in a curly form, even after carding. Therefore, under load, each fibre may carry a different stress and would not break at the same time. Possibly, the fibres may break in a form of

one by one during composite failure; this seriously reduced the load carrying capacity of the plant fibre composite. This was one of the main reasons that the tested strength was far smaller than the value predicted by the modified model. Therefore, for further works, an effectiveness factor is suggested to be taken into account to describe the fibre failure strength in the composite. Although, mentioned above, it appears that taking account of voids in the modified model could be a simple way to effectively model the influence of interfacial bonding.

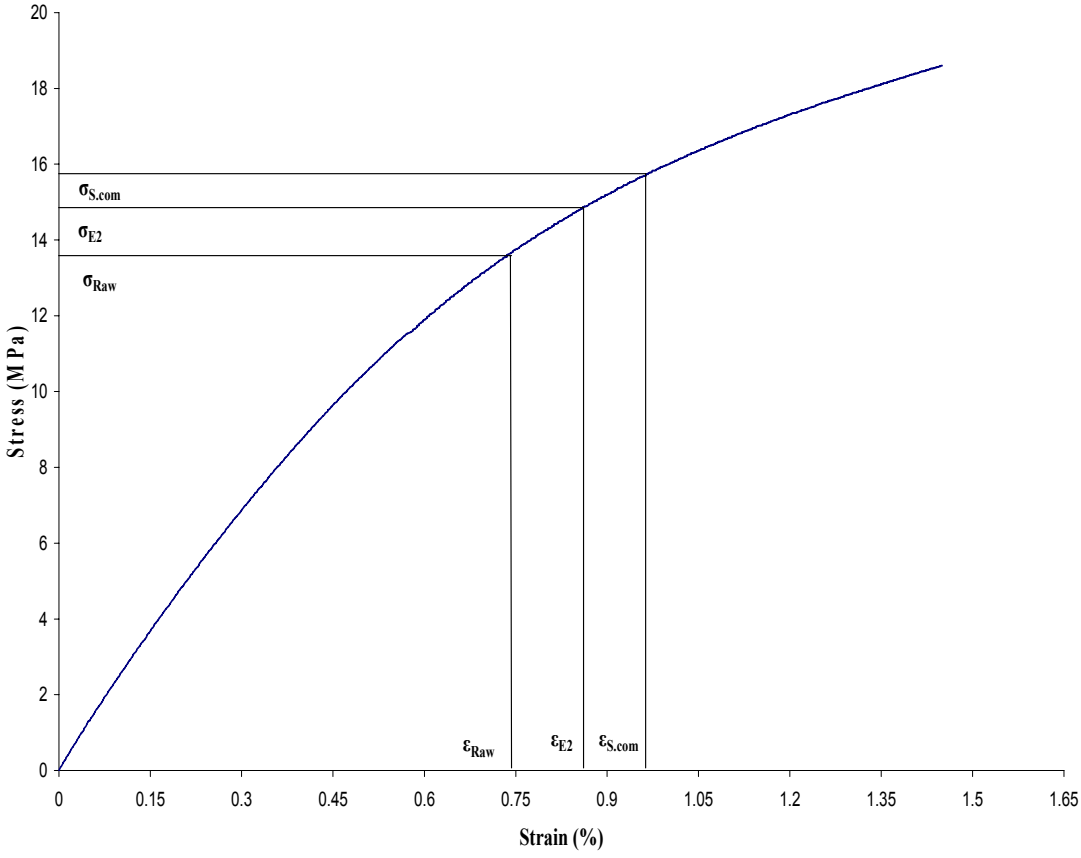

Figure 4.4.5: Stress-strain curve for polypropylene used to obtain the matrix stress at the failure strain of each long aligned fibre composite

Table 4.4.7: The matrix stress at the failure strain of the composite

Treatment	Failure strain of the composite (%)	Matrix stress at the failure strain (MPa)
Raw	0.75	13.79
E2	0.87	14.89
S.com	0.97	15.44

Table 4.4.8: Experimental composite tensile strength compared to calculated values using mathematical model

Treatment	Tensile strength of composite (MPa) according to "rule of mixtures"	Tensile strength of composite (MPa) according to modified model	Experimental tensile strength of composite (MPa)
Raw	214.7	125.2	50.9
E2	170.1	128.1	67.5
S.com	140.2	130.2	73.1

Chapter 5: Conclusions

5.1 Bag Retting and White Rot Fungal Treatments

The study found that white rot fungi and bag retting treatments removed non-cellulosic compounds such as wax, pectin, hemicellulose and lignin (see wet chemical analysis and FT-IR). The removal of non-cellulosic compounds, especially pectin, leads to separate hemp fibres from their bundles. This reduction of non-cellulosic compounds is also believed to be responsible for the observed increase in both crystallinity and thermal stability of the fibre evidenced by XRD and thermal analysis. In addition, white rot fungi and bag retted treatments supposed to increase surface roughness of fibre by fungal hyphae.

5.2 Chelator/enzyme Treatments

All chelator/enzyme treatments removed wax, pectin, lignin and other non-cellulosic compounds from hemp fibre, as well as separated hemp fibres from their bundles. As a consequence, the crystallinity and thermal stabilities of the treated fibres increased.

5.3 Composite Results

For white rot fungi and bag retted treatments, the removal of non-cellulosic compounds along with increased surface roughness associated with increased effective surface are believed to increase exposure of OH groups (as supported by zeta potential), and increase mechanical interlocking, giving increased interfacial bonding resulting in increased composite strength for bag retting and white rot fungi treatments despite the reduction in fibre strength.

For chelator\enzyme treatment, removal of non-cellulosic compounds is suspected to have increased the amount of OH groups exposed on the fibre surface, which could assist in bonding with the matrix in the presence of MAPP, as evidenced by the increase in composite tensile strength, despite the reduction in fibre strength. It should be noted that treatment with EDTMP.Na5 alone gave the best performance and would be the cheapest and most environmentally friendly to perform.

Long aligned fibre composites, which were fabricated by film-stacking and hot-pressing, generally presented higher tensile strength than short fibre reinforced composite fabricating through injection moulding, supporting that film-stacking and hot-pressing could be a suitable method to fabricate long fibre thermoplastic composites.

5.4 Composite Tensile Strength Modelling

Both the single fibre pull-out test and the Bowyer and Bader model were used to determine the interfacial shear strength (IFSS) of injection moulded untreated and S.com treated fibre composites. The single fibre pull-out test and the Bowyer and Bader method yielded different results; IFSS was found to be lower for the single fibre pull-out test compared to the Bowyer and Bader model, which is not surprising considering the different conditions and assumptions of these tests. However, both the single fibre pull-out test and the Bowyer-Bader model give higher IFSS for white rot fungi treated fibre composites than that for untreated fibre composites. This further demonstrates that white rot fungi (S.com) treatment increases the interfacial bonding between fibre and matrix, which is likely to be due to removal of non-cellulosic compounds such as wax, pectin, and lignin as well as the increased roughness of the fibre surfaces. The tensile strength of short fibre composites was predicted using the Bowyer-Bader model, which indicated

that in order to produce a strong composite, as well as the need to use strong fibre, the following are required:

- good fibre-matrix interfacial adhesion
- as great a proportion of the fibres as possible need to be longer than the critical fibre length (L_ε), fibres need to be oriented as well as possible in the loading direction
- good matrix strength

Long aligned fibre composites were fabricated by film-stacking and hot-pressing. The tensile strength of untreated and treated fibre composites measured and compared with results obtained by modelling taking account of voids. Although, the results obtained from experimental and mathematical modeling were different, both experimental and mathematical showed that tensile strength of the E2 and S.com treated fibre composites were higher than for untreated fibre composites, which is likely to be as result of improved hemp fibre interfacial bonding with PP by treatment. Therefore, taking account of voids in composites strength modeling could give good prediction reasonably.

Chapter 6
Recommendations

The results obtained from this study have proved that bag retting and white rot fungi treatment and chelator/enzyme treatment are effective and environmentally friendly methods to improve the interfacial bonding between PP and hemp fibre. Some recommendations for future work have been proposed as follow:

- During storage required for the industrial production of hemp fibre composites, hemp fibre would decay due to standard bacterial and fungal processes. Assessing the decay that occurs during storage such that it could be taken account of for further processing, is recommended for future research.

- The application of natural fibre composites is limited mainly to low-strength non-structural components. Therefore, future work should be conducted to improve the mechanical properties of the composites so that they can be used for structural components. It might be possible, based on the results of this current thesis, that long aligned fibre composites could be fabricated with high-volume fibre content to obtain high mechanical properties.

- Natural fibre reinforced thermoplastic composites are recyclable, but not biodegradable. It is therefore suggested that bio-derived and/or biodegradable polymer matrices reinforced with hemp fibre to produce novel biocomposites to replace and substitute for hemp fibre–reinforced petroleum based plastic composite, thus offering agriculture, environmental, manufacturing, and consumer benefits.

Reference

1. Hill S. Cars that grow on trees. New Scientist 1997; (2067): p. 36-39
2. Karus M, Kaup M. Natural fibres in the European automotive industry. Journal of Industrial Hemp 2002; 7(1): p. 119-131
3. Wambua P, Ivens J, Verpoest I. Natural fibres: can they replace glass in fibre reinforced plastics? Composites Science and Technology 2003;63(9): p.1259-1264
4. Mohanty AK, Misra M, Drzal LT, Selke SE, Harte BR, Hinrichsen G. Natural Fibres, Biopolymers, and Biocomposites: An Introduction. In: Mohanty AK, Misra M, Drzal LT, editors. Natural fibres, biopolymers, and biocomposites. Taylor & Francis. Boca Raton, Florida, p.1-36 (2005)
5. Pickering KL, Beckerman GW, Alan SN, Foreman NJ. Optimising industrial hemp fibre for composites. Composites: Part A. 2007; 38: 461-468
6. Pickering KL, and Ji C. The effect of poly [methylene(polyphenyl isocyanate)] and maleated polypropylene coupling agents on New Zealand radiata pine fibre/polypropylene composites. J Reinf Plast Comp 2004; 23: p. 2011-2024
7. Pedro J, Franco H, Gonzalez AV. Fibre-Matrix Adhesion in Natural Fibre Composites. In: Mohanty AK, Misra M, Drzal LT, editors. Natural fibres, biopolymers, and biocomposites. Taylor & Francis. Boca Raton, Florida, p.177-230 (2005)
8. Clarke AF, Wang XG, Hurren CJ. Degumming of bast fibres. United States Patent. US2004/0191888 AI (2004)
9. Daniel G, Volc J. Cryo-FE-SEM & TEM immune-techniques reveal new details for understanding white-rot decay of lignocelluose. C.R. Biologies 2004; 327: p. 61-871
10. Kashyap DR, Vohra PK, Chopra S, Tewari R. Applications of pectinases in the commercial sector: a review. Bioresour Technol 2001;77: p.215-227

11. Camarero S, Garc´ıa O, Vidal T. Efficient bleaching of non-wood high-quality paper pulp using laccase-mediator system. Enzyme Microb Technol 2004; 35: p.113–120
12. Stuart T, Liu Q, Hughes M, McCall RD, Sharma HSS, Norton A. Structural biocomposites from flax—Part I: Effect of bio-technical fibre modification on composite properties. Composites: Part A 2006; 37: p.393–404
13. Bismarck A, Mishra S, and Lampka. Plant fibres as reinforcement for green composites. In: Mohanty AK, Misra M, Drzal LT, editors. Natural fibres, biopolymers, and biocomposites. Taylor & Francis. Boca Raton, Florida, p.37-109 (2005)
14. Pervaiz M, Sain MM. Carbon storage potential in natural fibre composites. Conservation and Recycling 2003; 39(40): p. 325-340
15. Lilholt H, Lawther JM. Natural organic fibres. In: Kelly A, and Zweben C. editors, Fibre reinforcements and general theory of composites Comprehensive composite materials. vol. 1.
16. Mclntosh DJ, Barge R, Brown T, 5 minute guide to industrial hemp in New Zealand. Compiled by New Zealand hemp industries association
17. Schafer T, Honermeier B. Effect of sowing date and plant density on the cell morphology of hemp (*Cannabis sativa* L.) Industrial Crops and Products 2006; (23): p. 88–98
18. Beckerman G. Performance of hemp-fibre reinforced polypropylene composite materials. PhD Thesis of Material and Process Engineering, the University of Waikato 2008.
19. Pe′rez J, Mun˜oz-Dorado J, de la Rubia T, Martı′nez J. Biodegradation and biological treatments of cellulose, hemicellulose and lignin: an overview. Int Microbiol 2002; 5: p.53–63
20. Madsen B. Properties of Plant Fibre Yarn Polymer Composites. PhD Thesis, the Technical University of Denmark 2004.

21. Rowell RM, Han JS, Rowell JS. Characterization and factors effecting fibre properties. Natural Polymer and Agorofibres Composites. E.L.A. L. a. M. Frolline, L.H.C., Editor. 2000
22. Goda K, Sreekala MS, Gomes A, Kaji T, Ohgi J. Improvement of plant based natural fibers for toughening green composites—Effect of load application during mercerization of ramie fibers. Composites: Part A 2006; (37): 2213-2220
23. Anne Belinda Thomsen. Hemp raw materials: The effect of cultivar, growth conditions and pretreatment on the chemical composition of the fibres. Master Thesis, the Technical University of Denmark 2004
24. Manson JAE, Wakeman MD, Bernet N. Composite processing and manufacturing-an overview. In: Kelly A, Zweben C, editors. Comprehensive composite materials, vol. 2. Elsevier, 2000. p.577-609
25. Van de Velde K, Kiekens P. Thermoplastic polymers: overview of several properties and their consequences in flax reinforced composites. Polymer Testing 2001; 20(8): p. 885-893
26. Muzzy JD. Thermoplastics-Properties. Comprehensive Composite Materials. In: Kelly A, Zweben C, editors. Comprehensive composite materials, vol. 2. Elsevier, 2000. p. 57-77
27. Lawrence T. Interfaces and interphases. In: Daniel B, Miracle and Steven L, Donaldson, editors. ASM Handbook, vol. 21. p. 169-180
28. Matthews FL, Rawlings RD. Composite Materials: Engineering and Science. Chapman and Hall (1994)
29. Pedro J, Franco H, Gonzalez AV. Fibre-Matrix Adhesion in Natural Fibre Composites. In: Mohanty AK, Misra M, Drzal LT, editors. Natural fibres, biopolymers, and biocomposites. Taylor& Francis. Boca Raton, Florida, 2005. p.177-230

30. Lonergan GY. Physiological and degradative behaviour of a white rot fungus PhD Thesis, School of Engineering and Science Swinburne University of Technology Australia
31. Call HP, Mucke I. History, overview and application of mediated lignolytic systems, especially laccase-mediator system. Journal of Biotechnology 1997; 53: p.163-202
32. Hofrichter M. Review: lignin conversion by manganese peroxidase (MnP). Enzyme and Microbial Technology 2002; 30: p. 454-466
33. Alexopoulos CJ, Mims CW, Blackwell M. Introductory mycology John Wiley & Sons, INC.
34. Gutierrez A, Jose C.del Rio, and Martinez MJ. The biotechnological control of pitch in paper pulp manufacturing. Trends in Biotechnology 2001; 19: p. 340-348
35. Breen A, Singleton F. Fungi in lignocellulose breakdown and biopulping. Current Opinion in Biotechnology 1999; 10: p. 252-258
36. Lois J. Forde Kohler. Ronald J. Improving softwood mechanical pulp properties with Ophiostoma piliferum. Tappi Journal 80 (3): p. 135-139
37. Tamerler CB, et al. Production of lipolytic enzymes in batch cultures of Ophiostoma piceae. Journal of Chemical Technology and Biotechnology 76: p. 991-996
38. Ouajai S, Shanks RA. Composition, structure and thermal degradation of hemp cellulose after chemical treatments. Polymer Degradation and Stability 2005; 89: p. 327-335
39. Sharifah HA, Martin PA. The effect of alkalization and fibre alignment on the mechanical and thermal properties of kenaf and hemp bast fibre composites: part 1 – polyester resin matrix. Composites Science and Technology 2004; 64: p. 1219-1230
40. Nowack B. Review: Environmental chemistry of phosphonates. Water Res 2003; 37(11): 2533-2546

41. Bledzki AK, Gassan J. Composites reinforced with cellulose based fibres. Prog. Polym, Sci 1999; 24: p. 221-274
42. Pickering KL, Abdalla A, Ji C. The effect of silane coupling agents on radiate pine fibre for use in thermopiastic matrix composites. Composites: Part A 2003; 34: p. 915-926
43. Wang Q, Fan XR, Gao WD, Chen J. Characterization of bioscoured cotton fabrics using FT-IR ATR spectroscopy and microscopy techniques. Carbohydrate Research 2006; 341. P. 2170–2175
44. Pendey KK, Pitman AJ. Examination of the lignin content in a softwood and a hardwood decayed by a brown-rot fungaus with the Acetyl Bromide Method and Fourier Transform Infrared Spectroscopy. J polym Sci Part A Polym Chem. 2004; 42: 2340-2346
45. Andersson S, Wikberg H. Studies of crystallinity of Scots pine and Norway spruce cellulose. Trees 2004; 18: p.346-35
46. Smole MS, et al. X-ray study of pre-treated regenerated cellulose fibres. Mat Res Innovat 2003;7: p. 275-282
47. Tserkia V, Zafeiropoulosb NE, Simonb F, Panayiotoua C. A study of the effect of acetylation and propionylation surface treatments on natural fibres. Composites: Part A 2005; 36: p. 1110-1118
48. Ouajai S, Shanks RA. Composition, structure and thermal degradation of hemp cellulose after chemical treatments. Polymer Degradation and Stability 2005; 89: p. 327-335
49. Dietrich F, Gerd W. Wood Chemistry, Ultrastructure, Reactions. Walter De Gruvter (1984)
50. Reddya N, et al. Structure and properties of high quality natural cellulose fibers from cornstalks. Polymer 2005; 46: p. 5494–5500
51. Blanca M, et al. The effect of xylanase on lignocellulosic components during the bleaching of wood pulps. Bioresource Technology 2005; 96: p. 21–30

52. Andersson S, et al. Crystallinity of wood and the size of cellulose crystallites in Norway spruce (Picea abies). J wood Sci 2003; 49: p. 531-537
53. Truong M. Establishment of Protocols for Natural Fibre Density Measurement. 2007; CIC Project No. 07-020-07
54. Haines PJ. Principles of thermal analysis and calorimetry. Royal society of chemistry (2002)
55. Singh R, Arora S, Lal K. Thermal and spectral studies on cellulose modified with various cresyldichlorothiophosphates. Thermochimica Acta 1996; 289: p. 9-21
56. Tian CM, Guo HZ, Zhang HY. Study on the thermal degradation of cotton cellulose ammonium phosphate and its metal complexes. Thermochimica Acta 1995; 25: p. 243-251
57. Aggarwal p, Dollimore D. The combustion of starch, cellulose and cationically modified products of these compounds investigated using thermal analysis. Thermochimica Acta 1997; 291: p. 65-72
58. Sun RC, Tomkinson J, Geng ZC, Wang NJ. Comparative studies of hemicelluloses solubilized during the treatments of maize stems with Peroxymonsulfuric Acid, Peroxyformic Acid, Peracetic Acid, and hydrogen characterizations. Holzforschung 2000; 54: p. 492-496
59. Sharifah H A, Martin P A. The effect of alkalization and fibre alignment on the mechanical and thermal properties of kenaf and hemp bast fibre composites: part 1 – polyester resin matrix. Composites Science and Technology 2004; 64: p. 1219-1230
60. Sefain MZ, et al. Thermal behaviour of linen and chemically treated linen fibres. Polymer degradation and stability 1995; 50: p. 195-198
61. Wielagea B, Lampkea T, Marxb G, Nestlerb K, Starkeb D. Thermogravimetric and differential scanning calorimetric analysis of natural fibre and polypropylene. Thermochimica Acta 1999; 337: p. 169-177

62. Alkan M, Demirbas O, Dogan M. Electrokinetic properties of kaolinite in mono-and multivalent electrolyte solutions. Microporous and Mesoporous Materials 2005; 83: p. 51-59
63. Li H, Wei S, Qing C. Discussion on the position of the shear plane. Journal of Colloid and Interface Science 2003; 258: p. 40-44
64. Kleinschek KS, Ribitsch V. Electrokinetic properties of processed cellulose fibres. Colloid and Surfaces, A: Physicochemical and Engineering Aspects 1998; 140: p. 127-138
65. Kleinschek KS, Ribitsch V. Determination of the adsorption character of cellulose fibres using surface tension and surface charge. Mat Res Innovat 2002; 6: p. 13-18
66. Ribitsch V, Kleischek KS. The influence of classical and enzymatic treatment on the surface charge of cellulose fibres. Colloid Polym Sci 1996; 274: p. 388-394
67. Mallick PK. Particulate and short fibre reinforced polymer composites. In: Kelly A, Zweben C, editors. Comprehensive Composite Materials. vol. 2. Polymer matrix composites, Elsavier, 2000. p. 291- 333
68. Suresh G. Process Modeling. In: Daniel B, Miracle and Steven L, Donaldson, editors. ASM Handbook, vol. 21. p. 423-440
69. Joseph PV, et al. Effect of processing variables on the mechanical properties of sisal-fibre reinforced polypropylene composites. Composites Science and Technology 1999; 59: p. 1625-1640
70. Fu SY, Lauke B. Effects of fibre length and fibre orientation distributions on the tensile strength of short-fibre reinforced polymers. Composites Science and Technology 1996; 56: p. 1179-1190
71. Singleton ACN, Baillie CA, Beaumont PWR, Peijs T. On the mechanical properties, deformation and fracture of a natural fibre/recycled polymer composite. Composites Part B 2003; 34: p. 519-526

72. Suddell BC, Evans WJ. Natural fibre composites in automotive applications Natural fibres, biopolymers, and biocomposites. In: Mohanty AK, Misra M, Drzal LT, editors. Natural fibres, biopolymers, and biocomposites. Taylor & Francis. Boca Raton, Florida, p. 231-260 (2005)
73. Brooks R. Injection molding based techniques In Kelly A, Zweben C, editors. Comprehensive Composite Materials. Elsavier Science Ltd: Oxford. (2000)
74. Keller A. Compounding and mechanical properties of biodegradable hemp fibre composites. Composites Science and Technology 2003; 63(9): p.1307-1316
75. Tomas Astrom B. Thermoplastic composites manufacturing. In: Henry SD, Moosbrugger C, editors. ASM handbook. vol. 21. Composites, Material Park, 1990. p. 570-578
76. Gibson AG. Continuous molding of thermoplastic composites. In: Kelly A, Zweben C, editors. Comprehensive Composite Materials. vol. 2. Polymer matrix composites, Elsavier, 2000. p. 979-997
77. Wakeman MD, Rudd CD. Compression molding of thermoplastic composites. In: Kelly A, Zweben C, editors. Comprehensive Composite Materials. vol. 2. Polymer matrix composites, Elsavier, 2000. p. 915-965
78. Manson JAE, Wakeman MD Bernet N. Composite processing and manufacturing-an overview. In: Kelly A, Zweben C, editors. Comprehensive Composite Materials. vol. 2. Polymer matrix composites, Elsavier, 2000. p. 577-609
79. Shibata S, Cao Y, Fukumoto I. Press forming of short natural fibre-reinforced biodegradable resin: Effects of fibre volume and length on flexural properties Polymer Testing 2005; 24: p. 1005–1011
80. Doan TTL, Gao SL, Mäder E. Jute/polypropylene composites 1. Effect of matrix modification. Comp Sci Tech 2006; 66: p. 952-963

81. Herrera-Franco PJ, Valadez-Gonzalez. A. A study of the mechanical properties of short natural-fibre reinforced composites. Composites: Part B 2005; 36: p.597-608
82. Valadez-Gonzalez A, Cervantes-Uc JM, Olayo R, Herrera-Franco PJ. Effect of fibre surface treatment on the fibre-matrix bond strength of natural fibre reinforced composites. Composites: Part B 1999; 30: p. 309-320
83. Drzal LM, Rich MJ, Camping JD, Park WJ. Interfacial shear strength and failure mechanism in graphite fibre composite. Proceeding of 35th Annual Technical Conference Reinforced Plastics/Composites Institute, Section 20-C. 1980. p. 1–7.
84. Tripathi D, Jones FR. Review: Single fibre fragmentation test for assessing adhesion in fibre reinforced composites. Journal of materials science 1998; 33: p.1-16
85. Kalaprasad G, Joseph K, Thomas S, Pavithran C. Theoretical modelling of tensile properties of short sisal fibre-reinforced low-density polyethylene composites Journal of Materials Science 1997; 32(16): p. 4261-4267.
86. Joseph PV, Mathew G, Joseph K, Thomas S, Pradeep P. Mechanical properties of short sisal fiber-reinforced polypropylene composites: Comparison of experimental data with theoretical predictions. Journal of Applied Polymer Science 2002; 88(1): p. 602-611.
87. Kelly A, Tyson WR. Tensile properties of fibre-reinforced metals: Copper/Tungsten and Copper/Molybdenum. Journal of the Mechanics and Physics of Solids 1965; 13: p. 329-350.
88. Thomason JL. Micromechanical parameters from macromechanical measurements on glass reinforced polyamide 6,6. Comp Sci Tech 2001; 61: p. 2007-2016
89. Hirsch TJ. Modulus of elasticity of concrete affected by elastic moduli of cement paste matrix and aggregate. Journal of the American Concrete Institute 1962; 59: p. 427-447.

90. Bowyer WH, Bader MG. On the re-inforcement of thermoplastics by imperfectly aligned discontinuous fibres. J Materials Sci 1972; 7: p. 1315-1321
91. Sui GX, Wong SC, Yang R, Yue CY. The effect of fibre inclusions in toughened plastics–Part Π: determination of micromechanical parameters. Comp Sci Tech 2005; 65: p. 221-229
92. Bader MG, Bowyer WH. An improved method of production for high strength fibre-reinforced thermoplastics. CPSOA 1973; 4: p. 150-156
93. Madsen B, Thygesen A, Lilholt H. Plant fibre composites – porosity and volumetric interaction. Comp Sci Tech 2007; 67: p. 1584–1600
94. Thygesen A, Thomsenc AB, Daniel G, Lilholt H. Comparison of composites made from fungal defibrated hemp with composites of traditional hemp yarn. Industrial Crops and Products 2007; 25: p. 147–159
95. MacKenzie JK. The elastic constants of a solid containing spherical holes. Proc Phys Soc 1950; B63:2.
96. Thygesen A. Properties of hemp fibre polymer composites -An optimisation of fibre properties using novel defibration methods and fibre characterization. PhD Thesis, the Royal Agricultural and Veterinary University of Denmark 2006.
97. ASTM D2734-94. ASTM Standard Test Methods for Void Content of Reinforced Plastics 2003.
98. Madsen B, Lilholt H. Physical and mechanical properties of unidirectional plant fibre composites—an evaluation of the influence of porosity. Comp Sci Tech 2003; 63: p.1265-1272
99. ASTM D3800-99. ASTM Standard Test Method for Density of High-Modulus Fibers 1999.
100. ASTM D3379-75. Standard test method for tensile strength and Young's Modulus for high-modulus single-filament materials 1989.

101. ASTM D638. ASTM Standard Test Method for Tensile Properties of Plastics 2004.
102. ASTM D792. ASTM Standard Test Methods for Density and Specific Gravity (Relative Density) of Plastics by Displacement 2000.